The Effects of L4/5 Fusion on the Adjacent Segments in the Lumbar Spine

A Thesis submitted to The University of Manchester for the degree of Doctor of Philosophy in the Faculty of Engineering and Physical Sciences

2015

Francisco Mauricio Martínez Lozada

School of Mechanical, Aerospace and Civil Engineering

Table of Contents

List of Figures

List of Tables

Abbreviations

LBP	Low Back Pain
PLF	Posterolateral Fusion
PEEK	Polyether ether ketone
L1	Lumbar vertebra L1
L2	Lumbar vertebra L2
L3	Lumbar vertebra L3
L4	Lumbar vertebra L4
L5	Lumbar vertebra L5
S1	Sacral vertebra S1
L1/2	Intervertebral disc between L1 and L2 vertebrae
L2/3	Intervertebral disc between L2 and L3 vertebrae
L3/4	Intervertebral disc between L3 and L4 vertebrae
L4/5	Intervertebral disc between L4 and L5 vertebrae
L5/S1	Intervertebral disc between L5 and S1 vertebrae
PLIF0NF	Posterior lumbar interbody fusion with two 0º cages inserted and no fusion
PLIF0F	Posterior lumbar interbody fusion with two 0º cages inserted and fusion achieved
PLIF4NF	Posterior lumbar interbody fusion with two 4º cages inserted and no fusion
PLIF4F	Posterior lumbar interbody fusion with two 0º cages inserted and fusion achieved
HS	Healthy Spine Model
ROM	Range of Motion
3D	Three-dimensional
C1-C7	Cervical vertebrae
T1-T12	Thoracic vertebrae
ALL	Anterior Longitudinal Ligament
PLL	Posterior Longitudinal Ligament
TL	Transverse Ligament

CL	Capsular ligament
LF	Ligament Flavum
ISL	Interspinous Ligament
SSL	Supra spinous ligament
SIL	Sacroiliac ligament
FSU	Functional spinal unit
CT	Computed Tomography
DDD	Degenerative Disc Disease
ALIF	Anterior Lumbar Interbody Fusion
TLIF	Transverse Lumbar Interbody Fusion
XLIF	Extreme Lateral Interbody Fusion
FEA	Finite Element Analysis
FEM	Finite Element Method
IGES	Initial Graphics Exchange Specification
PLIF	Posterior Lumbar Interbody Fusion

Nomenclature

MPa	Megapascal (10^6 Pascal)
GPa	Gigapascal (10^9 Pascal)
mm	Millimetres
^{o}	Degrees
cos	Cosine of an angle
sin	Sine of an angle
{F}	Force matrix
[K]	Stiffness matrix
{u}	Displacement matrix
E	Young's modulus
N	Newton
v	Poisson's ratio
x	Displacement on Hooke's Law

Abstract

Lumbar intervertebral disc disorder is a spinal condition that affects the normal function of the intervertebral discs mainly due to the natural aging process. This condition can manifest itself in pain and limited motion in the legs, amongst others.

Posterolateral Fusion (PLF) and Posterior Lumbar Interbody Fusion (PLIF) are two of the most used surgical procedures for treating lumbar intervertebral disc disease. Although these procedures are commonly used and performed successfully the impact in terms of the stresses developed in the posterior implants employed and in the spinal components adjacent to the surgical site has not been exhaustively investigated. In addition, the consequences of the procedure on the reduction of the Range of Motion of the lumbar spine is not clearly understood.

The objective of this research is to investigative the effect of one-level spinal fusion of lumbar segment L4-L5 on the stresses and the range of motion at the remaining, adjacent lumbar levels. Four 3 dimensional finite element models of a lumbosacral spine were created from Computer Tomography data (CT scan). The models were used to investigate four surgical scenarios, including the use of 0^o and 4^o interbody cages, in addition to the un-instrumented spine for flexion, extension, torsion and lateral bending motions. The predictions obtained from the models enabled the mechanical behaviour of the lumbar spine following fusion surgery using 0^o and 4^o cages to be investigated and compared. In addition, a clinical study was performed to quantify the reduction in the range of motion for subjects who had undergone L4/5 posterior lumbar interbody fusion surgery. The clinical results were compared to those of subjects who had not undergone surgery and to the range of motion predictions from the computational model.

The results from this research demonstrate that the insertion of posterior instrumentation does not have an impact on the spinal structures above the L3/4 intervertebral disc. However, the pedicle screws and the insertion of the interbody cages causes stress levels in the area adjacent to the surgical site to rise which could promote accelerated degeneration of the discs. Additionally, this study demonstrates how the pedicle screws are affected by the surgical spinal fusion techniques.

Furthermore, the investigation demonstrates how posterior lumbar interbody fusion causes the range of motion of patients that had undergone this surgery to decrease. The results from the comparison of the behaviour of the use of 0^o and 4^o interbody cages in L4-5 posterolateral fusion demonstrates that the stress levels in the adjacent vertebrae, intervertebral discs and pedicle screw fixation system increase when 4^o are used cages than when 0^o cages were employed.

The results from the in-vitro study show a decrease in the range of motion of the subjects who had undergone L4/5 posterior lumbar interbody fusion surgery when compared with the subjects with no low back pain history. This indicates that the PLIF surgery combined with the normal disc degeneration is subjected to higher stresses than the healthy spine.

Declaration

No portion of the work referred to in the Thesis has been submitted in support of an application for another degree or qualification of this or any other university or other institute of learning.

Copyright

Acknowledgements

First, I would like to express my deepest gratitude to Prof. Teresa Alonso-Rasgado, Prof Colin Bailey, Mr Rajat Verma and Mr Saeed Mohammad for their guidance, patience and support to improve this work.

I also want to thank Dr Alan Walmsley and to the Bioengineering Research Group. Without their help and suggestions, I could not have finished this project.

I would also like to thank my parents for the moral support I have always received from them and which is invaluable to me.

I am indebted to all my friends who have supported me over the last few years during this journey.

Last but not least, I wish to gratefully acknowledge the PhD scholarship financial support provided by the National Council on Science and Technology of Mexico (CONACYT).

Chapter I – Introduction

1.1 Overview

Lumbar intervertebral disc disorders are a frequent problem in humans that increase with age. In general, these problems take place in the lumbar area of the spine due to the combination of the higher compressive loads and mobility associated with this region of the spine during daily activities. Depending on the pathology, different surgical treatments are used to stabilize and restore the degenerated or damaged parts of the lumbar spine in order to facilitate the recovery of the affected segment.

In cases where non-operative treatment is insufficient for treating lumbar intervertebral disc disorders, for example, where structural changes are severe or pain is recurrent, then spinal instrumentation may be used. Spinal instrumentation is a widely used surgical technique, which is employed for a range of clinical problems including trauma, deformity and degeneration of the intervertebral discs. Instrumentation used in these procedures includes pedicle screw fixation systems, which prevent any undesirable movement in the damaged segment, alleviating the load on the degenerated disc [1-6]. This surgical approach is commonly known as Posterolateral Fusion (PLF). However, where additional stabilization and mechanical support are required, a Posterior Lumbar Interbody Fusion (PLIF) surgical technique may be used. In this case the damaged or degenerated intervertebral disc is surgically removed and replaced with intervertebral cages, which are then filled with bone graft to promote bone growth in the void between the two fixed vertebrae [7-10].

When performing fusion operations of these types, either PLF or PLIF, surgeons are naturally concerned with the effect of such procedures on the rest of the lumbar spine. Although clinical studies have shown that fusion techniques provide effective stability at the surgical site, the effect of these procedures on the adjacent intervertebral discs and vertebrae bodies is not well understood by clinicians. For example, the motion at the site of the procedure is restricted and the behaviour at the adjacent sites is altered, which could cause an increase in stress at adjacent segments that may lead to accelerated degeneration of the intervertebral disc that is situated above and/or below the fixed segment [11-13]. Hence it is important to understand the consequences of surgical interventions on the lumbar spine.

1.2 Research Background

Posterolateral Fusion and Posterior Lumbar Interbody Fusion surgical procedures are the most common methods used to stabilise the damaged lumbar spine after lumbar decompression surgery. However, there is controversy in the published literature on the effect of fusion on the adjacent spine.

For example, Yan *et al.* [14] reported no significant change in stress in the adjacent disc following pedicle screw instrumentation of one segment of their 4 level lumbar spine model. Other investigators have, however, reported increased stresses at adjacent levels [11, 15-17]. Cunningham *et al.* [17] reported a 45% increase in adjacent disc stress following instrumentation in their cadaveric study; In other study Zhong *et al.* [18], comparing an intact model and an instrumented model, reported an increase on the level of stress for up to 80% (from .6 [MPa] to 1.1 [MPa]).

Researchers have developed models to investigate the biomechanical behaviour of various aspects of lumbar spinal fusion procedures, including the pedicular screws and rods [1, 19], interbody cages (both stand-alone or in conjunction with pedicle fixation systems) [4, 5], posterior interbody fusion [11], and posterior interbody fusion as compared to artificial disc replacement [11]. However, many of the studies model less than five levels in the lumbar spine and concentrate on reporting the range of motion (ROM) at the surgical site and in the immediately adjacent segments. Although range of motion is important, as reduced ROM is generally associated with increased stability whereas increased ROM denotes greater instability [11], a deeper, fuller understanding of the biomechanical effect of lumbar fusion can be obtained by considering more levels of the spine and by calculating and considering the stresses in the spinal elements of these levels.

In recent years great advances have been made in the basic knowledge of the function and the form of the vertebral column, however further investigation is required in this structure in order to provide solutions and recommendations to surgeons for solving specific kinds of problems.

1.3 Objectives and Research Methodology

The aim of the research described in this thesis was to investigate and compare the performance of the Posterolateral Fusion (PLF) and Posterior Lumbar Interbody Fusion (PLIF) surgical techniques undertaken on the L4/5 lumbar segment. In addition, for PLIF, 0º and 4º intervertebral body fusion cages were considered. The effect of these techniques on the stresses and range of motion in the adjacent intervertebral discs and vertebral elements were studied using three-dimensional (3D) finite element models.

Four (3D) models of the five-level lumbar spine and sacral bone were developed to undertake this research in order to simulate the following scenarios:

a) Un-instrumented spine.
b) Spine with a pedicle screw fixation system implanted.
c) Spine with a pedicle screw fixation system and two 0^0 or 4^0 interbody cages implanted.
d) Spine with a pedicle screw fixation system and two 0^0 or 4^0 interbody cages implanted following fusion across the L4-L5 vertebrae.

Four motions: flexion, extension, torsion and lateral bending in addition to the standing position were considered. Average von Mises stresses and Range of Motion (ROM) at the surgical site and at adjacent vertebral bodies and intervertebral discs were compared for all the scenarios and motions. The numerical models were validated using ROM data from the published literature.

Furthermore, an innovative clinical study was undertaken that entailed comparing the range of motion from an *in-vivo* investigation using subjects that had undergone a L4/5 posterior lumbar interbody fusion (PLIF) using 4º intervertebral body fusion cages on average 1.8 years previously to the ROM of subjects who had no history of low back pain conditions and had not undergone lumbar interbody fusion. ROM from these two groups were compared. Additionally, predictions from ROM for the 3D finite element models, un-instrumented and four degree PLIF, were compared with the results from the *in-vivo* investigation.

In addition to this introductory chapter, this thesis is composed of six further chapters that are presented as follows: Chapter II describes the anatomy of the spine emphasizing the lumbosacral region, its different sections, components, materials, biomechanics and the ROM of this part of the spine.

Chapter III describes the most common intervertebral disc disorders in the lumbar spine and the surgical techniques used to treat them, including Posterolateral Fusion (PLF) and Posterior Lumbar Interbody Fusion (PLIF). The instrumentation used to correct the vertebral alignment and to stabilize the damaged segments is also discussed in this chapter.

Chapter IV presents a literature review of the different methods used to construct and study the lumbar spine using the finite element analysis. This chapter also explains the different procedures and devices used on numerous *in-vivo* investigations to measure the ROM of the lumbar spine.

Chapter V describes the *in-vivo* investigation used to analyze and compare the range of motion between patients that had and had not undergone L4/5 Interbody lumbar fusion. This chapter also presents a comparison of the ROM results between the two groups of participants in the study.

The next Chapter, Chapter VI, describes in detail the development of the 3D computational models. This chapter explain the process used to create the geometry of the healthy Lumbosacral spine and the techniques used to alter the geometry of this model to simulate the different fusion procedures investigated. Furthermore, this chapter also describe the loads applied to the models to simulate different motions of the spine and the physiological boundary conditions used to simulate the interaction between the elements that constitute these models.

Chapter VII presents the results from the investigation describing the effect on the vertebral bone and intervertebral discs following Posterolateral Fusion and Posterior Interbody Fusion using 0º PEEK and 4º PEEK interbody cages. This chapter also presents a comparison of the performance of the 0º and 4º cages for the different fusion scenarios. In addition, a comparison between the experimental results and the numerical models predictions are discussed.

Finally, Chapter VIII presents the conclusions of the different computational analyses and the experimental tests as well as describing recommendations for future work

Chapter II - Spine

2.1 Introduction

The Spine or Vertebral Column is a structure formed by muscles, tissues, vertebras, intervertebral discs and ligaments. This arrangement of bone and tissues transfers the loads of the upper body right to the pelvis and permits the required physiological motion of the upper body while protecting the spinal cord from potentially damaging forces and motions produced by movement or trauma. [20-26]

This chapter describes the anatomy of the spine emphasizing the lumbosacral region, its different sections, components, materials, biomechanics and the ROM of this part of the spine. The main elements of the spine, including the vertebrae, intervertebral discs, ligaments and spinal muscles and their constitutive components, are described. The types of osseous tissue, trabecular and cortical bone, found in the spinal structures are identified and their mechanical properties discussed. The ROM at the different levels of the spine is described including factors, which can affect the ROM.

2.2 Anatomy

Depending of the anatomy of the individual, the spinal column is formed by 33 to 34 bony segments. Based on the anatomy of the bones, its different physical properties and biomechanics, these bones can be grouped in five different sections: the cervical region that contains 7 vertebras (C1 - C7), the thoracic area that has 12 vertebras (T1 - T12), the lumbar section that has 5 vertebras (L1 - L5) the sacral area that also contains five vertebras (S1 - S5) and the cocygeal zone that has 3 to 4 fused vertebras depending on the anatomy of the individual. Figure 2.1 shows the position of the location of the different sections mentioned previously.

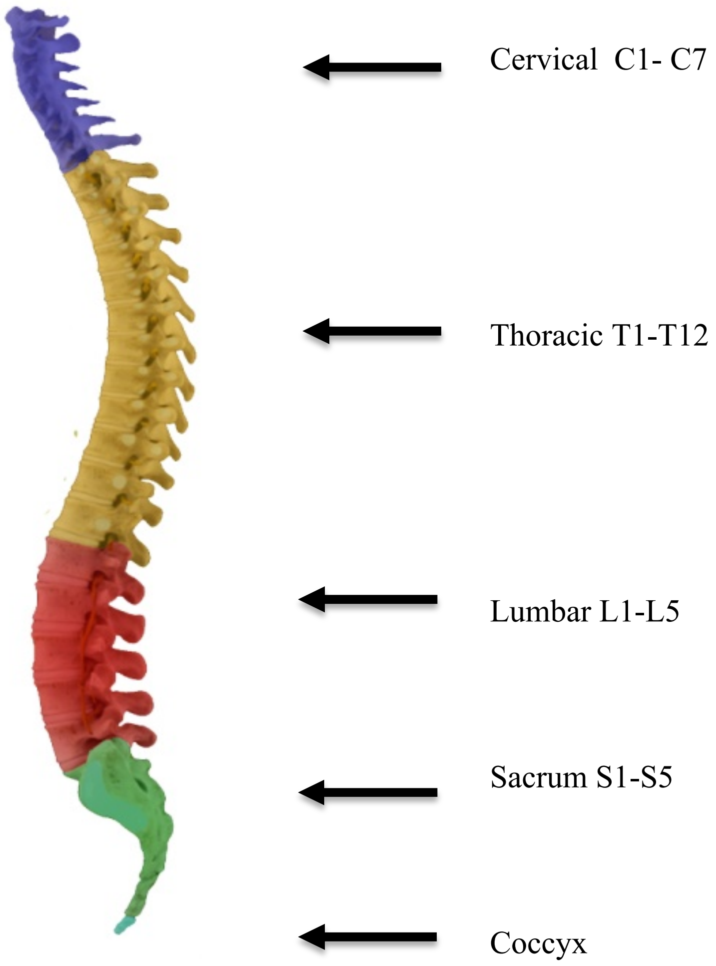

Figure 2.1 Regions of the Spine

The alignment of all the bone elements in the spine is largely determined by the intervertebral discs. While in the frontal or posterior view the spinal column are in a straight alignment, as shown in the Figure 2.2, in the sagittal plane the anatomies of these soft tissues generate four curves along the five sections. The function of these curves is to increase the spinal column flexibility and also to function as a spring to provide the shock absorbing capacity when external loads are applied to this structure. In old age, as the discs tend to degenerate, the four curves gradually disappear transforming the vertebral column into a C-shape form. [22, 23]

The next figure (Figure 2.2) shows the curves of the spine in the three principal views. These curves are convex anteriorly or lordotic in the cervical and the lumbar spine, and convex posteriorly or kyphotic in the thoracic and sacral regions [21, 23, 27]

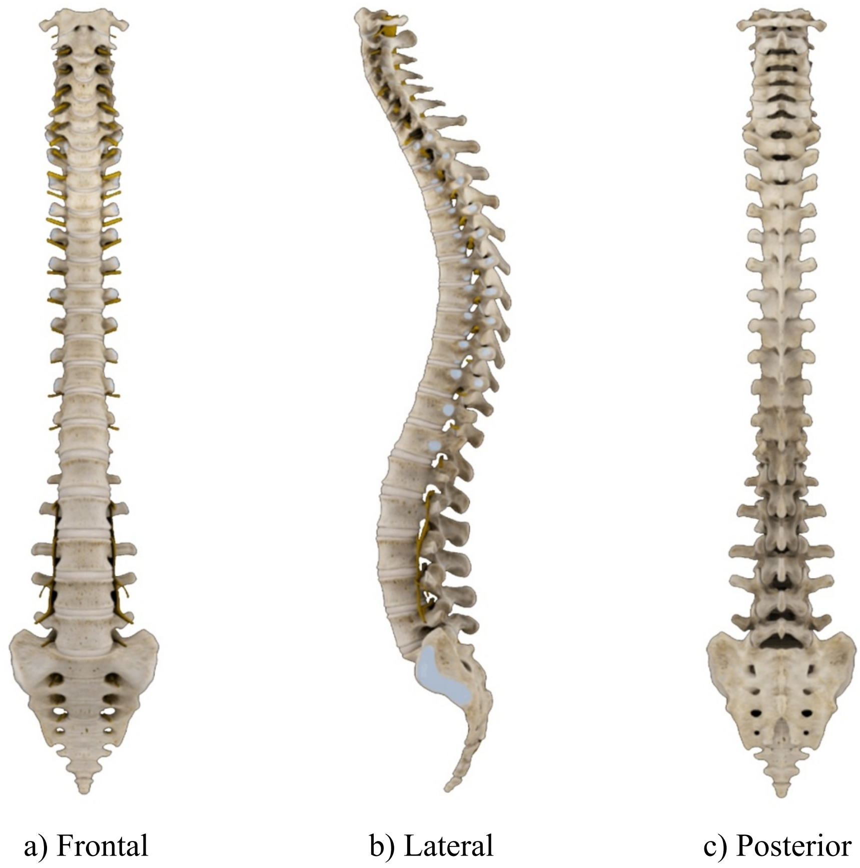

Figure 2.2 Curves of the spine [28]

2.3 Osseous Tissue

The osseous tissue or bone tissue is a rigid and connective material that can function as support or protection for different organs of the body. This solid structure is always involved in a continuous remodelling process in which old bone tissue is replaced by new osseous tissue, which gives the bone the ability to repair itself and alter its properties in response to changes in mechanical demand.[29]

According to histological examination, bone tissue is classified into cortical and trabecular bone. However, at macroscopic levels these types of bone can also be differentiated by their density or porosity levels. The cortical or compact bone is the type of bone with most presence in the human skeleton. This type of bone contributes up to 80% of the total skeleton mass and is found primarily in the mid section of the long bones. The trabecular bone, also called cancellous bone, contributes the other 20% of the skeleton mass. This bone is found primarily at the centre of the vertebral bodies, the pelvis and at the end of the long bones. [30]

The vertebral bodies are composed of both types of bone. The porous trabecular bone is located at the centre of the vertebral body while the cortical bone surrounds the trabecular bone with a solid fine shell.[31]

2.3.1 Bone Mechanical Properties

Due to its anatomy the osseous tissue can be considered as a two-phase material formed by collagen fibres and minerals. According to some studies the mineral particles and the collagen fibres inserted in the bone matrix are the reason that the bones present anisotropic and viscoelastic mechanical properties. [32]

As an anisotropic material the strength and stiffness of the bone depends on the loading conditions that this structure is subjected, being stronger in the longitudinal direction than in the transverse direction, tolerating higher compressive loads than tensile loads.[33, 34]

To characterise the mechanical behaviour of the bone, several studies had tested the cortical and the trabecular bone under different loading conditions in order to obtain the stress-strain curve that is the relationship between the internal forces resulting from a load applied to a certain material and the deformation that the material undergoes.[35]

These curves are different for each material, however they present similar characteristic zones known as the elastic region, the plastic region and the failure mechanism regions.

The elastic region is the first region in these curves. In this region the material is deformed for as long as the loads are applied. Once the load is removed the material recovers its original form. In this region, specific mechanical characteristic such as Young's Modulus can be obtained. The second zone is known as the plastic region.

In this part of the graph the deformation caused by the applied load is irreversible, causing permanent changes in the shape of the material. The third zone is when the material reaches it maximum stress at which point it fractures. Figure 2.3 shows the strain-stress curve of bone and the different regions.

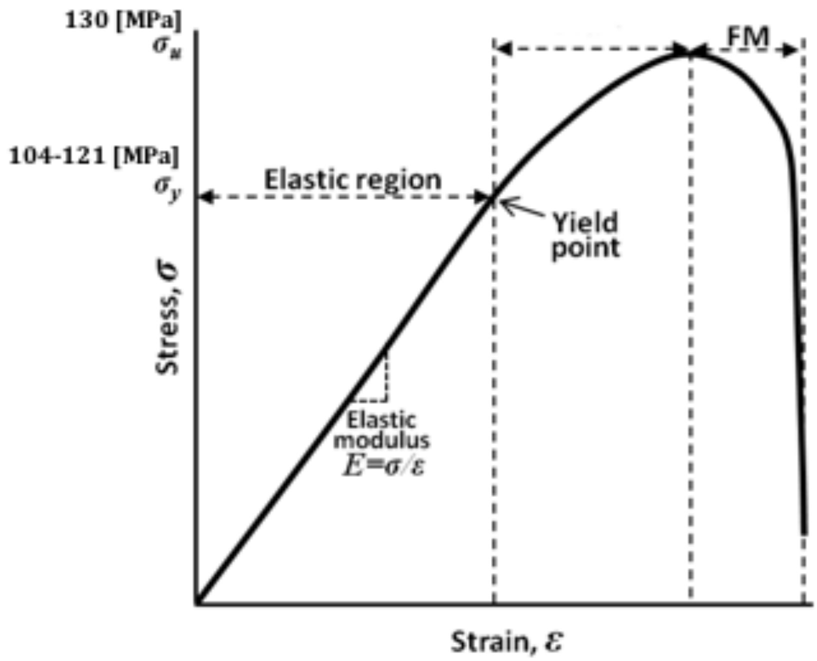

Figure 2.3 Strain-Stress curve of bone (Limb). Modif[36]

Stress-strain curves are different for each material. Figure 2.4 and 2.5 show the stress and strain-curves for the cortical and trabecular bone respectively. It can be seen from these figures that for both materials the bone supports greater stress under compression than under tensile loading.

The stress-strain curve for the cortical bone, Figure 2.4, shows the different stages as mentioned previously. The first region for compressive loading, from the origin (A) to the yield point (Bc) is the elastic region where the bone can return to its original position if the loads are removed. The second zone, from the Bc point to the ultimate compressive stress Cc is the plastic region which for this type of bone (cortical) is almost non-existent. The failure zone extends from the point Cc to Dc which is the point where the bone begins to fracture until it totally fails at Ec.

The stress-strain curve for the cortical bone under tensile loading only displays two regions. The elastic region, from the origin to the yield point and the plastic region, from the yield point to the ultimate tensile strength Ct where the material fails instantaneously.

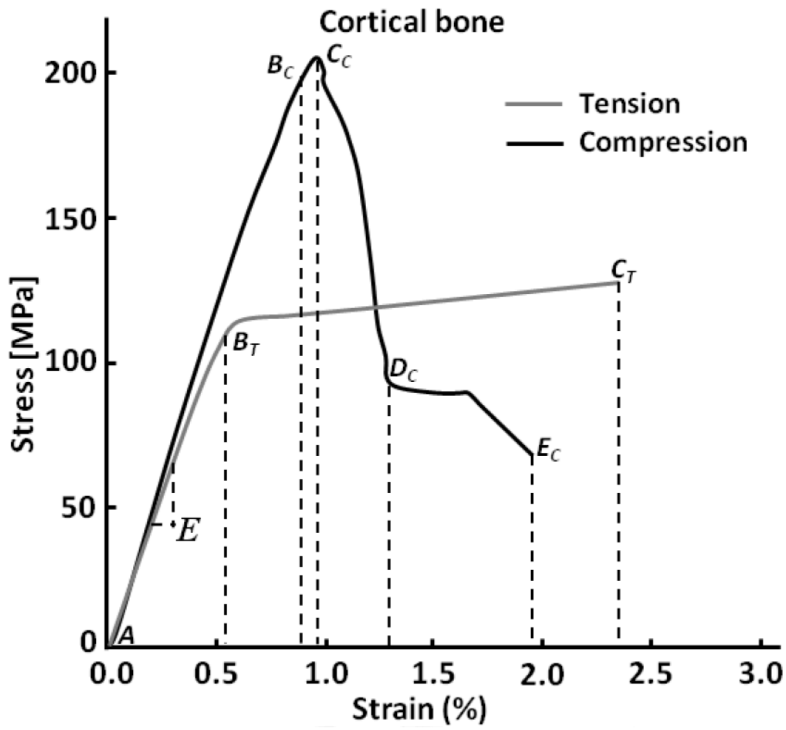

Figure 2.4 Strain-Stress curve of cortical bone. Modif [37, 38]

As for the compression stress-strain curve of the cortical bone, the graph for the trabecular bone contains the 3 different deformation regions (Figure 2.5). The elastic region (A-Bc), the plastic region (Bc-Cc) and the failure region (Cc-Dc) where fracture starts to take place before failure occurs.

For the stress-strain curves under tensile loading the trabecular bone displays three deformation regions, unlike cortical bone, which presents just two. The elastic region comprises from point A to the yield point Bt, the plastic region from Bt to the ultimate tensile stress Ct and the failure region, from Ct to Dt where microfractures start to occur until the material fails totally at point Et

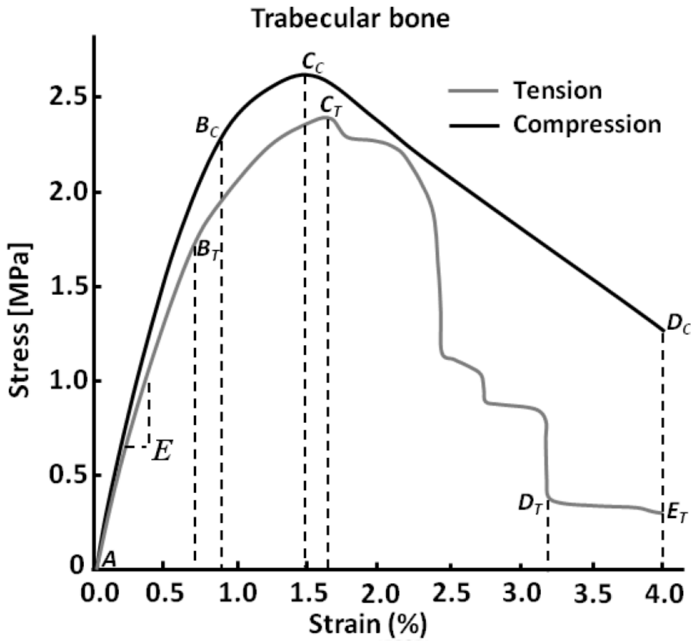

Figure 2.5 Strain-Stress curve of trabecular bone. Modif [37, 38]

2.4 Vertebra

The vertebrae are the bones that form the vertebral column. A vertebra, despite its position in the vertebral column, is formed by a vertebral body, a vertebral arch, the posterior elements, the articular, transverse and spinous processes, and the pedicles. As well as the other bones in the vertebral body, the vertebrae are composed of two types of bone, the cortical bone and the trabecular bone. With age, like all the other bones in the body, these structures lose mineral content that change their physical properties decreasing its strength and size.

The principal mechanical function of the vertebras is to sustain and transmit the compressive loads of the upper part of the body. For this reason, the basic design of the vertebrae in the various regions of the spine from C3 to L5 is approximately the same. However, because of the compressive forces along the trunk, these bony structures are not in the same bone amount along the spine as the quantity of cortical bone increases progressively from the top to the bottom, meaning that the vertebral bodies increase in size towards the lumbar region.[22]

Figure 2.6 Anatomy of the Vertebrae[28]

2.4.1 The Lumbar Spine

The lumbar spine refers to the vertebrae in the lower back of the human body. This section consists of five separate vertebrae named L1, L2, L3, L4 and L5 from the top to the bottom. Due to the loads that this region bears, these five vertebrae are considerably more robust and larger in size compared with the thoracic or cervical vertebras.

This type of vertebra can be divided into three parts, the vertebral bodies, the pedicles and the posterior elements. These three elements have their own function in the lumbar spine. The function of the vertebral body is to support and transmit all the loads from the trunk. As mentioned before, this part consists of a trabecular bone matrix surrounded by a cortical shell. The posterior elements refer to the irregular bone mass on the posterior part of the vertebra; this part receives the different muscle forces that act on the vertebra from the back muscles and transmit them to the pedicles, with the function to bear and transfer the forces from the posterior elements to the vertebral body.

Figure 2.7 Lumbar Vertebra[28]

2.4.2 The Sacral Spine

The sacrum is a single bone located within the two hip bones. This bone, which contains five fused vertebrae, is triangular in shape and is curved so that it has a concave anterior surface and a correspondingly convex posterior surface. The sacral bone articulates above with fifth lumbar vertebra and below with the coccyx. This bone has two large lateral surfaces that articulate with the pelvic bones transmitting the upper body weight to the lower extremities.

Figure 2.8 Sacral Vertebra[28]

2.5 Intervertebral Discs

The intervertebral discs are soft tissue structures situated between each vertebra of the spine constituting 20 - 33 % of the entire height of the vertebral column. These discs transmit the loads from the superior vertebra to the inferior vertebral body providing mobility to the spine allowing complex motion of the joint while also function as a shock absorber material between the vertebras. [23, 39, 40]

These soft tissues are exposed to a different kind of forces and moments. During the standing or sitting position the intevertebral discs are mainly subjected to compressive loads, but as the individual performs different motions as flexion, extension, lateral bending or rotation, tensile or shear stresses are generated in different parts of the discs. [41, 42]

The principal loads to which the disc is subjected can be divided into two major categories. Both categories depend on the duration and the magnitude of the load. The first group represents the short duration, high amplitude load, and causes more damage in the disc, while the second group is the long duration-low amplitude load represented by the loads that are caused by normal physical activity.[43]

While the discs have different heights and sizes along the different sections of the spinal column, these structures maintain the same configuration and are divided into three regions, the Nucleus Pulposus, the Annulus Fibrosus, and the Cartilaginous End-plates as shown in Figure 2.9.

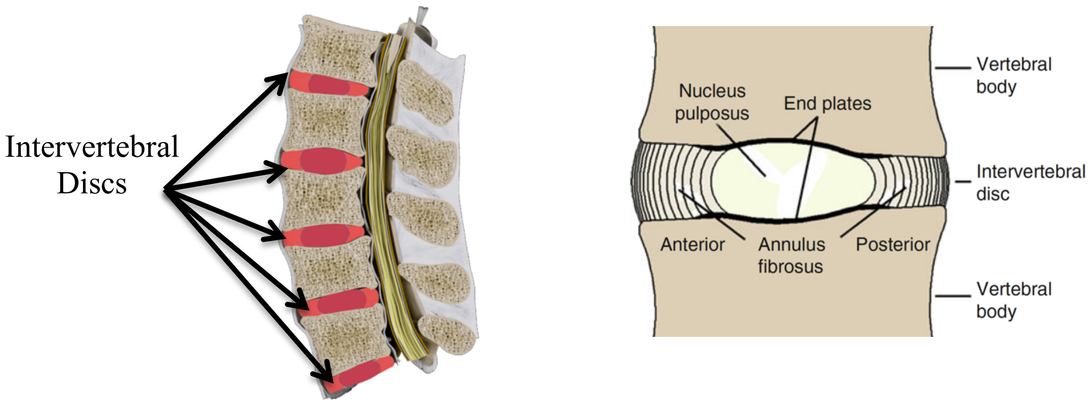

Figure 2.9 Intervertebral Discs. Modif [28, 44]

The nucleus pulposus is located in the central area of the intervertebral discs surrounded by the collagen fibres of the annulus fibrosus as shown if Figure 2.10. This structure is formed of a random mesh made of proteoglycans, collagen and mainly water that constituted 70 to 90% of this element. This random organization of the nucleus pulposus tissue and the large content of water in a normal healthy intervertebral disc, leads to obtaining isotropic mechanical properties in this part of the disc.

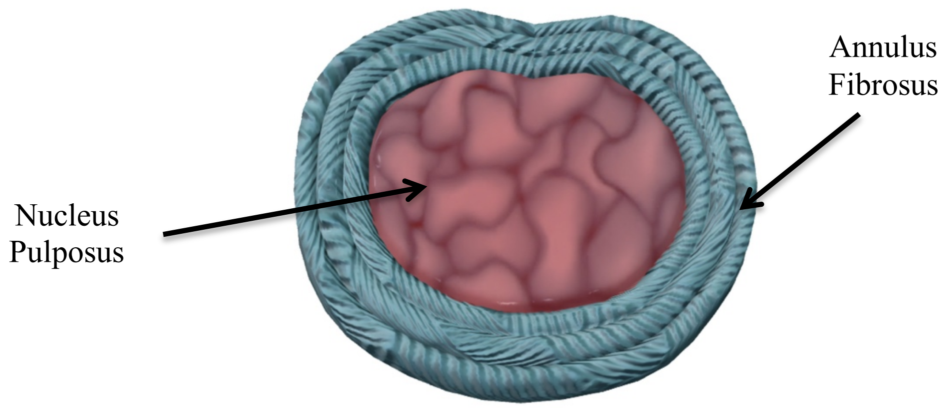

Figure 2.10 Nucleus Pulposus surrounded by collagen fibres. Modif.[45]

When the disc is subjected to different kinds of loads the nucleus pulposus is pressurized within the intervertebral disc as show in Figure 2.11. This pressure is constrained by the surrounding annulus fibrosus fibres and the end plates enabling this tissue to absorb and transmit the compressive loads throughout the entire spine. The total pressure within the nucleus pulposus is called the swelling pressure.[46, 47]

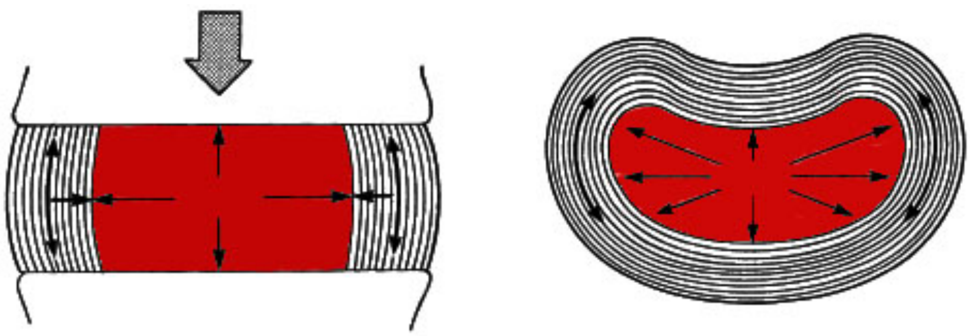

Figure 2.11 Swelling pressure. Modif. [23]

As mentioned before, the intervertebral discs vary in their size and shape throughout the different levels of the spine. One of the differences of the nucleus pulpous, when regarding these changes, is that in the lumbar area the size of the nucleus increase and the capacity to swell becomes greater compared with discs in other vertebral areas.[48]

The annulus fibrosus is located surrounding the nucleus pulposus. This part of the disc is composed by 50% water while the other 50% of this segment is a stiff structure composed of fibrous tissue made of collagen fibres inserted in a proteoglycan grid, which are arranged in concentric laminated layers around the nucleous pulposus and attached to the cartilaginous end plates.

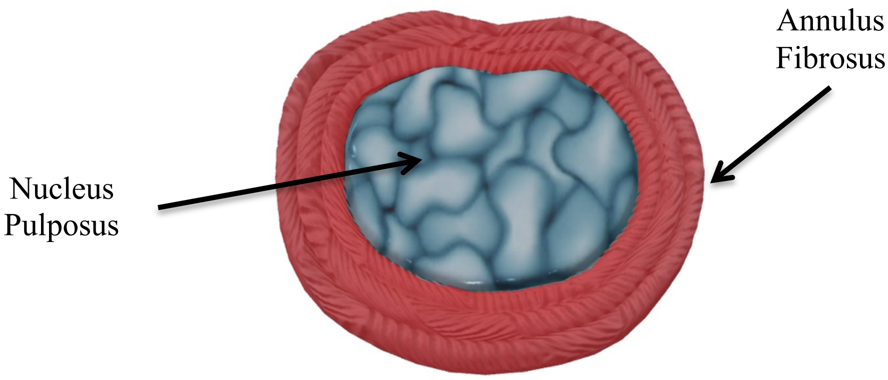

Figure 2.12 Annulus fibrosus surrounding the nucleus pulposus. [45].

These layers alternate their orientation at 30 and 150º relative to the adjacent endplates affecting the tensile circumferential modulus, which affects the compressive mechanical properties of this part of the intervertebral disc.

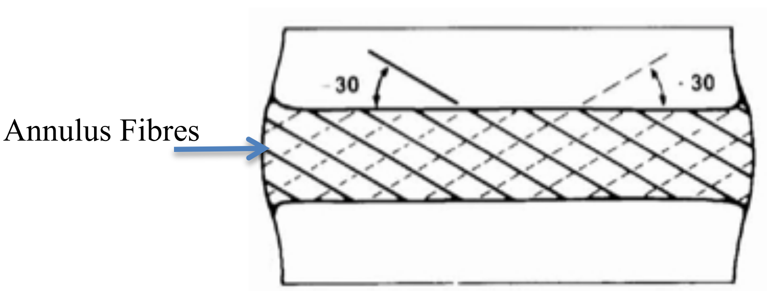

Figure 2.13 Fibres oriented about 30º in the intervertebral disc.[23]

Due to the high water content and the fibrous tissue, the annulus fibrosus can be analysed as a composite material, for this reason various investigations had analysed this arrangement as an anisotropic component. However to simplify the study of this part of the invertebral disc other investigations had considered this fibrilar matrix as an isotropic material and included a solid material that represented the different layers of fibres.

In contrast to the nucleus pulposus that is only subjected to compressive loads, the annulus fibrosus is subjected to compressive and tensile forces due to the different motions of the spine. As an example, this behaviour can be observed in flexion or extension movements. In the flexion movement the nucleus pulposus and the anterior part of the annulus fibrosus are subjected to compression loads while the posterior part of the fibrous structure is affected by tensile forces. This conduct is the same in the extension motion with the difference that when the lumbar spine extends the compression loads affect the posterior part of the annulus and the tensile loads affect the anterior part.

The Cartilaginous End-Plates are located between the intervertebral disc and the vertebral bodies. Their principal functions are to provide nutrients like glucose and oxygen to the intervertebral discs and to distribute the loads across the vertebra. Like the other components of the intervertebral disc, the structure and mechanical properties of the end plates vary spatially, though these characteristics have not been widely studied. [22]

2.6 Ligaments

The ligaments have many different functions in the spine but the main purposes of these tissues are to keep the vertebrae together, providing support to the entire spinal column, and to constrain the motions of the different segments of the spine, preventing overtension and injuries by restricting motions between the vertebrae within a permitted range.

These tissue are composed of type I collagen fibres, elastin and water that form an extracellular matrix. The arrangement of the fibre matrix produced means that, in contrast with other soft tissue in the body, these tissues can resist tension forces from vertebra to vertebra but when they are subjected to compression forces they buckle.

There are seven principal ligaments in the spine, and although they are all similar, they vary in size, orientation, and attachment points. These ligaments in the spine are the Anterior Longitudinal Ligament (ALL), the Posterior Longitudinal Ligament (PLL), the Intertransverse Ligaments (ITL), the Capsular Ligaments (CL), the Ligament Flava (LF), the Interspinous Ligaments (ISL) and the Supraspinous Ligaments (SSL) as shown in Figure 2.14.[23, 49-51]

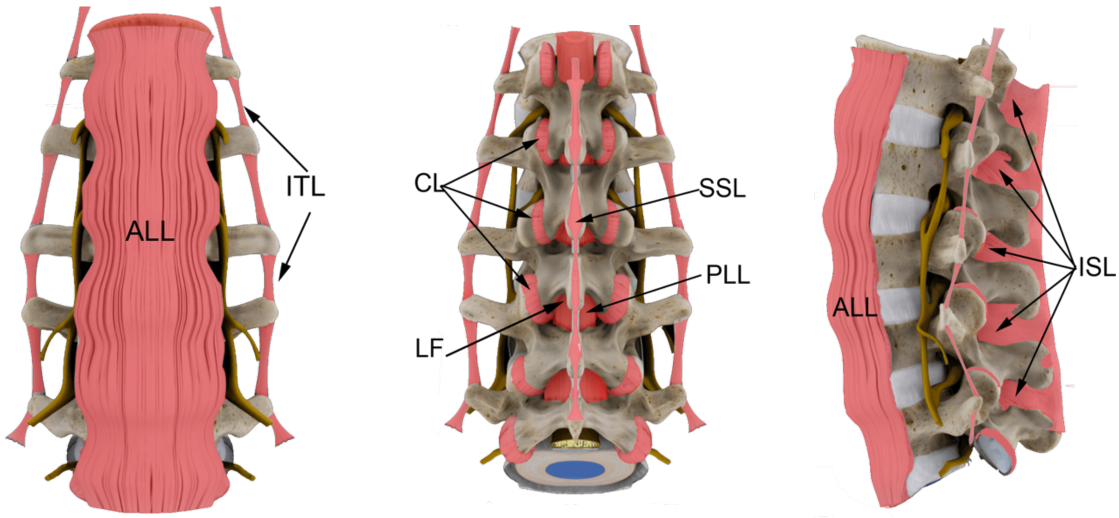

a) Frontal View   b) Posterior View   c) Lateral View

Figure 2.14 Ligaments in the Lumbar Spine. Anterior Longitudinal Ligament (ALL), the Posterior Longitudinal Ligament (PLL), Intertransverse Ligaments (ITL), Capsular Ligaments (CL), Ligament Flava (LF), Interspinous Ligaments (ISL), Supraspinous Ligaments (SSL). Modif.[52]

The ligaments exhibit viscoelastic mechanical behaviour. These structures shrink when tensile loads are applied recovering their original form when the load is removed. However, when this tissue reaches the yield point, due to its mechanical properties, the structure cannot recover its original shape.

Figure 2.15 presents the stress-strain curve for the ligaments. This curve can be divided into three zones, the toe zone and the linear zone, that fits within the physiological loading and the failure zone that starts when the loads are greater than the physiological loading, creating micro fractures in the tissue until the ligament totally fails.

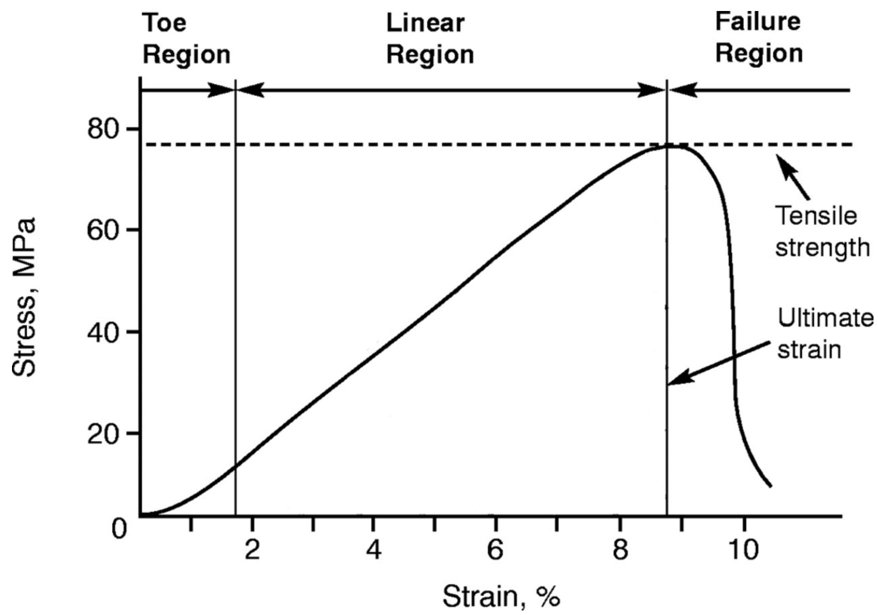

Figure 2.15 Strain-Stress curve of the ligaments (Medial Collateral Ligament) Modif.[38, 53]

The ligament's mechanical properties like the intervertebral disc and the soft tissue tend to decrease with age. When the ligaments fail this generally occurs at the attachment point with the vertebra. Due to the fact that the principal function of these tissues is to provide stability to the spine, ligament failure can then affect the range of motion between two adjacent vertebras, damaging the intervertebral discs.

2.7 Spinal Muscles

The spinal muscles, like most other muscles, have several biomechanical functions. Through their activity these tissues create body movements generating bending moments and torques. Beside these actions, the muscles also provide stability to the vertebral column and serve as a response to the unwanted loads applied by external forces.

A spinal column without the support of the muscles is not a stable structure and cannot carry even the weight of the trunk. The requirement for maintaining stability becomes even more critical when the spinal column is required to support an external load or carry out certain task. Muscles provide the necessary spinal stability when the external load is imposed upon it, as well as during every instant of the physiological motion.

According to their position relative to the spine, back muscles can be classified as postvertebral and prevertebral. Within this division, the postvertebral muscles can be divided into deep, intermediate and superficial muscles. The spinal column stability and movement of this structure is attributed primarily to the deep muscle classification although all of these groups of muscles contribute to these functions in some way. The prevertebral muscles have no further divisions. This group of muscles refers to the abdominal muscles, *the external oblique, internal oblique, transversus abdominis and the rectus abdominis.*

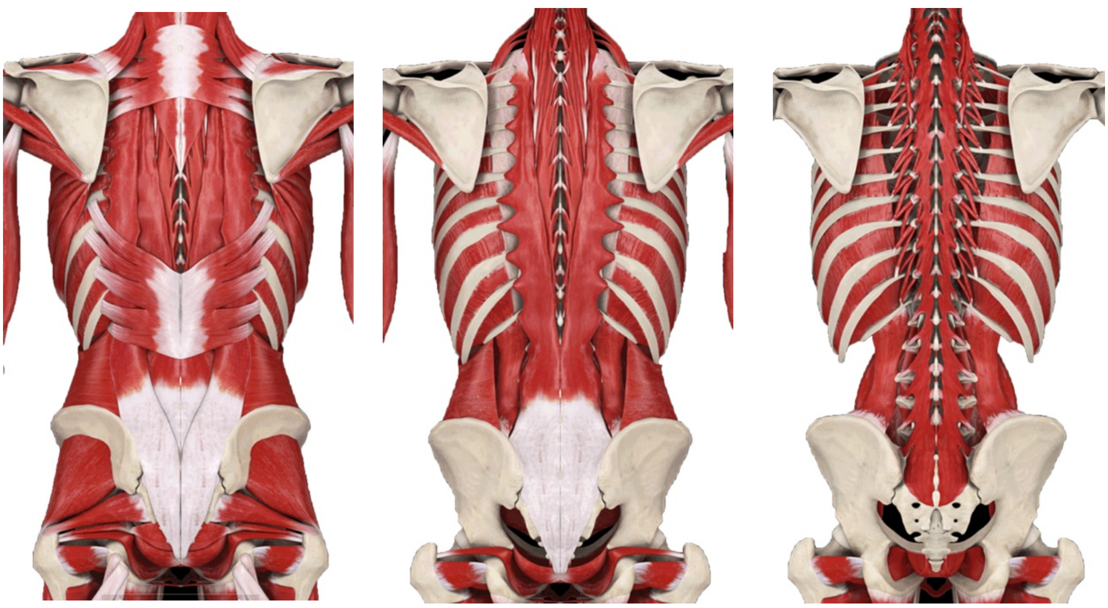

a) b) c)

Figure 2.16 Muscles in the lumbar spine.[52]

2.8 Biomechanics of the Lumbar Spine

The biomechanics of the spine refers to the mechanical behaviour relating to the movements, loads and forces that affect this structure. As mentioned before, the vertebral column transfers loads and permits movement while protecting the spinal cord. These physiological motions are difficult to measure because they are different depending on the age and sex of each individual. A comprehensive knowledge of spinal kinematics is of predominant importance for the understanding of all aspects of the clinical analysis and management of spine problems. [21, 54, 55]

For biomechanical purposes the spine can be subdivided into an arrangement of two adjacent vertebras and all the connecting ligaments, muscles and tissues between them. This setting is called a functional spinal unit (FSU). This array of two vertebrae is the smallest possible representation of the spine that can demonstrate the biomechanical characteristics of the vertebral column. For the characterization of the mechanical properties of a Functional Spinal Unit, the lower vertebra is fixed while the loads are applied to the upper vertebra. After that condition is applied, all the movements and displacements can be measured.[23]

a) Frontal View b) Lateral View c) Lateral Medial View

Figure 2.17 Functional Spinal Unit.[28]

Due to the six degrees of freedom and because of the combination of different loads, spinal motion is often complex. These loads can be divided into two types, the physiological type, referring to the common loads due to the normal day activity like flexion, extension, lateral bending and rotation as shown in the Figure 2.18. The traumatic load types are referring to the loads that take place during accidents. These loads are short in time but great in amplitude.[56]

Flexion Extension Lateral Bending Rotation

Figure 2.18 Motions of the Spine.[46]

Biomechanically speaking, the lumbar region is the most robust segment in the spine. This segment resists the greatest loads, forces and moments in the vertebral column. This region is subjected to compression for almost all the common day activities like standing, walking, running or sitting. The compressive forces on this segment depend on the position of the lumbar vertebras and the anatomy of these bones. Different studies suggest that for a standing position, the load applied to the lumbar spine is approximately 55 to 60% of the total body weight.

2.9 Range of Motion

As mentioned before, the physiological motions are difficult to measure. The range of motion (ROM) is different at each level of the spine and depends on many different factors like the age of the subject, the gender or the structural properties of the disc. However various investigations, using autopsy material, radiographic *in-*

vivo measurements or CT Scans have shown an agreement of a range of values for the ROM of individual motion segments [23, 27, 56-58]

It is important to have knowledge of the normal ROM of any part of the spine in order to understand the effects that any disease or implant can cause to the biomechanics of the spine. As mentioned before each section of the spine has its own particular anatomy, for this reason each region has its distinctive ROM.

2.9.1 Cervical Spine

To explain the ROM of the cervical spine it is necessary to divide this region in to two parts; the Skull-C1-C2 region and from C2 to C7. The Upper Cervical region (Skull-C1-C2) is the most complex join of the axial skeleton. For the flexion/extension motion the joint between these bones have the same ROM in the sagittal plane. For the lateral bending motion, the joint between the skull-C1 has a movement of approximately 89º while the movement at the C1-C2 joint is nearly insignificant. On the other hand for the axial rotation motion there is a large axial rotation at the C1-C2 joint, while in the upper joint this movement is minimal due to the geometric anatomy of the articulation.[23]

For the lower part of the cervical spine (C3-C7) most of the motion in flexion/extension is in the middle part of this region as it can be seen in the Table 2.1 at the end of these chapter. For these joints the C5-C6 interspace is generally considered to have the largest ROM for this movement. However, for the lateral bending and the axial rotation movements the anatomy of the vertebras play an important role on the ROM. Due to the resemblance anatomy of this part of the cervical spine with the thoracic vertebrae, in particular because of the inclination of the facet joints, as shown in Figure 2.19, the range of motion for these movements decreases from the joint C2-C3 into the caudal direction of this part of the spine[59, 60]

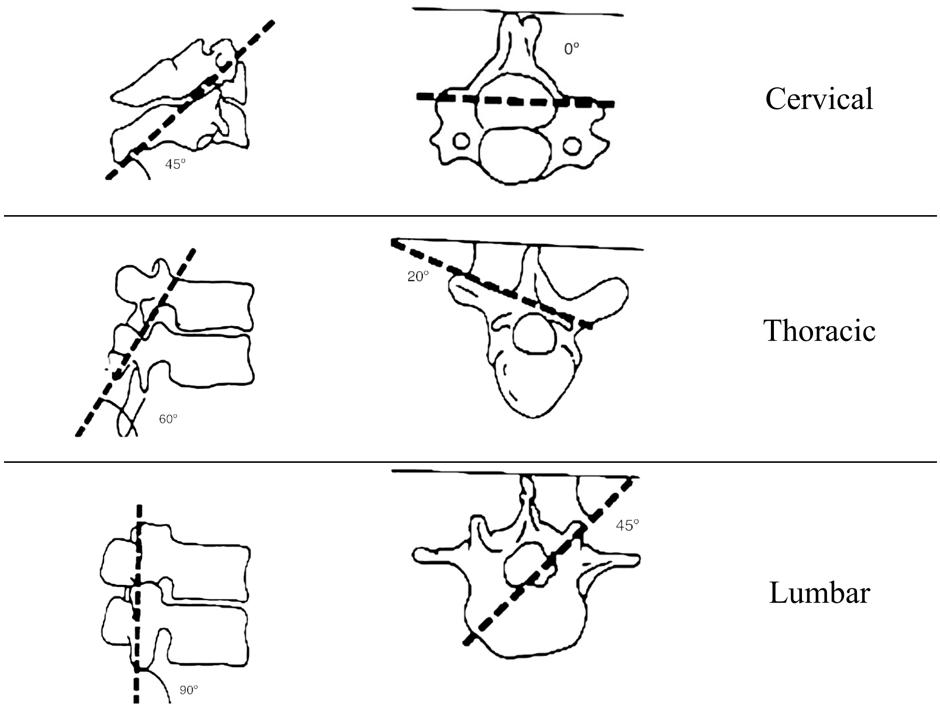

Figure 2.19 Facet Joints Orientation[38]

2.9.2 Thoracic Spine

The thoracic spine appears to be a rigid structure when it is compared with the ROM of the cervical or the lumbar spine. As well as the other regions of the spine, the vertebrae and the intervertebral disc in this part of the body increase in size from the top to bottom, affecting the ROM on the different anatomical planes.

As the anatomy of the upper thoracic vertebras resemble the cervical bones' structure the rotational movement of these joints present a range of motion of about 9º which decreases down to 2º in the lower part of this region. In contrast to the flexion and extension movements the upper part of the thoracic spine, that presents a ROM of 4º, is less flexible than the joints near the lumbar spine that increase the movement to about 12º at the T12-L1 joint.

2.9.3 Lumbar Spine

As this section of the spine is the area that carries the highest loads of the vertebral column, the vertebras and the intervertebral disc are the biggest in size of the whole lumbar spine. This characteristic allows a wider ROM in the sagittal plane and in the frontal plane, which means a ROM of 12 to up to 17º for the flexion and the extension movements and a mobility of about 6 to 8º for the lateral bending motion.

Another characteristic of these vertebrae of this part of the body is that the angle of the facet joints is nearly 90º as shown in the Figure 3.2. This characteristic affects the rotation of these vertebrae limiting the ROM between 1 and 2º for all the joints of the lumbar spine.

The next table shows the most representative values for the rotatory ROMs of the spine in the traditional planes of motion.

Table 2.1 Rotatory ranges of motion at different levels of the spine [23]

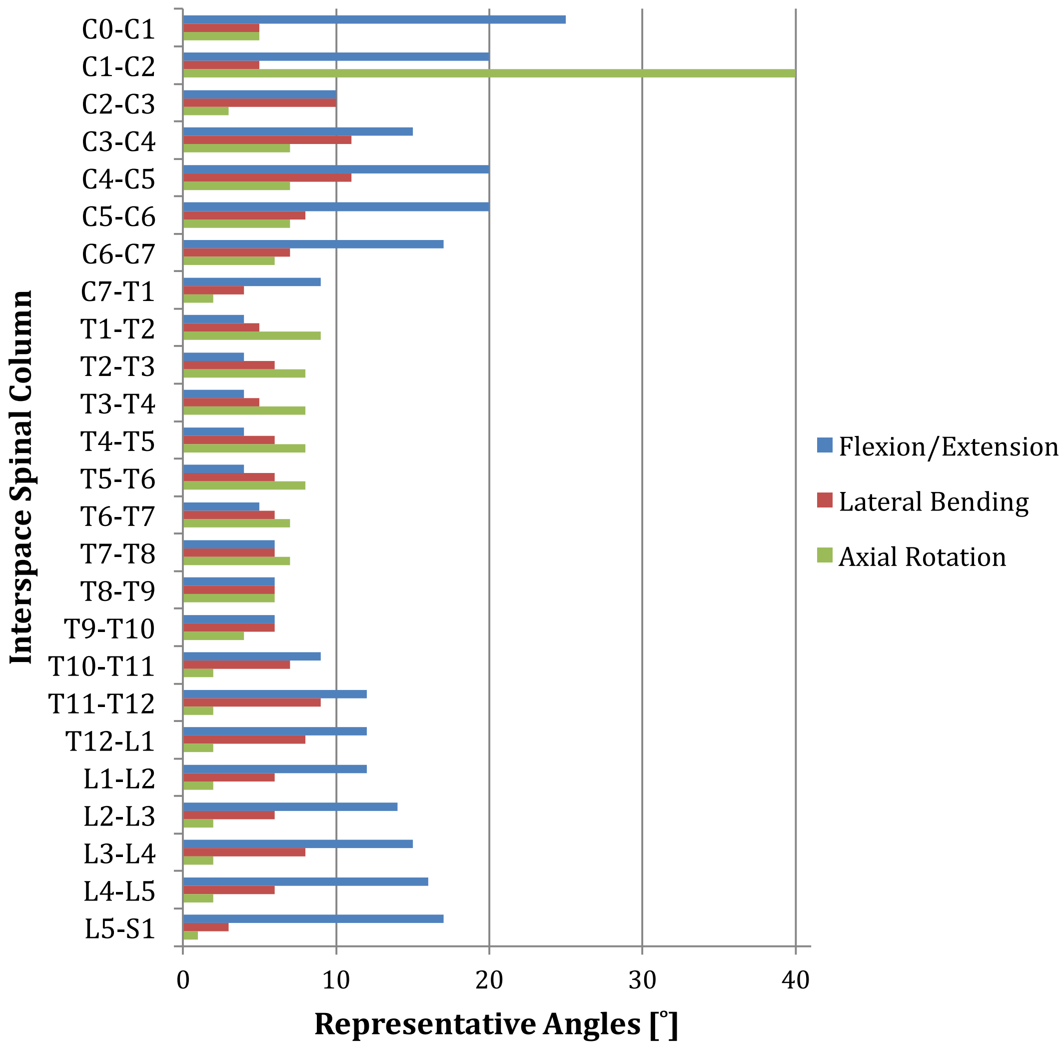

Chapter III – Lumbar Intervertebral Disc Disorders

3.1 Introduction

Low back pain (LBP) is a common term used to describe discomfort or soreness in the lumbosacral region. Research has determined that 60% to 90% of the adult population will be affected by this problem at some point in their life. [61, 62] However, as Anderson [63] pointed out, most patients with this kind of problem make a fast recovery without any functional consequences.

Although low back pain is a frequent problem, often the exact cause of the pain cannot be identified. It is important to state that low back pain is not a disease but an indication of alterations in the structure of the spine.[64]

Although the most common cause of LBP is a strain of the muscles or sprain of the ligaments surrounding the spine, LBP can also be caused by other disorders such as, spinal stenosis, herniation of the intervertebral disc, kyphosis, scoliosis, trauma, and various additional circumstances created by a degenerative spinal condition.

This chapter will describe how intervertebral disc disorders affect the lumbosacral spine, the instrumentation and surgical procedures used to alleviate pain and stabilize the affected, damaged segment and complications that can occur after the surgical procedures.

3.2 Intervertebral Disc Disorders

Intervertebral Disc Disorders refers to a group of circumstances that affect the normal structure or function of the lumbar intervertebral discs. As opposed to the degeneration affecting other joints like the knee or the hip, which are not always visible on CT-Scans or Magnetic Resonance images, a proportion of the population will present some evidence of intervertebral disc degeneration at some point in their lives.[65, 66]

3.2.1 Degenerative Disc Disease

The term Degenerative Disc Disease (DDD) refers to all the structural failures, tissue weakening and degenerative changes resulting from ageing, poor nutrition, genetic factors, trauma or heavy lifting that affect the intervertebral discs. This disease typically begins to have an effect on people when they are in their late 20s and according to Powell *et al.* [67], the disease is present in one third of the healthy population between 21 and 40 years old.

Because of the loss of water content, this spinal condition affects the mechanical function of the spine creating instability of the segments altering the loads, stress distribution and reducing the space between two adjacent vertebrae as seen in Figure 3.1. These changes can also affect the ligaments in the injured area, damage the intervertebral end plates and reduce the ROM in flexion-extension and lateral bending.

Studies suggest that repetitive loading affects and promotes the degeneration of the intervertebral discs. For this reason, the L4/5 and L5/S1 discs situated in the region that bears the major stresses in the lumbar spine are the most common discs that present degenerative conditions. [68]

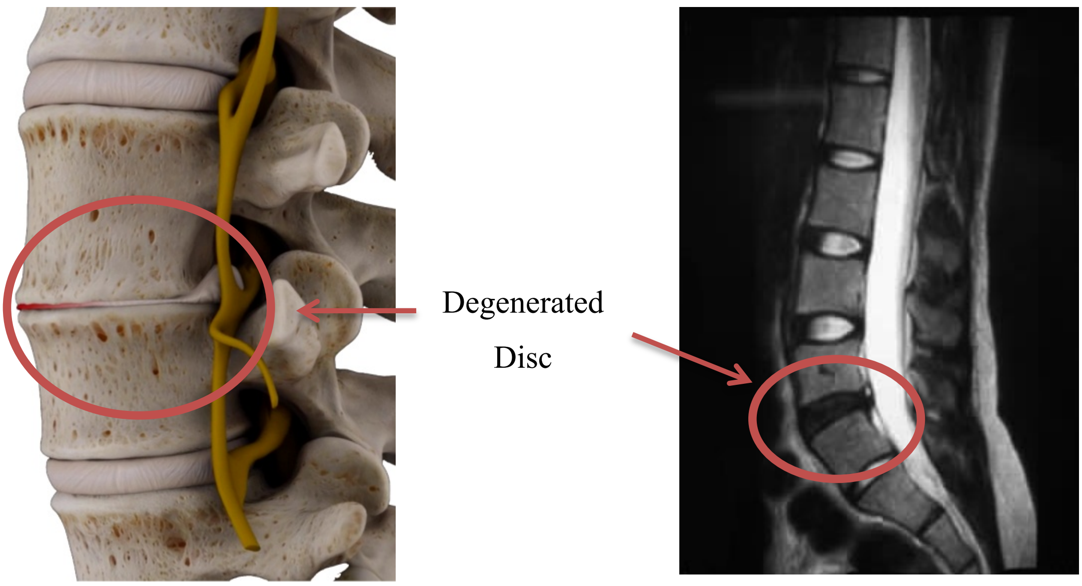

Figure 3.1 Degenerative Disc Disease Explain Figure[28]

The location of the spinal cord and the many nerve endings surrounding the spine make it difficult to define a specific symptom for the degenerative spine. The symptoms can vary from limited motion or pain in the spine to loss of sensitivity in the legs and toes or in some cases sexual dysfunction.

Most patients with this disorder can be managed with a non-operative treatment that consists of medication to manage the pain and physical therapy to restore the normal function of the lumbar spine. However, when there are severe structural changes or the pain is recurrent, despite the medication, an operative treatment is required. For cases of degenerative disc disease associated with severe structural changes, spinal fusion is the most common surgical technique used to alleviate pain and restore stability in the damaged segment.

3.2.2 Herniated Intervertebral Disc

An intervertebral disc is herniated when its nucleus pulposus, annulus fibrosus or the cartilage endplates expand beyond the margins of the adjacent vertebral bodies. This condition typically occurs as a result of ageing due to the degeneration of the matrix of the annulus fibrosus, affecting mainly individuals between 30 and 50 years old and primarily the lumbar spine at the L4/5 and the L5/S1 levels.[69]

Intervertebral disc herniation is the main reason for which spinal surgery is performed. The main symptom of this disorder is radicular pain, which is a particular type of pain that radiates into the lower limbs due to the mechanical deformation or compression of the nerve root, however this disorder can also present bladder and bowel dysfunction and low back pain.

Lumbar disc herniation can be classified according to the resulting structural damage, namely protrusions, extrusion and sequestrations, as illustrated in Figure 3.2. A protruded intervertebral disc is when the disc widens beyond its limits but the outer layers of the annulus fibrosus remain intact maintaining the nucleus pulposus inside the annulus fibrosus matrix. A disc extrusion occurs when the nucleus of the intervertebral disc expands beyond the layers of the annulus fibrosus, rupturing the fibre layers. A disc sequestration is when a part of the nucleus pulposus, having penetrated the annulus layers, is then separated from the structure detaching itself totally from the intervertebral disc.[70]

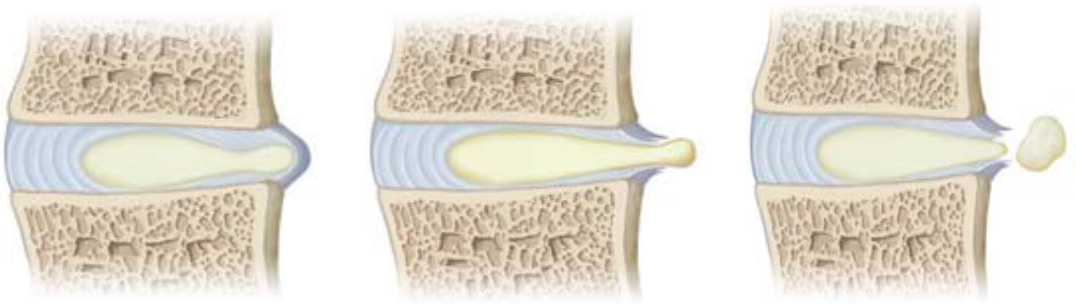

a) b) c)

Figure 3.2 a) Protruded Disc b) Extruded Disc c) Sequestered Disc[71]

There are two types of procedures for a herniated disc, a conservative and an operative treatment. The conservative treatment consists of rest, analgesic medication and physiotherapy while the operative procedure consists of the decompression of the neural canal or the removal of the damaged part of the intervertebral disc also called Discectomy. Historically, these treatments have excellent outcomes relieving the pain of the patients, who can regain their daily activities, however in some cases when the herniation of the intervertebral disc is recurrent, lumbar fusion surgery is the optimal solution to restore the stability of the lumbar spine.[72, 73]

3.2.3 Spondylolisthesis

In the spine, when a vertebra has slipped forward over another the condition is called Spondylolisthesis, as shown in Figure 3.3. This condition mainly affects individuals over 35 years old and can be classified into five different categories. These categories are: *Congenital Spondylolisthesis*, meaning that this condition is present from birth being the result of incorrect bone formation; *Isthmic Spondylolisthesis* caused by defects or breakage of the vertebra as a result of small stresses; *Degenerative Spondilolysthesis* caused by the degeneration and weakening of the intervertebral disc; *Traumatic Spondylolisthesis* that as the names implies is generated by an injury that causes the movement of the vertebra; and *Pathological Spondylolisthesis* meaning that the vertebra was affected by a disease such as a tumour.[74, 75]

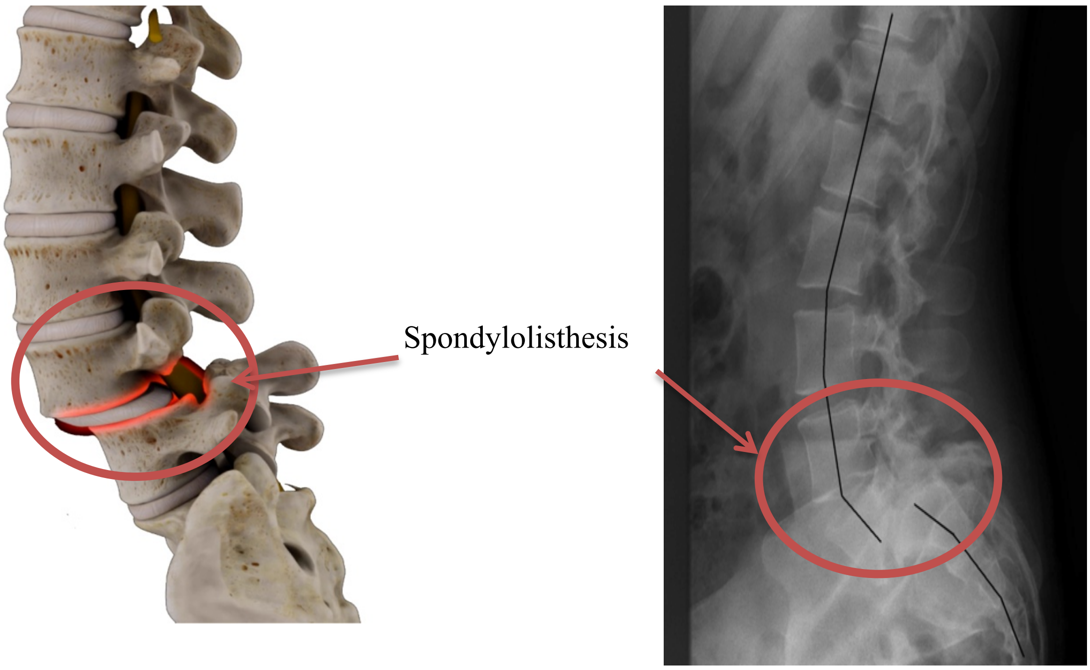

Figure 3.3 Spondylolisthesic Spine[28]

Of the five categories, degenerative spondylolisthesis is the most common cause of degenerative disc disorder in the lumbar spine. The clinical presentation for this kind of injury is mainly pain in the lower back, however this disease is also associated with leg pain and bladder or bowel dysfunction.

Depending on the percentage of anterior slippage of a vertebra from its correct position this condition can be divided into four grades. Grade I corresponds to the first 25% of slippage of the vertebra, Grade II is from 26-50%, Grade III from 51-75% and Grade IV corresponds to between 75% and complete slippage of the vertebra (100%)

The first step in treating this condition, depending of the grade of displacement, is conservative treatment, which includes resting, taking medication to reduce pain, and the use of a brace to reduce motion in the affected area while the patient improves the strength and mobility of the damaged spine. If the conservative treatment fails to improve the patient's condition, non-conservative treatment will be necessary to alleviate the pain and correct the vertebra position.

The options for surgical treatment depend on the morphology of the affected area as well as the grade of slippage of the vertebrae. Operative treatment for this problem focuses in relieving the pain of the patient and restoring lumbar stability. While different surgical techniques are available to treat lumbar spondylolisthesis, lumbar interbody fusion is one of the most commonly employed and reliable procedures used to correct the damaged lumbar spine.

3.3 Spinal Instrumentation for Spinal Fusion

When the vertebral column suffers a deformation or a fracture as a result of disease or trauma, spinal instrumentation is needed to stabilize the spine. In recent years as a result of the development of new techniques and new materials, the number of choices for spinal instrumentation has substantially increased.

Every region of the spine has particular anatomical and biomechanical properties and so, for a successful outcome, it is necessary to choose the appropriate implant and technique that best fits the individual characteristics and the surgeon's preferences.

The principal objectives of internal fixation in a damaged spine are:

- To support the vertebral column when the vertebrae are damaged in order to reduce the rehabilitation time providing stability to the whole damaged structure.
- To prevent or correct the form and vertebral alignment resulting from spinal deformities.
- To reduce or eliminate the pain attributable to the disruption of the spinal cord and to prevent any further damage caused by the instability of the spine.
- To reduce or diminish the movement between vertebrae in order to promote bone fusion.

Surgeons and biomedical engineers need to understand the factors that contribute to successful procedures with positive patient outcomes. Major factors in achieving a successful outcome are the function of the fixation devices and their influence on the biomechanics of the vertebral column.

Confirming the approach and the instrumentation is a key decision made during preoperative planning. It requires an understanding of the anatomy, and the indications and limitations of each approach in order to achieve the desired surgical result. This study will focus on the most common surgical approach for intervention in the lumbar region, the posterior approach. This procedure is used when a posterior decompression is needed in addition to the stabilization of the damaged segment of the spine. An advantage of this approach is the relative ease of access to the spine, but as in all surgical interventions, the decision to use this approach depends on the clinical problem, the anatomic location, and the surgeon's preference.

In this investigation no vertebral elements of the spine will be replaced, rather they will be stabilized to allow vertebral fusion, which generally occurs within four or five months after surgery

Surgeons use many different types of instrumentation in order to achieve correct stabilization of a damaged segment by eliminating motion and hence promoting correct bone fusion between two vertebrae. There are three principal systems of posterior implants that are used to stabilize the spine namely:

- Rods with the implementation of Pedicle Screws,
- The use of Translaminar or facet screws, and
- The application of distraction frames typically attached via pedicle-screws, hooks, or wires.

Each one of these methods has its own characteristics and advantages, and they may be combined with other techniques in order to achieve a better result or to treat different pathologies. This study will assess the most common devices used in spinal surgery, pedicle screws, used alone or with the addition of intervertebral body fusion cages.[76]

3.3.1 Pedicle Screws and Rods

These devices have been used since the late 1980s. The system is formed by screws inserted at each side of the vertebra through the pedicles into the central part of the vertebral body and by rods that can be of different diameters and lengths (Figure 3.4). The rods are used to align and link the screws to restore the height of the degenerated intervertebral disc, to correct the position of the vertebrae and to achieve a rigid stabilization between the damaged segments.[77]

a) Screws and Rods

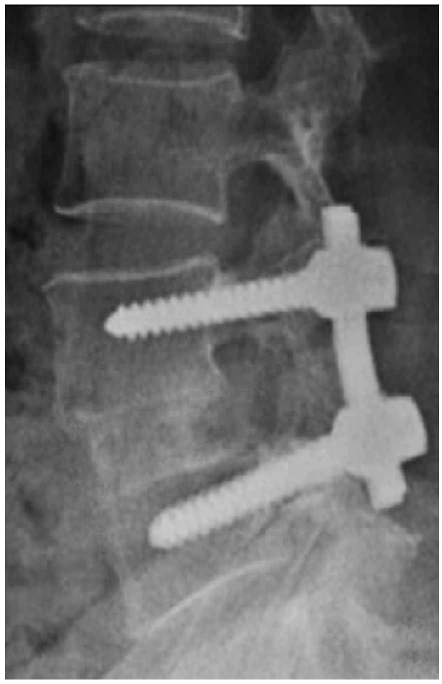

b) Screws inserted at the vertebrae[78]

Figure 3.4 Pedicle screw assembly

These devices, despite being largely successful and the most common method of achieving a correct fusion of the spine, can produce problems at the site of implantation. For example, problems may arise as a result of poor bone quality, that can affect the adequate fixation of the screws. In addition, breakage of the screws and rods may occur (Figure 3.5), or a loading situation may be encountered that exceeds the load-bearing capacity of the implant.

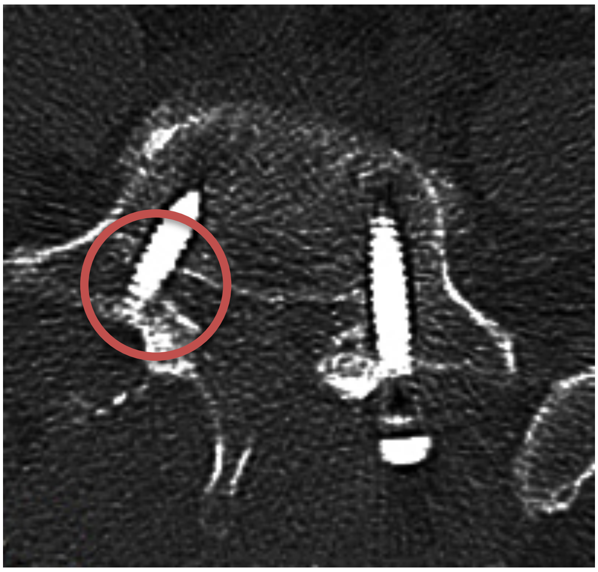

a) Pedicle Screws inserted

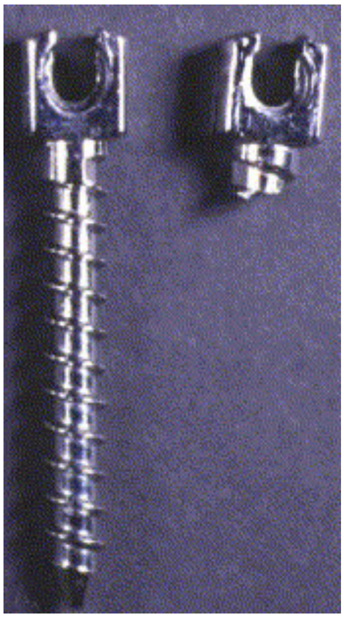

b) Broken Screws

Figure 3.5 Broken pedicle screws[79]

In addition, problems may arise as a result of human error such as poor surgical technique, use of an inadequate diameter or length of screw, fracture of the pedicle during the surgery, an infection or a nerve injury that can occur when the decompression process takes place. [80-82]

The pedicle screws and rods may be made either of stainless steel or titanium alloy (Ti6Al4V), but of the two, titanium alloy is the more frequently used in the field because it allows for the use of better magnetic resonance images, has higher resistance to corrosion and fatigue, and has superior biocompatibility. The diameters of the screws can vary from 4.0mm to 7.0mm depending on the anatomy of the vertebra, the pedicle shape or the segment of the spine.

Once the damaged segment is stabilized and bone fusion is achieved, the fixation devices are no longer required for correct function of the spine. However, the implants are not removed unless the pedicle screws or the linking rods cause pain or discomfort to the patient.

3.3.2 Interbody Cages

An interbody cage is a medical device that is inserted between two vertebrae after intervertebral disc removal. This instrument serves as a bridge between the two vertebral bodies and is used to maintain the restored height after the decompression of the degenerated intervertebral disc while improving the stability of the damaged section and reducing screw or rod failures (Figure 3.6).

Figure 3.6 Pedicle screw and interbody cages assembly[83]

These devices are usually rectangular boxes or cylinders but may have a different form depending on the damaged section of the spine or the surgical procedure. As a consequence of the curvature of the spine, these cages are designed with different angles with respect to the sagittal plane to best fit the gap left by the degenerated intervertebral disc. This investigation will focus on the rectangular shaped cages with an angle of 0º and an angle of 4º, as shown in Figure 3.7.

0° Cages 4° Cages

Figure 3.7 Intervertebral Cages

These Interbody fusion cages are usually made from Titanium alloy or from a medical grade thermoplastic polymer, Polyether Ether Ketone, commonly known as PEEK. Studies have shown that the cages made of these two materials provide a stable rigid fixation when they are used in conjunction with posterior instrumentation such as pedicle screws and rods [84, 85]. However, some other studies have indicated disadvantages with the use of titanium versus the use of PEEK interbody cages [86, 87].

One disadvantage of using the titanium devices is the unreliable diagnostic assessment of bone growth. The use of this material limits visualization of soft tissue structures like the intervertebral discs on CT Scans or on MRIs and affects the surgeon’s ability to give a correct evaluation of the fusion between the vertebrae because of the radiolucency of titanium. Previous studies have shown that PEEK interbody cages represent a better choice biomechanically in comparison with the titanium devices because the stiffness of the material is closer to that of cortical bone [84, 87]. Although this phenomenon is not fully understood, the material of the intervertebral cage can promote osteopenia or stress shielding, which can cause migration or instability of the implant that may result in a non-fusion of the damaged segment. This study will evaluate PEEK cages for the reason described above and because their use is common practice.

A key element of these cages is that regardless of the material used or the shape of the cages, all these devices are filled with bone graft material to promote arthrodesis. This means that the material inserted in these cages promotes bone growth between the two vertebral bodies achieving a joint ossification improving and accelerating the fusion performance.

3.3.3 Bone Graft

Bone graft refers to the implanted bone used to promote bone growth between adjacent bone segments or across a fracture with the objective of repairing the bone or fusing two or more bones in order to regain stability in a damaged area. The fusion of bone after a fracture is often a natural process, however, when this process is surgically induced, like the fusion of two vertebrae, it is called arthrodesis.

Depending on where the bone graft is obtained, the implant tissue can be divided into 5 categories, namely: autograft, allograft, xenograft, synthetic materials and a combination of these four. [88]

Autograft or autologous bone graft uses tissue obtained from the host, usually taken from the iliac crest or spinal processes, and implanted in the same individual (see Figure 3.8). This type of bone graft is the best possible graft because it supports all the three physiological processes required. Autografts present perfect biocompatibility and are the most common bone grafts used in surgical procedures in the lumbar spine.

Allograft refers to the implanted bone tissue being collected from a donor. This tissue is commonly collected from the iliac crest, fibula or a rib. The disadvantage of this kind of bone graft is that, because tissue is obtained from a donor, it has to go through a process of sterilization, decontamination, and preservation prior to grafting, which can lead to deterioration of the mechanical properties of the graft, causing it to lose up to 50% of its ultimate compressive strength. Although this kind of transplant is the second most common tissue transplant after blood, disease transfer is one possible additional disadvantage associated with allografts.

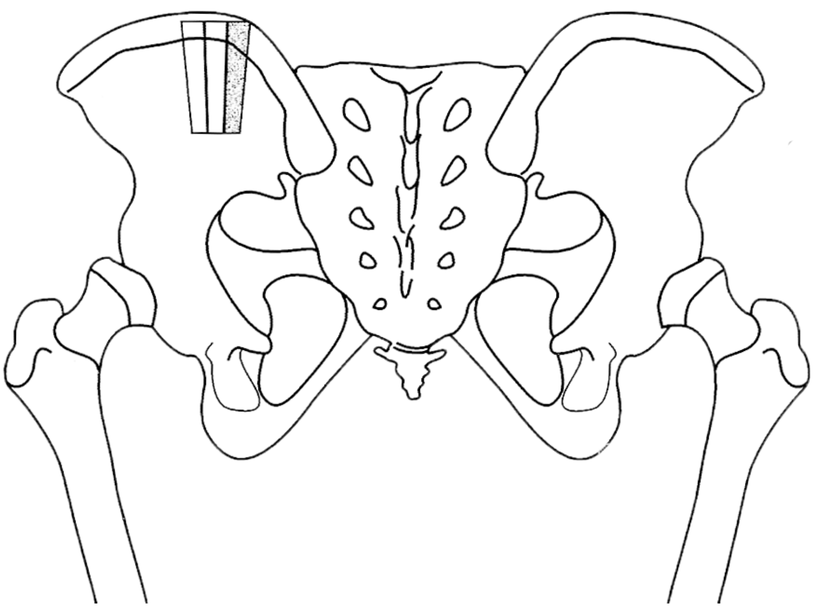

Figure 3.8 Bone Graft harvesting from Iliac Crest[89]

The Xenograft category refers to the transplantation of bone tissue from one species into a different species. As for the allograft category, this bone graft requires an aggressive process of sterilization that has a detrimental effect on the physiological processes, possibly eliminating the osteoinductive process. The most commonly used animal graft is from bovine tissue that has been reported to be biocompatible with human bone tissue.

Each of these categories has its advantages and disadvantages. However every type of tissue implant needs to support three physiological processes in order to obtain a functional bone graft. The processes involved are:

Osteogenesis, that is the capacity of the implanted material to form new bone; Osteoinduction, which refers to the ability of undefined cells, hosted in the implanted tissue, to promote new bone; and Osteconduction, which refers to the capability of the bone graft material to support the attachment of new bone cells.

Synthetic graft materials are composed of different ceramics such as hydroxyapatite, tricalcium phosphate, calcium carbonate, bovine collagen or a mixture of these elements (Figure 3.9). One of the advantages of these materials is that they do not transmit any disease. Although these materials are available in large quantities, they do not have osteogenic or oesteoinductive properties, which has a major detrimental effect on the strength of the new tissue, which can lead to a failure of the bone fusion.

a)

b)

Figure 3.9 Bone graft inserted into interbody cages [90]

The graft material is inserted into the interbody cages to promote bone growth and achieve correct bone fusion. The next section will explain the most common stabilization techniques, the posterior fusion procedures and how they affect the lumbar spine.

3.4 Stabilization Techniques and Posterior Fusion Procedures

Lumbar spinal fusion is one of the most common surgical procedures used to alleviate pain and rectify the position of the vertebrae in the lumbar spine.[91, 92] This surgical procedure consists of fixation between the vertebrae adjacent to the damaged disc, or the removal of the intervertebral disc in order to insert one or two interbody cages to restore the height of the inter-vertebral space, or to correct the position of the slipped vertebra. As the name indicates, the objective of lumbar spinal fusion is to fuse two vertebrae in order to restrict the motion of the segments involved either to reduce further degeneration of the intervertebral disc or to relieve pain as a result of nerve compression. [93, 94]

Depending on the pathology and the surgeon's preferred technique, the fusion procedure may be carried out using different approaches such as Posterolaterlal Fusion (PLF), Anterior Lumbar Interbody Fusion (ALIF), Posterior Lumbar Interbody Fusion (PLIF), Transforaminal Lumbar Interbody Fusion (TLIF) or Extreme Lateral Interbody Fusion (XLIF). It is important to emphasize that all the devices used in these procedures do not replace any vertebra or function of the intervertebral disc. The main function of the devices is to stabilize the damaged section during the fusion of the spine, which can take up to four or five months. [95]

3.4.1 Posterolateral Fusion (PLF)

Spinal fusion was first reported by Cloward in 1952 [96]. In this report Cloward describes the fusion of two adjacent vertebrae using cadaveric bone and emphasizes the dangers of infection of this procedure. In 1953 Watkins introduced the use of screws and bone grafts to provide a better fixation of the vertebras [97]. Since then, reports of spinal fusion have introduced more elements and devices to improve the outcome of this approach. [96-99]

Under general anaesthesia, the patient is usually placed in the prone position, because the approach is from the posterior aspect of the patient. As shown in Figure 3.10a, a midline incision is made so the surgeon has access to the damaged area. With the posterior elements exposed (Figure 3.10b), the surgeon retracts all the muscles in the area in order to decompress the damaged intervertebral disc.[94]

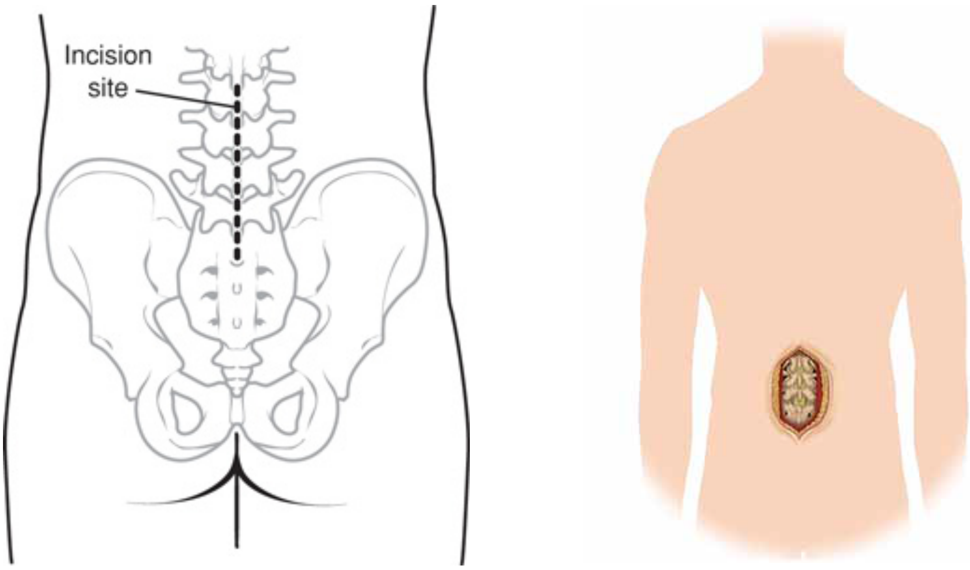

a) b)

Figure 3.10 a) Incision at the lower back b) Incision created to access the damaged spine

In common with all stabilizing techniques, posterolateral fusion (PLF) eliminates the motion of the damaged area but with the difference that this approach leaves the intervertebral disc untouched (Figure 3.11). Although, for this particular surgery, no instrumentation is required, several studies have reported that adding different devices to fix the vertebrae, like wires, hooks, or pedicular screws increases the fusion rate, and reduces the recovery time.[95, 100]

When compared with either a non-operative treatment or lumbar decompression alone, several studies have demonstrated that PLF achieves more desirable results.

However, other studies indicate that this kind of surgery, although it permits adequate load sharing in the anterior part of the vertebra, it does not provide the level of stability of other methods such as Posterior Lumbar Interbody Fusion (PLIF) with additional instrumentation.[94, 101]

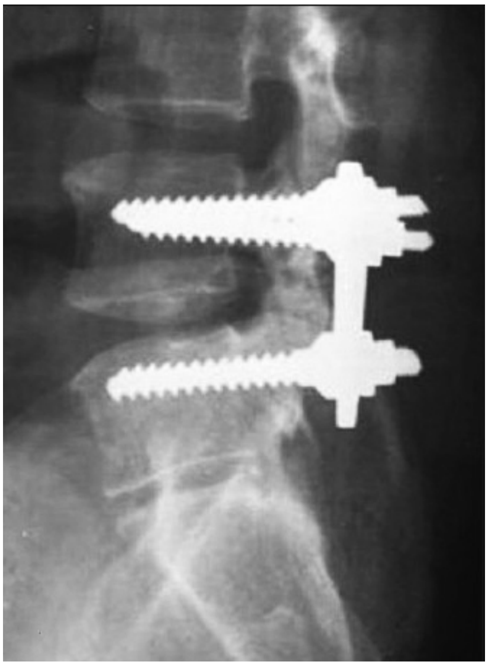

Figure 3.11 Posterolateral Fusion at L4-5 Level [102]

3.4.2 Posterior Lumbar Interbody Fusion (PLIF)

As its names indicate, PLIF is a method in which access to the damaged area of the spine is obtained via the posterior aspect of the body. This method was first introduced by Cloward in 1963 and consists of the total removal of the damaged intervertebral disc and the insertion of interbody fusion cages that support the vertebrae and restore the height of the intervertebral space (see Figure 3.12). [103]

The interbody cages are filled with bone graft material, which grows around these devices to create a solid fixation between the affected vertebrae. Correct fusion of the spine can take up to four or five months after the surgery. Consequently, pedicle screws are inserted bilaterally to restrict any movement of the functional spinal unit in order to promote correct bone graft growth. [95]

Because of the insertion of the interbody cages and the posterior instrumentation, this method provides a more rigid fixation than PLF achieving complete fusion in up to 90% of cases. The high rate of complete fusion is partly a consequence of the vascularity of the region. Using PLIF, the blood supply between the bony elements increases, improving the bone graft growth, which increases the desired fixation.[100]

Figure 3.12 Posterior Lumbar Interbody Fusion at L4-5[83]

However, PLIF has the disadvantage that the duration of the surgery is prolonged because of the difficulty involved in the surgery. Because of the posterior approach the surgeon has to operate near the spinal cord, and so this surgery can be associated with problems such as cerebrospinal fluid leak, paraplegia, and nerve root injury among others. Although this method provides a more rigid fixation that improves the fusion rate, these devises can also result in the collapse of the vertebra over the interbody cages or the migration of these devices or the bone graft.

Because PLF and PLIF are the most common techniques used to stabilize the lumbar spine and are preferred by many surgeons, this investigation will evaluate only PLF and PLIF using two PEEK interbody cages.[94]

3.5 Complications after Surgery

As with any other surgical intervention, spinal surgery can result in the presentation of complications following the intervention. The most common problems for this kind of surgery are infections, dural tears, pseudoarthrosis, graft migration, neurologic injury or implant related complications.

Of these complications, neurologic injury is the most serious consequence that can occur due to spinal fusion surgery. As explained before, for the Posterolateral Fusion and for the Posterior Lumbar Interbody Fusion, the surgeon gains access from the back of the patient retracting the muscles and nerve roots that surround the damaged area. Because of this, blood flow to the nerve roots can be reduced which can cause the malfunction of these nerves. Although this problem is not common, studies have reported the rate of this complication as being as high as 7%. [104]

Hardware complications are rare for this type of surgery; however, various studies indicate that when problems related to the devices occur, usually the patient needs to be subjected to revision surgery. The most common implant related problems are the breakage of the pedicular screws and the migration or the subsidence of the interbody cages.[105]

The migration of the cages refers to the unwanted movement of the implant from its initial position (Figure 3.13). This problem can occur due to instability across the fusion segment, the loss off contact between the interbody cage and the vertebral end plate or due to the wrong size or location of the cage. This problem can be eliminated with careful preparation for the surgery, and selecting the correct size of the interbody cages. Also some studies suggest that the use of posterior devices such as pedicle screws can be used to prevent this problem [106]

Subsidence of an interbody cage refers to the insertion of a cage into the vertebral body. This problem can lead to instability of the segment producing the failure of the fusion. This problem is commonly caused by poor bone quality although the material of the cage and the design of this device can also be factors that generate this condition. Other studies suggest that changes in the shape of the interbody cages could improve the outcome of this problem. However, the consequences of proposed changes to interbody cage shape are not fully understood. [107-109]

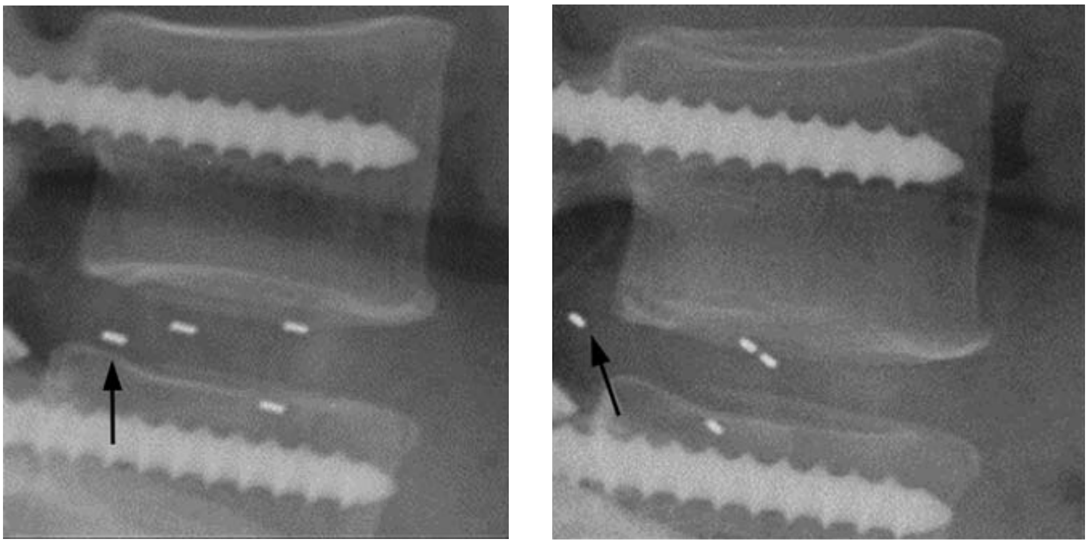

a) b)

Figure 3.13 Initial and final position of an Interbody Fusion cage after an unwanted implant migration[104]

As mentioned before, pedicle screw breakage can be caused due to human errors like a poor surgical technique or inadequate election of the diameter or length of the screw. The breakage of the screws is usually seen in multilevel fusions or related to the absence of anterior devices such as PEEK interbody cages, causing elevated stress in the screws. This problem is usually related to a loss of stabilization causing a failure of fusion and even possible neurological damage. The breakage of a screw often requires surgical revision and the removal of the broken screw [110]

The complications mentioned above are problems that are caused directly from the interaction of the devices and the bone or soft tissue in the spine in the damaged area. However, some studies suggest that the insertion of mechanical devices can also affect the neighbouring areas developing further disc degeneration. This process of further degeneration or the development of an abnormal process next to a spinal fusion segment is called Adjacent Segment Disc Disease.

3.5.1 Adjacent Segment Disc Disease

Adjacent Segment Disc Disease refers to the manifestation of degenerative conditions at the neighbouring joints where implants were inserted or in the case of this study, adjacent to where intervertebral fusion was achieved. While this degeneration could be the result of aging as diverse studies suggest, other investigations have shown that almost 30% of patients that undergo fusion spinal surgery develop this degenerative condition. [111-113]

The stiffness of the implants used for the surgeries described above, directly affects the amount of load transmitted to the other levels next to the damaged area. This condition affects the biomechanics of the spine changing the ROM, the intradiscal pressure or the stresses in the contiguous elements during the different motions of the spine. Despite this, it is not entirely clear whether these surgical procedures provoke degeneration of the neighbouring elements, instead the changes in the biomechanics of the spine could explain the development of Disc Degeneration.[114, 115]

In order to study if the insertion of mechanical devices is a factor that promotes degeneration in the neighbouring segments, several investigations have undertaken follow-up studies of patients with these conditions [112, 116, 117]. These studies reported that more than a third of the patients that had undergone lumbar fusion also developed adjacent segment degeneration. However, in contrast to these results, other studies which evaluated patients that had undergone lumbar fusion against a similar group of patients that preferred a non-surgical treatment found no difference in the rates of adjacent disc degeneration [13, 112]. For these reasons, it is unclear as to whether insertion of Lumbar Interbody Cages or Pedicular Screws has an effect on the adjacent segments.[118]

Figure 3.14 shows an example of degeneration of the superior intervertebral disc adjacent to the surgical site.

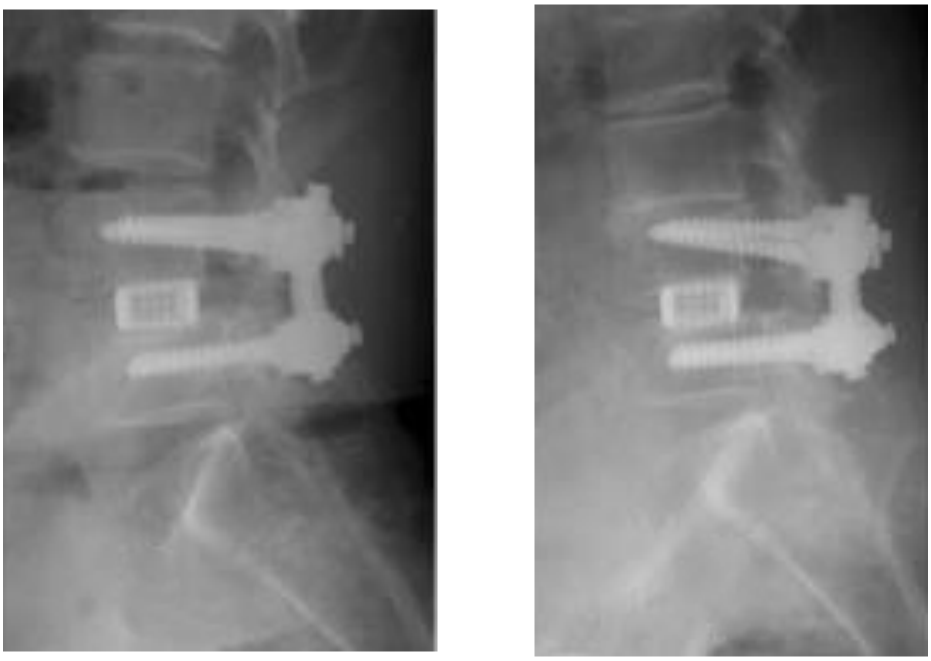

Figure 3.14 Adjacent Lumbar Disc Degeneration after a PLIF surgery at L4-5 [119]

This chapter has explained the most common diseases that affect the intervertebral discs in the lumbar spine causing low back pain and has described the instrumentation used to stabilize or fuse the affected region. This chapter also explained the techniques used in this study to repair the damaged spine describing also the complications of the surgery and the possible problems caused by the insertion of these devices.

The next chapter will present a brief explanation of the different techniques used to create a 3D finite element model of the lumbar spine. Also the next chapter will describe the most used techniques to measure the range of motion of the lumbar spine for *in-vivo* investigations.

Chapter IV: Finite Element and Motion Analyses of the Lumbar Spine – Literature Review

4.1 Introduction to the Finite Element Method

The finite element method, also known as finite element analysis, is a numerical method used to obtain approximate solutions to equations that describe the behaviour of various engineering problems in diverse areas including solid mechanics, fluid mechanics, electromagnetics or in this case biomechanics.

The finite element method involves partitioning of the components of a complex problem into a finite set of simple elements. These elements, that have associated material and structural properties defined, are formed and connected by nodes. These nodes and elements are rearranged into a mesh that represents the physical shape of the geometry of the problem. Consideration of this mesh results in a set of algebraic matrix equations that are solved at the nodes.[120]

The first practical use of this method took place in the aircraft industry in the early 1950s when Turner *et. al*. presented their new method to model the dynamic stiffness properties and displacements of a structure [121]. The first report of the use of this method in the biomechanical field was in 1972, when Brekelmans *et al.* investigated the stress affecting a human femur under the action of physiological loads [122]. Since then, rapid improvements in computational processing and greater availability of robust and accurate modelling software have permitted more complex models to be developed.

To solve a finite element stress analysis for a linear elastic material, Hooke's law is used to relate the deformation of an elastic material and the stress applied to it.

$$F = kx \tag{1}$$

Where F is the force, k is the constant factor (stiffness) and x is the displacement.

As mentioned previously, application of the finite element method to the mesh formed by the nodes results in an algebraic matrix that is solved for the field variables at the nodes. Since each node of this matrix has a displacement, the same number of equations as nodes in the mesh is created resulting in a system of linear algebraic equations expressed as

$$\{F\} = [k]\{u\} \tag{2}$$

Where {F} is the applied force vector, [k] is the stiffness matrix and {u} is the displacement vector to be determined. Once the displacements [u] are known, then the stresses and strains can be determined using Young's modulus

$$E = \frac{\sigma}{\varepsilon} \tag{3}$$

Where E is Young's modulus, σ is the stress and ε is the strain.

To solve this system of equation the finite element analysis software, Abaqus/CAE 6.10© (Dassault Systèmes), used for the analysis described in this thesis, uses Newton's method. This method uses a series of small increments in order to find a better approximation to the solution. [123]

4.2 Application of the Finite Element Method to the Spine Research

One of the first attempts to study the spine using finite element analysis was undertaken by Belytschko *et al.*[124]. This study investigated the material constants and the stress distributions that affect the lumbar spine, finding a good correlation between the model and their experimental analysis. In recent years the finite element analysis has been used to understand the behaviour of the healthy and the injured spine as well as has helped to explain the performance of implants or fixation systems used to stabilize the damaged lumbar spine.

As computational methods and surgical interventions continued to grow, further investigations are needed to provide improved approximations to the real function and motion of the spine. For this reason, in order to create a computational model that correctly represents the behaviour of the lumbar spine is necessary to understand how other studies had simulated the components that conform this part of the body.

4.2.1 Vertebrae Models

The principal characteristics to recreate an appropriate model of a vertebra are the geometry and the material properties. Although some studies use generic geometries that represent the average dimensions of a vertebra [125-128], the most used approach to create the geometry of this part of the spine is the use of Computed Tomography (CT) [50]. This imaging method allows the extraction of the surface geometry and in some cases can also provide information regarding the bone mineral density, which can be used to assign the material properties to the vertebra. [24]

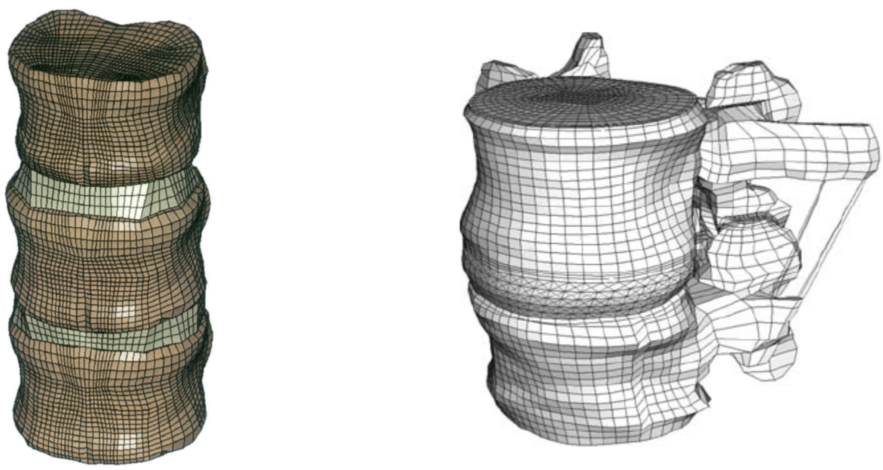

a) b)

Figure 4.1 Different approaches to create the geometry of a vertebrae a) Vertebra created from anatomical generic geometry [126] b) Vertebra created from CT scans[129]

In order to select the proper materials for a vertebra model some studies have use the bone mineral density data obtained from the CT scans as mentioned before. This technique consists in to assign a Young's modulus value to an element based on the brightness of the CT scan image [130, 131]. Other studies oversimplify this structure only considering this structure as a rigid body [132-134], nonetheless the most common method used to assign materials to a finite element analysis of a vertebra is to assign different materials properties to the cortical shell and the trabecular bone. Although the materials properties used to simulate the bone vary depending on the study, the cortical and trabecular are often represented as isotropic, elastic plastic materials.

4.2.2 Intervertebral Discs Models

Due to its complex structure, different methods had been used to recreate the geometry of the intervertebral discs. For instance, as seen with studies of the vertebrae, commercially available models have been used to study the disc structure [126]. In other cases, the shape of the discs has been considered to be axisymmetric to reduce the computational time used to analyse this part of the spine, as show in Figure 4.2 [135, 136]. Other studies have used measurements taken from *in-vitro* studies to recreate the geometry of the intervertebral disc [135, 137]. However, the most used method to recreate the geometry of the intervertebral disc is with the use of CT scans or magnetic resonance imaging (MRI), where the nucleus pulposus and the annulus fibrosus can be clearly identified. [24]

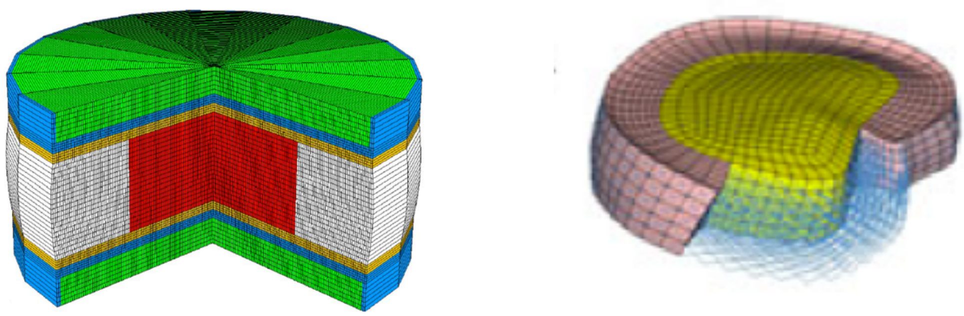

a) b)

Figure 4.2 Different approaches to create the geometry of the intervertebral disc a) Axisymmetric model of an Intervertebral Disc b) Isotropic and incompressible model of an intervertebral disc [135, 138]

To simulate the materials properties for the intervertebral disc some studies have simulated the ground substance of the annulus fibrosus using an anisotropic material formulation, however other studies simulated this part of the intervertebral disc as an isotropic material that contains cable, truss or rebar elements that simulate the fibres that exist around the nucleus pulposus.

As mentioned in Chapter 2, the nucleus pulposus is constituted mostly by water, for this reason this part of the intervertebral disc is often simulated as an incompressible fluid or in some cases as a hyper elastic material.

4.2.3 Ligaments

In most of the research that investigate the behaviour of the lumbar spine, at least seven ligaments are included in the finite element model. These ligaments are the Anterior Longitudinal Ligament (ALL), the Posterior Longitudinal Ligament (PLL), Ligament Flavum (LF), Capsular Ligament (CL), Interspinous Ligament (ISL), Supraspinous Ligament (SSL), Intertransverse Ligament (ITL). When the 5 vertebrae of the lumbar spine are simulated in conjunction with the sacrum or with the pelvic bone two more ligaments are generally added, the Iliolumbar Ligament (ILL) and the Sacroiliac Ligament (SIL).[139-143]

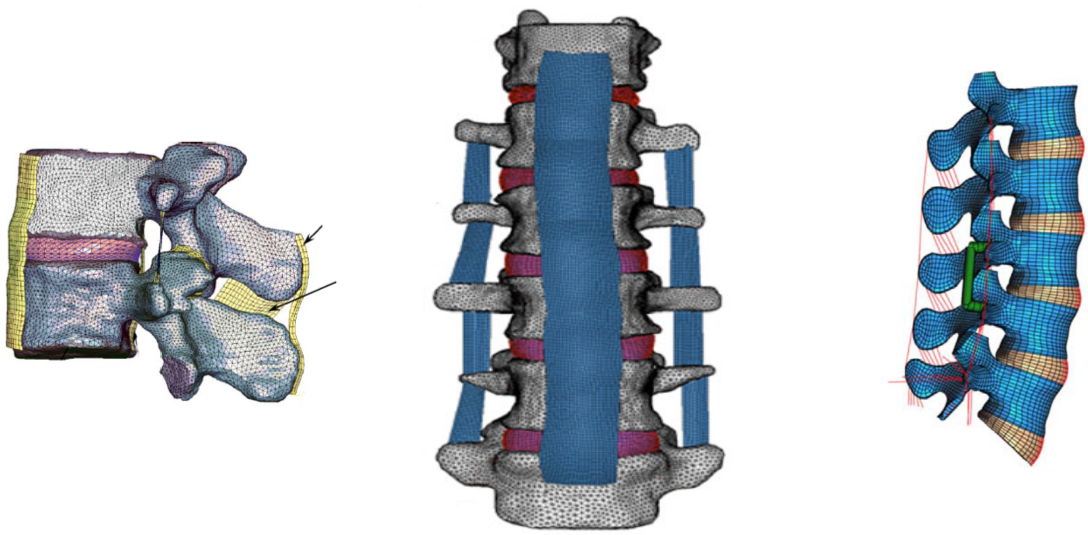

a) b) c)

Figure 4.3 Different approaches to simulate the ligaments in the lumbar spine a) Solid ligaments [144] b) Surface ligaments [145] c) Spring Elements ligaments [146]

Although some studies as El Rich *et al.,* Tsuang *et al.* or Wagnac *et al.* had studied and simulated the ligaments as three dimensional structures or as surface structures, most of the studies that simulate segmental models of the spine reproduce the ligaments as non linear spring elements which only had stiffness characteristics during tension. [129, 144, 145, 147, 148]

4.2.4 Lumbar Segment Models

As explained in Chapter 2, the FSU consisting of two vertebrae, the intervertebral disc and all the connecting ligaments between the bone structures, is the most basic vertebral arrangement to study the biomechanics of the spine. When two or more FSU are connected it is called a segment model. These segment models have been created with the purpose to study the behaviour of large segments of the spine under different scenarios.

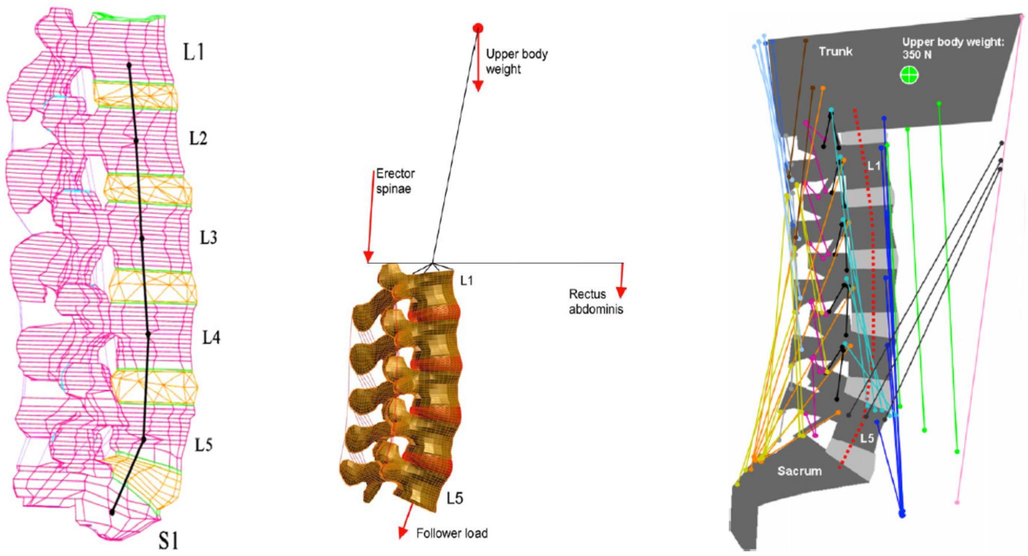

a) b) c)

Figure 4.4 Different loads configuration to reproduce the anatomical motions of the lumbar spine[149-151]

One of the key factors to consider in these segment models is how the loads are applied to simulate the different motions to which the segment is subjected. For the lumbar spine some studies have simulated the standing position by just applying a load to the upper vertebra of the segment model, however some studies have demonstrated that this approach does not simulate the correct behaviour of the lumbar spine. The most common used method to simulate this motion is by applying a follower load that consists of a compressive load that follows the lordotic curve of the lumbar spine. [24, 149, 150]

To simulate the flexion, extension, torsion and lateral bending motions some investigation have applied pure moments to the cranial vertebra, however most of the studies use a combination of the follower load combined with moments applied in the upper vertebra of the segment.

4.2.5 Pathological Models of the Spine

The creation of a segment model of the lumbar spine can also be used to study the biomechanical effects that a disease or a post-surgical scenario could cause to this part of the spine. In these cases, the material properties of the segment or the geometry of the vertebrae or the intervertebral discs are altered to simulate the characteristics of the pathology studied.

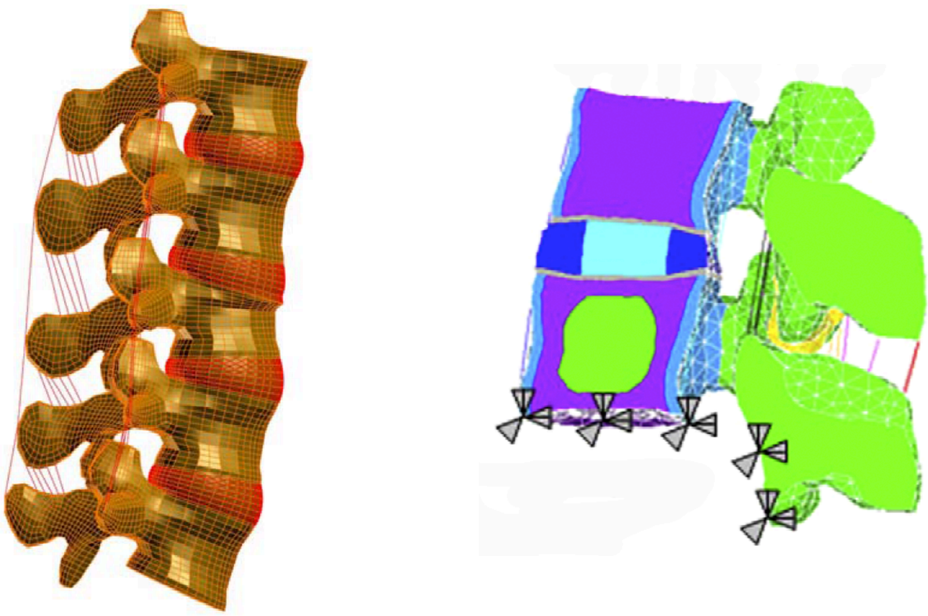

a) b)

Figure 4.5Pathological models simulating osteoporosis and a kyphoplasty treatment. [51, 150]

For example, in separate studies Villagra *et al*., Rohlmann *et al.* and Zhang *et al.* investigated the effects of osteoporosis and bone cement on the vertebral bodies predicting that the presence of bone cement inside the vertebral bodies cause only a minimal increase in the peak von Mises stresses predicted for these structures and the adjacent intervertebral disc. [51, 126, 150]

4.2.6 Modelling of the Devices and Instrumentation used in the Lumbar Spine

As same as the models that reproduce a pathological condition a number of investigations had been performed in order to study the behaviour of the spine when medical devices are inserted. These studies evaluate how the implants contribute to stabilize a damaged segment or how the medical devices implanted alter the adjacent elements to the surgical site. The range of study of these investigations extends from the analysis of the instrumentation devices employed such as the different posterior implants used to fix the vertebrae, the position and design of the intervertebral cages, to the investigation of the biological materials and the effect on the adjacent intervertebral discs and the effect of the implants on the bony elements.

For example, Liu *et al*.[152] studied the impact of the Dynesys screw system and the effect that this device implanted at the L3/4 level caused on the spine, finding a decrease in the ROM at the surgical level and an increase of 10% to 22% in the ROM at the adjacent level. This study also found an increase in the annulus fibrous maximum von Mises stress at the adjacent levels and demonstrated that the Dynesys device cannot restore normal loading to the spine. In another study, Rohlmann *et al*. [146] studied the Dynesys system and a rigid fixation system implanted at the L3/4 level finding small variations in how these two implants affect the spine.

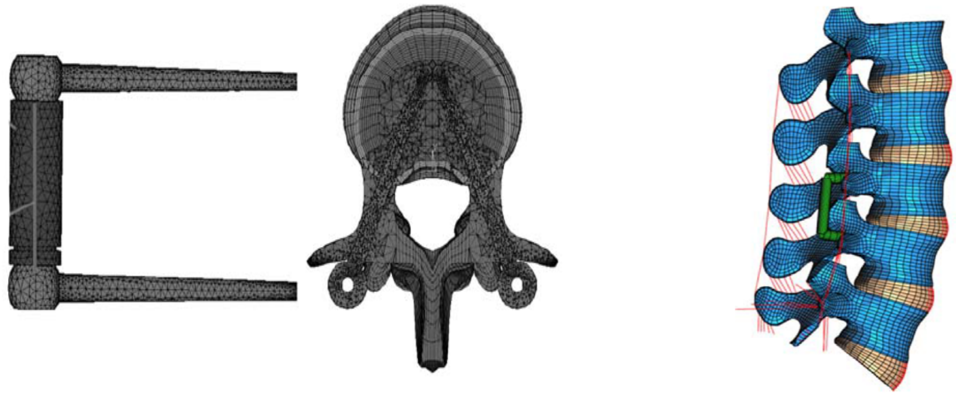

a) b)

Figure 4.6 Different models with spinal instrumentation inserted. a) Liu et al. investigation of screws inserted at the L3/4 level b) Rohlmann et al. comparison of 2 fixation devices [146, 152]

The next table presents a summary of the models reviewed in this chapter. All the models described in this review created the geometry of the spine from CT scans images, with exception of the Kap-Soo et al. study, which created the geometry of the spinal components from measurements of an in vitro study. Three of the models presented in this review studied the healthy lumbar spine while the others investigations analysed two instrumented spines and a osteoporotic FSU. Excluding the Kap-Soo et al study that considered the vertebrae components as rigid elements, all the other studies considered the vertebrae as a homogenous elastic material.

The table 4.1 also shows the different approaches used to represent the intervertebral discs assigning elastic, viscoelastic or hyper elastic material behaviour to the annulus ground substance. In addition, to simulate the motions of the spine, four of the models presented used a compressive follower load, while the Zhang et al study only applied an axial load to the top of the upper vertebra and the Lie et al just applied moments to the L1 vertebra.

Table 4.1 Summary of the elements, material properties and loads of the finite element models reviewed

	Model	**Young's Modulus [MPa] Vertebra Components**			**Young's Modulus [MPa] Intervertebral Discs Components**			**Type of Load**	**Ligaments**
		Cortical Bone	*Trabecular Bone*	*Posterior Elements*	*Nucleus Pulposus*	*Annulus Ground Substance*	*Annulus Fibres*		
Kap-Soo et al. [149]	T12 – Sacrum Healthy Model	Rigid Elements			Rigid Elements			Follower Load	-
Rohlmann et al. [150]	L1 – L5 Healthy Model	10, 000	50	3500	Incompressible	3.5		200 [N] Follower Load	Non-linear Spring Elements
Zhang et al. [51]	Osteoporotic L1 – L2 FSU	8040	34	2345	1	4.2	455	400 [N] Axial Load	Linear Link Elements
Liu et al. [152]	L1-L5 Instrumented Spine	E_x= 11,300 E_y= 11,300 E_z = 20,000	E_x= 140 E_y= 140 E_z = 200	3500	1666.7	Viscoelastic C_{10}=0.42 C_{01}= 0.105	357-550	Moments applied at L1	Tension Only Link Elements
Rohlmann et al. [146]	L1-L5 Instrumented Spine	10,000	200/140	3500	Incompressible	Hyperelastic C_{10}=0.3448 D_1= 0.30	Non - Linear	200 [N] Follower Load	Non-linear Spring Elements
Renner et al. [151]	Healthy L1-S1 Spine	12000	100	3500	L1/L4 - 2.5 L4/L5 – 3 L5/S1 – 2.25	Mooney-Rivlin Material	Non - Linear	Follower Load/Moments	Non-linear Truss Elements

4.3 Motion Capture Analysis

Motion capture analysis refers to the techniques or methods that allow to measure and study the human motion. These studies are used to understand how the whole human body or a specific part performs under different postures, activities or loading conditions. These analyses have always been conducted used the technology available at the time of the study. For example, ancient civilizations employed drawings or sculptures to study the animal gait, in the renaissance Leonardo da Vinci sketched in detail studies about stair climbing and at the end of the 1880's Edward Muybridge used photography to capture the motion of a horse in his study about animal locomotion. Since then, new technology such as video tracking and lately computer software has been developed and used to study of the human motion.

4.4 Motion Capture Analysis of the Spine

The study of the lumbar spine motion can be divided into two main categories, i*n-vivo* and *in-vitro* studies. *In-vitro* studies refer to the tests or experiments performed outside a living organism in an artificial environment while *in-vivo* studies refers to the experimentation that take place in a living organism.

Cadaveric, or *in-vitro* studies test present advantages such as better control over experimental variables, accurate measurements directly from the studied specimen or the ease to repeat a test, however one of the principal limitations of this type of study is the failure to replicate the precise conditions of a living organism. In the other hand, *in-vivo* studies present advantages such as a precise loading and physiologic response that an *in-vitro* study cannot replicate, however the results of *in-vivo* studies can be affected by different factors such as the skin motion or the subject's health. For these reasons to study the range of motion of the human spine many different techniques had been developed to acquire the motion information either from cadaveric studies (*in-vitro*) or from clinical trials (*in-vivo*).

4.4.1 X-Ray images

X Ray images are commonly used to detect a fracture or pathology of the skeletal system; however, these images can also be used to identify the motions of the bone structures inside the human body. For example, Percy *et al*., Boden *et al.* and Dvorak *et al.* use x-rays images to measure the segmental and the total range of motion of the normal lumbar spine.[153-155]

These three *in-vivo* investigations used healthy subjects with no history of low back pain to calculate the angular motion between the L1 vertebra and the sacrum. Boden *et al.* and Pearcy *et al.* just studied the ROM of the lumbar spine for the flexion and extension motions while Dvorak *et al.* also calculated the lateral bending movement. These investigations established that all the intervertebral joints or the complete segment present more movement for the flexion motion than for the extension motion.

For these investigations al least three radiographs per subject were necessary to conduct the study. Although the use of x-ray provides clear images of the lumbar spine, many investigations have reported the risk that this procedure can cause due to the radiation exposure.

a)

b)

c)

Figure 4.7 X ray images used to measure the ROM of the lumbar spine b) X-Ray image of the extended lumbar spine c) X-Ray image of the flexed lumbar spine [153, 154]

4.4.2 Fluoroscopy

Fluoroscopy is an imaging technique that allows the examination of interior parts of the body in real time. This method is often used in medicine to observe the internal motion or structure of organs such the heart, however some investigations have also used this procedure to study the range of motion of the spine.

Ahmadi *et al.* used video fluoroscopy to investigate the lumbar spine kinematics in patients with lumbar segmental instability. For this investigation 15 healthy subjects and 15 volunteers diagnosed with lumbar segmental instability were used. This study found that the mayor difference between these two groups occur in the L5/S1 segment where the segment registered a hypermobility in patients with lumbar spine instability compared with the control group.[61]

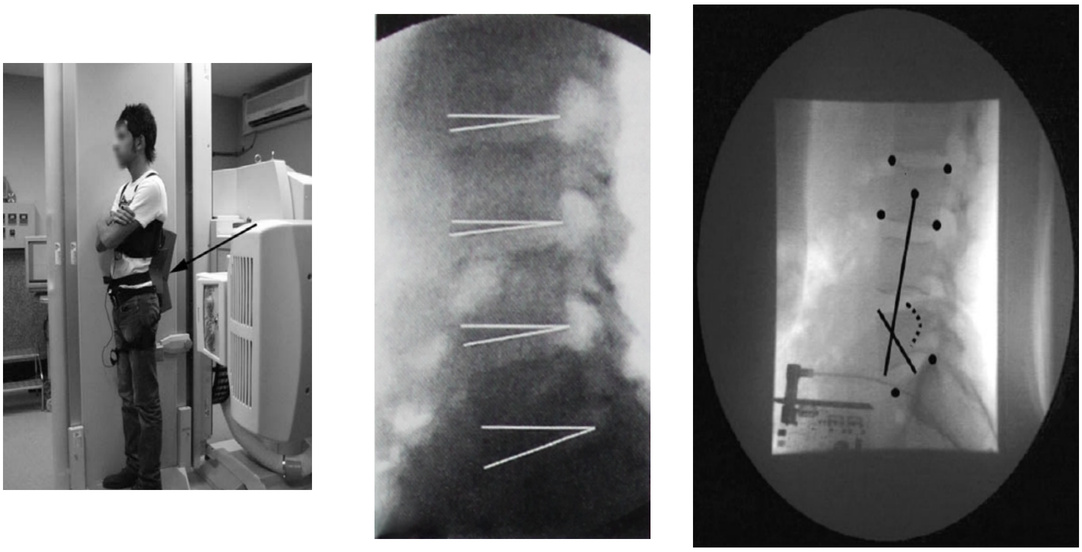

a) b) c)

Figure 4.8 Fluoroscopy Images to measure the ROM of the Lumbar Spine[61, 156, 157]

In other study Okawa *et al*. used video fluoroscopy to study the range of motion of the lumbar spine in healthy subjects, patients with low back pain and patients with degenerative spondylolisthesis. This study reported a decrease in the range of motion and a reduction in the angular velocities of patients with degenerative spondylolisthesis, compared against the results from the healthy subjects and the patients with low back pain. Also this results showed no statistical difference between the range of motion of the healthy subjects and the participants with low back pain.[157]

4.4.3 Magnetic Resonance Imaging

Magnetic Resonance Imaging or MRI is a medical procedure that uses magnetic fields and radio waves to produce images of the internal structures in the body that an x-ray procedure cannot generate. MRI scans are considered a safe procedure, however due to the magnets used to generate the images, participants with metallic devices implanted cannot use this imaging method.

a) b) c)

Figure 4.9 Magnetic Resonance Image of an Extended and Flexed Lumbar spine [158]

Many investigations have used the magnetic resonance images to study the range of motion of the lumbar spine in healthy subjects. For example, Edmondston *et al.* studied the effect of the flexion and extension positions on the intervertebral discs founding a height increase in the anterior part of the disc between positions of supine flexion and extension and reporting that the range of motion from the L1 vertebra to the sacrum ranged from 22° to 77°. [158]

In another study Battie *et al*. used MRI to determine the influence of smoking on the degeneration of the intervertebral discs. This study found greater disc degeneration in the smokers' intervertebral disc, however the range of motion from full flexion to full extension between smokers (60.3°) and non-smokers (60.6°) were similar.[159]

4.4.4 Potentiometers

A potentiometer is an electronic device used to measure the voltage on a circuit. Many investigations use devices such as the CA-6000 Spine Motion Analyzer (Orthopaedic Systems, Hayward, California) that use six high precision potentiometers to measure the range of motion of the lumbar spine. For example, McGregor *et al*. and Troke *et al*. in different investigations use this device to investigate the motion of the lumbar spine in the normal population. Both studies agreed the range of motion gradually reduce with age, especially in the extension motion, however one substantial difference between the studies is that McGregor *et al*. found that the range of motion varies depending of the gender while Troke *et al*. found no difference in the range of motion in the lumbar spine between the sexes.[160, 161]

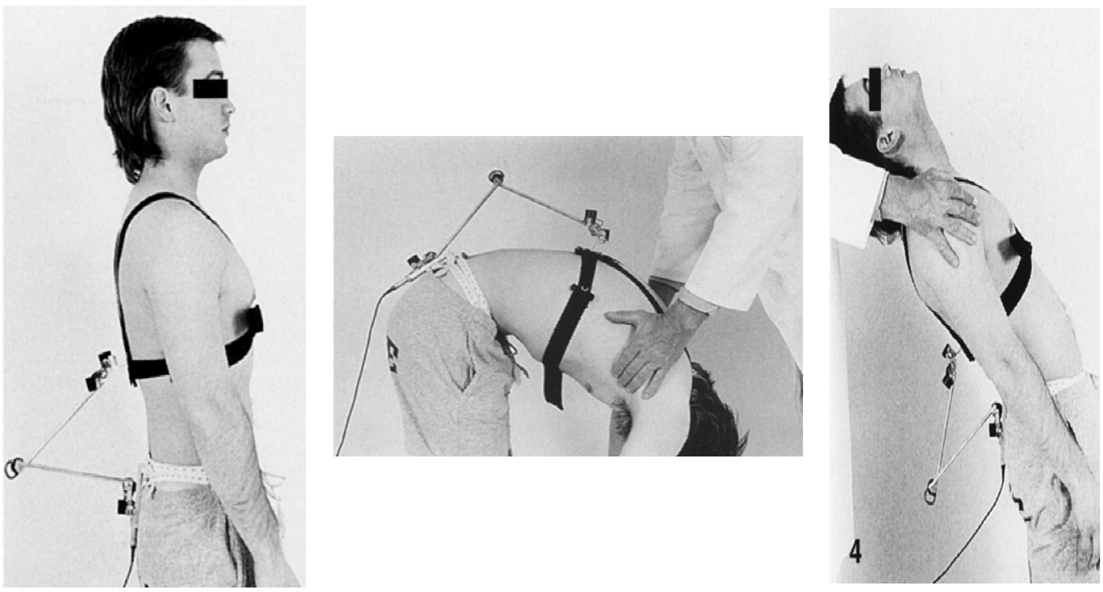

a) *b)* *c)*

Figure 4.10 Potentiometers used to measure the ROM of the lumbar spine[162]

In other study Dvorak *et al*. use this device on healthy subjects to measure the difference between actively and passively motions and also to investigate the changes in the range of motion of the lumbar spine during the course of one day. The results showed that the passive motion resulted in a greater range of motion compared with the active examination and that the range of motion in the lumbar spine increases during the course of the day.[162]

4.4.5 Strain Gauges

A strain gauge is a device that changes its electrical resistance in proportion to the amount of strain subjected. Different studies have used these devices to calculate the range of motion of the lumbar spine, for example O'Sullivan *et al*. tested the BodyGuard System (Sels Instruments, Vorselaar, Belgium) that use train gauges to analyse the lumbar spine posture of 18 healthy participants registering a range of motion of 60° for the flexion motion.[163]

In other study Cosmüller *et al*. also study the accuracy of a stain gauge device to study the range of motion of the lumbar spine. With this device the range of motion registered were 50.8 for flexion and 25.7 for the extension motion demonstrating a good agreement with other measuring devices. This study also reported no difference in the range of motion between genders however the results suggested a decrease on the flexibility in the lumbar spine with age.[164]

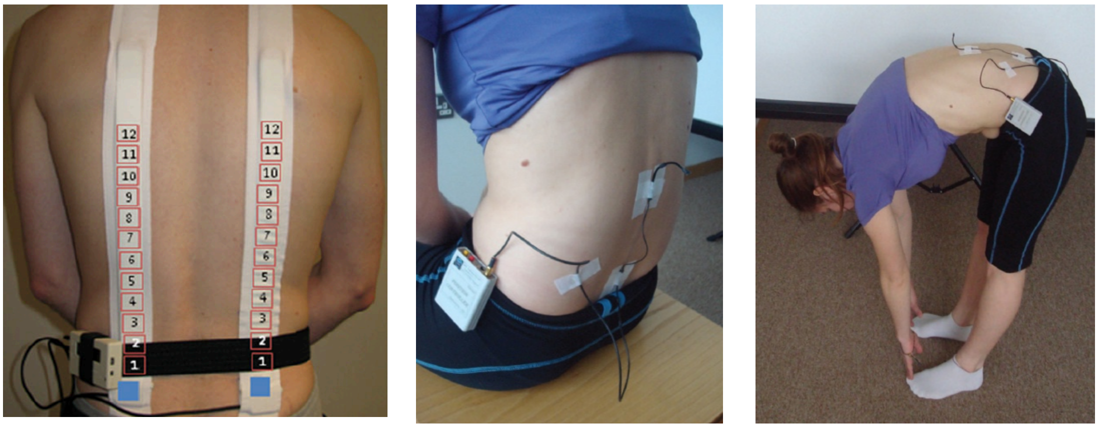

a) b) c)

Figure 4.11Strain Gauges used to measure the flexion and extension motions of the lumbar spine [163, 164]

Although these devices are a good alternative to measure the range of motion for the flexion and extension motions, these devices have not been yet tested for the axial rotation and the lateral bending motions.

4.4.6 Inertial Sensors Systems

Inertial sensors are electronic devices used to measure the position, orientation, velocity and gravitational forces of an object using gyroscopes, accelerometers and magnetometers. To measure the range of motion of the lumbar spine using these types of sensors, the devices are placed at the lower back of the subject over the L1 and the S1 vertebrae.

Different studies have been made to demonstrate that the use of inertial sensors is a valid technique to measure the motion of the lumbar spine. For example, in separate studies Ha *et al*. and Goodvin *et al*. compared the use of inertial sensors against an electromagnetic based system and an optical motion measurement system respectively. [165, 166]

Both studies found that the measures obtained from the use of inertial sensors resulted to be reasonably accurate compared to those made by the optical and electromagnetic devices. Goodvin *et al*. using the optical and inertial approaches at the same time reported that the results were within 3.1° between each other. In the study made by Ha *et al*. the inertial and electromagnetic systems were not used simultaneously due to the magnetic interference that the electromagnetic devices can produce, however this study showed no significant difference between both methods.

In another study Lee *et al*. use inertial sensors to investigate the differences in the range of motion between healthy subjects and participants with low back pain symptoms. This study found that the participants with low back pain not only have a reduced range of motion compared to the healthy subject but additionally showed a decrease in the motion velocity, especially in the extension motion.[167]

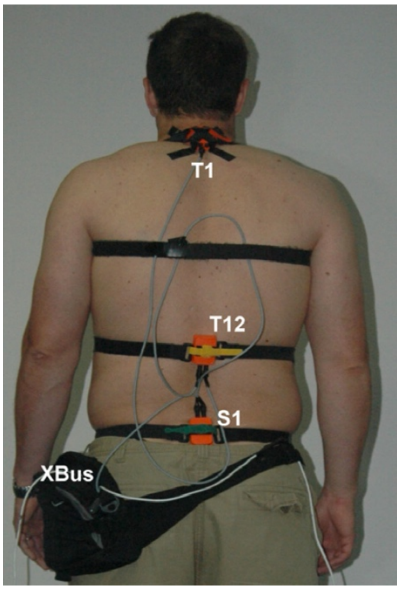

Figure 4.12 Three Inertial Sensors to measure the Range of Motion of the Spine[167]

4.4.7 Optical Systems

Optical Motion Capture systems use images taken from photographic or video cameras to track the motion of an object or a person. These systems usually use stationary cameras that sense markers or light sources attached to the subject of study. The system identifies the position and motion of these markers creating an image that can be analysed.

Many investigations have used optical systems to track the motion of the lumbar spine during different activities. For example Tojima *et al*. use the VICON System (VICONMX;Vicon Motion Systems Ltd.) to determine the range of motion of the lumbar spine in subjects with no history of low back pain. This study investigated the flexion, extension, lateral bending and torsion motions obtaining range of motion values of 41.9°, 17.4°, 16.3° and 8.4° for each motion respectively.[168]

This motion capture system was also used in an *in-vitro* study made by Lee *et al*. The objective of this study was to evaluate the differences in motion pattern of the lumbar spine after two different surgical procedures. For this investigation six human cadaveric lumbar spines were tested under different loading conditions before and after the surgical procedures finding that a both methods resulted in an increase in the range of motion causing instability in the lumbar spine.[169]

In other study Vismara *et al*. used an optical motion caption system to study the posture and fusion of the spine in obese subjects with and without chronic low back pain. This investigation showed that the range of motion of the thoracic segment was lower for obese subjects with and without low back pain however the range of motion in the lumbar spine remained similar among these three groups. [170]

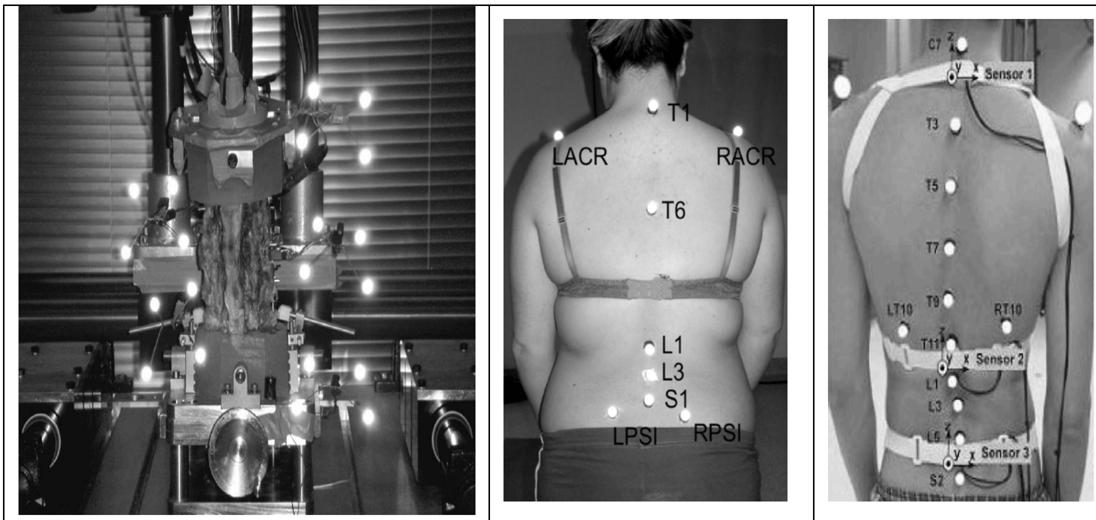

a) b) c)

Figure 4.13 Optical Motion Systems used to measure the range of motion of the lumbar spine in an in-vitro and two in-vivo studies [170, 171]

Table 4.2 presents a summary of the different techniques to measure the ROM of the lumbar spine. All the studies presented performed an in-vivo investigation with the exception of the Lee et al study that used frozen cadaveric spines. Most of the approaches presented do not represent any risk to the subjects examined, however the x-ray and fluoroscopy methods could present some risks to the subject due to the radiation exposure that is necessary for these techniques.

Table 4.2 Summary of different studies to measure the ROM of the lumbar spine

	Study Type	Technique Used	Motions Studied	Subject Condition	Risk
Percy et al.[155]	In vivo	X -Ray Images	Flexion and Extension	Healthy	Radiation Exposure
Dvorak et al.[153]	In vivo	X -Ray Images	Flexion, Extension and Lateral Bending	Healthy	Radiation Exposure
Ahmadi et al.[61]	In vivo	Fluoroscopy	Flexion in a lying prone position	Lumbar Segmental Instability	Radiation Exposure
Edmondston et al.[158]	In vivo	Magnetic Resonance Imaging	Flexion Extension	Healthy	Non metal subjects/Allergy to the contrast dye
Troke et al.[161]	In vivo	Potentiometers	Flexion, extension, lateral bending and torsion	Healthy	None/External Device
Dvorak et al.[162]	In vivo	Potentiometers	Flexion, extension, lateral bending and torsion	Healthy subjects	None/External Device
Lee et al.[167]	In vivo	Inertial Sensor Systems	Flexion and Extension	Low back pain Volunteers	None/External Device
O'Sullivan et al.[163]	In vivo	Strain Gauges	Sitting and flexion	Healthy	None/External Device
Ha et al.[166]	In vivo	Inertial Sensor Systems	Flexion, extension, lateral bending and torsion	Healthy	None/Non invasive
Goodvin et al[165]	In vivo	Inertial Sensor Systems	Flexion, extension and lateral bending	Healthy	None/Non invasive
Lee et al.[169]	In vitro	Optical Systems	Flexion and Extension	Frozen Cadaveric Spines (L1-L5)	-
Vismara et al.[170]	In vivo	Optical Systems	Flexion and lateral bending	Obese and Low back pain Subjects	None/Non invasive
Tojima et al.[168]	In-vivo	Optical Systems	Flexion, extension, lateral bending and torsion	Healthy	None/Non invasive

This chapter presented a literature review of the different techniques used to create a 3D finite element model of the lumbar spine. Many of the models developed to investigate the function of the lumbar spine and the effects of fusion techniques in this part of the body consider only a small number of lumbar spine segments and in doing so may only provide a restricted insight into the problem. In addition, analyses often focus on reporting one type of implant not considering the effects on how changes in the sagittal angle of the cage affects the range of motion of the lumbar spine or the outcome of the surgery. [172, 173]

For these reasons, unlike previous studies that only used a L1-L5 lumbar model, this investigation will study the lumbosacral spine (L1-S1). Also this investigation will evaluate the effects on the lumbar spine after two surgical procedures (PLF and PLIF) using a rigid posterior implant and two types of PEEK interbody cages. Moreover this study will evaluate the consequence of using two different intervertebral cages (0° and 4°) and the impact that these devices have on vertebrae, intervertebral discs and the ROM of the lumbosacral spine.

In addition, this chapter also describes some of the most used techniques and devices to experimentally measure the range of motion of the lumbar spine. Although *in-vitro* or invasive analysis can produce more accurate results often its cost or the risk for the patients in using these methods can cause a great limitation for these kinds of studies. For these reasons this investigation used inertial motion sensors, that showed to be a valid tool to measure the function of the lumbar spine, to study the differences in the range of motion of subjects that had undergone a L4/5 posterior lumbar interbody fusion (PLIF) and subjects who had no history of low back pain.

Chapter V Motion Capture Analysis

5.1 Introduction

Lumbar spinal fusion procedures are widely employed in the treatment of lower back disorders including displacement of one or more vertebra and certain cases of degenerative disc disease. The ROM of the lumbar spine is an important parameter as it can aid in the diagnosis of lower back disorders. In addition, it is widely recognized that surgical lumbar fusion procedures generally result in a reduction in ROM. [166, 174].

For this study an *in-vivo* investigation was carried out using subjects that had undergone a L4/5 posterior lumbar interbody fusion (PLIF) and subjects who had no history of low back pain conditions and had not undergone lumbar interbody fusion in order to calculate the ROM between the standing position and the flexed and extended positions. For the purposes of this investigation, the ROM was expressed as the angular separation of the L1 vertebra and the sacrum between the normal standing position and the maximally flexed or extended spine.

This chapter describe the equipment, the methodology and the data processing techniques used to measure the ROM on the lumbar spine of the two groups described previously. These results enable the study of the effects that a L4/5 posterior lumbar interbody fusion causes on the lumbar spine.

5.2 Background

The ROM of a joint, such as the knee, shoulder or ankle is an important measurement that can be used to evaluate the correct function of the segment. As well as these joints, the ROM of the lumbar spine is a common measure used to determine the functionality of the spine and to rate the dysfunction of this part of the body. Precise knowledge of the kinematics of the spine can aid in the detection of certain diseases in this region.[175-178]

There have been many studies that have attempted to quantify the ROM of the spine under various circumstances and using different methods. These studies can be divided firstly into two main categories, *in-vivo* and *in-vitro* studies. Cadaveric, or *in-vitro* experiments permit invasive and accurate fixation of pins or optical markers directly to the bone, however obtaining the samples with the required characteristics of the investigation present a problem. [179-183]

In-vivo tests could present many variables that can influence the results of the experiments, such as the skin motion, that can produce an error from .56º to 4.4º according to different studies, or the subject's health that can limit the mobility of the subject. However, there have been several major advantages associated with them, such as the natural motion of the spine during the tests and the normal muscle and ligament contractions. [181, 184, 185]

As mentioned in Chapter 4, to measure the ROM of the lumbar spine different visualization techniques have been employed including X-rays and MRI scans or the use of equipment such as electromagnetic tracking systems or video motion capture using reflective markers in order to accurately calculate the movement of this segment.[165, 166, 176, 183, 185-187]

5.3 Methodology

The methodology used in this work has been developed to measure the ROM of the lumbar spine. As the flexion and the extension motions are the most pronounced motions performed in the lumbar spine, the methodology used in this investigation consisted of the comparison of the angle between the L1 vertebra and the Sacrum (S1) in the standing position and the angle measured between these two bones when the spine is maximally flexed or extended.

For this experiment two wireless inertial motion-tracking sensors (MTw, Xsens Technologies, Enshede Netherlands) were placed over the spinous process of the L1 vertebra and the sacrum respectively on 10 subjects without any history of back problems and on 5 patients that had undergone L4/5 PLIF surgery.

With the sensors attached at the lower back, each subject was asked to perform 5 full flexion and 5 full extension motions. The information obtained from the two sensors was recorded using the MT Manager software provided with the equipment. After the trials were completed, the data was processed and analysed using the MATLAB (The MathWorks, Inc., USA) software to obtain the orientation of the two sensors during the tests. The orientation of the sensors was used to calculate the difference in angle in order to determine the ROM for the two motions for the subjects from the two groups, enabling a comparison with the predictions from the respective computational model to be undertaken.

This study required the approval of two ethical committees. Approval was obtained to conduct the tests on the subjects without lower back problems from the Ethics Committee of the University of Manchester (ref 12429). For the case of the patients that had undergone L4/5 PLIF surgery, the National Research Ethics Service Committee (NRES) approved the protocol (ref 13/NW/0488).

5.4 Subject Selection

Participants without a history of lower back pain and volunteers that had undergone an L4-5 lumbar fusion procedure were selected to perform the activities required to measure the ROM of the lumbar spine in the sagittal plane.

Prior to the trials each volunteer that accepted the invitation to participate in the study received a participant information sheet explaining the objective of the research, the protocol for the test and the reasons why they had been selected for the study. Each volunteer also received and signed a consent form confirming that they had been informed about the experimental protocol and the potential risks associated with the trials and that they agreed to participate in this study.

5.4.1 Participants without history of spine problems

To develop normative data for participants able to perform total flexion and extension motions in a normal way, 10 volunteers with these characteristics were recruited. If a subject presented with previous history of low back problems or injuries or had been treated for a lower back muscular problem the subject was excluded from the study.

Ten subjects (6 men and 4 women) aged 29±1.7 years old with a mean weight of 72.7 kg (SD= 12.4) and a mean height of 1.7 m (SD= .1) agreed to take part in the study. Table 5.1 shows the age, gender, height and weight of each subject.

Table 5.1 – Anthropometric information of participants with no history of low back pain

Participant	Age [Years]	Gender	Height [m]	Weight [kg]
1	26	F	1.64	65
2	26	M	1.74	76
3	28	M	1.63	62
4	30	M	1.74	70
5	28	F	1.61	65
6	29	F	1.65	66
7	29	M	1.82	90
8	30	M	1.80	79
9	31	F	1.53	62
10	29	M	1.81	97

5.4.2 Participants with an L4-5 posterior Lumbar Fusion

To obtain normative data for the ROM for patients that had undergone a L4-5 lumbar fusion procedure, 5 participants with this characteristic were recruited. The requirements for the subjects for this part of the study were that these patients had previously undergone L4/5 PLIF surgery and that they were able to perform the flexion and extension motions without any pain or discomfort.

The identification and selection of the volunteers was undertaken in collaboration with Salford Royal Hospital (Salford Royal NHS Foundation Trust, Salford, UK).

Five subjects (2 men and 3 women) aged 55±9 years old with a mean weight of 78 kg (SD= 12) and a mean height of 1.7 m (SD= .1) agreed to take part in the study. Table 5.2 shows the age, gender height and weight of each subject.

Table 5.2 - Anthropometric information of participants with an L4-5 posterior Lumbar Fusion

Participant	**Age [Years]**	**Gender**	**Height [m]**	**Weight [kg]**	**Time since surgery**
1	52	M	1.86	98	2 years, 1 month
2	53	M	1.76	75	1 year, 5 months
3	71	F	1.60	68	1 year, 3 months
4	46	F	1.69	70	1 year, 3 months
5	52	F	1.66	79	2 years, 7 months

5.5 Equipment

For this investigation two wireless inertial motion-tracking sensors (MTw, Xsens Technologies, Enshede Netherlands), of weight 30g and dimension 38 x 53 x 21 mm, were used to measure the ROM of the Lumbar Spine in the sagittal plane. These sensors use gyroscopes, magnetometers and accelerometers, to describe orientation, angular velocity and angular acceleration in 3 dimensions with a reported dynamic accuracy of 2°. The data provided by the sensors was used to measure the difference in angle between the standing position and the maximal flexion and extension motions. [188] One of the wireless inertial motion-tracking sensors used in the investigation is shown in Figure 5.1.

Figure 5.1 Xsens Sensors

5.5.1 Calibration

Before the beginning of the test and prior the attachment of the two MTw sensors on the subject's lower back, the sensors were calibrated by performing a heading reset on a flat surface. This calibration eliminates any structural magnetic disturbance and allowed the coordinate system of both sensors to maintain the same orientation during the tests with respect to the global system G, which is the system created by the earth's magnetic north and the local vertical axis as shown in the Figure 5.2.

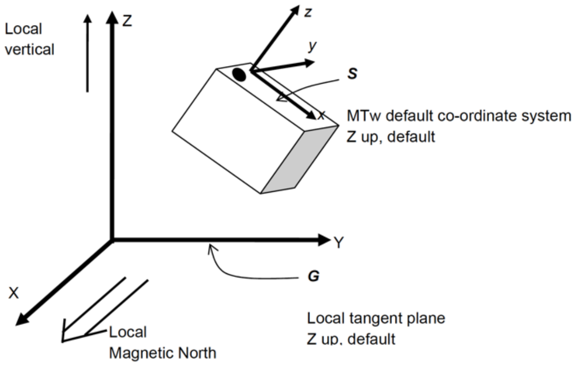

Figure 5.2 Xsens Sensors coordinate system [188]

The sensors were configured to wirelessly transmit the data to the Awinda Master Sensor Station (Xsens Technologies, Enshede Netherlands), shown in the Figure 5.3, at 100 Hz using the MT Manager software provided with the equipment. This software allowed all the information provided by the inertial sensors to be visualized and recorded [188].

Figure 5.3 Awinda Station

After the calibration, each sensor was attached directly to the skin of the participant using double-sided tape. One sensor was positioned over the L1 lumbar vertebra (the "L" sensor) and the second sensor over the S1 sacral bone (the "S" sensor) as shown in Figure 5.4.

Figure 5.4 Sensor Placing

5.6 Data Collection

Volunteers were first given thorough instructions regarding what was required during the trials. Next, the MTw sensors were calibrated and placed over the lower back of the subjects, and the participants were asked to perform two activities in order to measure the ROM of the Lumbar Spine in the sagittal plane.

For the first activity participants were requested to perform 5 repetitions of a maximal flexion motion in their normal comfort range from the standing position. For each trial, the participants, starting in the standing position, received the instruction to begin the forward bending motion. After the participants reached their maximal range of motion they were instructed to maintain this position for at least 2 to 5 seconds. After that, the participants were asked to return to the vertical position to prepare for the next trial. Figure 5.5 shows the 3 steps for the forward bending activity.

a) b) c)

Figure 5.5 Flexion Motion a) Starting position b) Maximal flexion position c) Final Position

For the second activity, participants were requested to perform 5 trials of a backward bending motion in their normal comfort range. Starting from the standing position, the volunteers were instructed to begin the backward bending motion. As with the previous forward bending activity, when the patients reached their maximal range for the extension motion, they were instructed to maintain the position for at least 2 to 5 seconds. After that, they returned to the vertical position to prepare for the next trial. Figure 5.6 shows the 3 steps for the backward bending activity.

a) b) c)

Figure 5.6 Extension Motion a) Starting position b) Maximal extension position c) Final Position

5.7 Data Processing

Once the subjects had concluded the forward and backward bending activities, the two MTw sensors were carefully removed in order to avoid any discomfort to the volunteers. As mentioned previously, the data from each trial was wirelessly recorded using the MT Manager software provided with the equipment.

Using the data recorded from the sensors, the ROM of the flexed and extended spine was calculated using the directional cosine matrix, shown below, which represents the orientation of each of the sensors attached to the back of the patients.[188]

$$R_{GS} = R_{\psi}^{Z} R_{\theta}^{Y} R_{\phi}^{X}$$

$$= \begin{bmatrix} \cos(\psi) & -\sin(\psi) & 0 \\ \sin(\psi) & \cos(\psi) & 0 \\ 0 & 0 & 1 \end{bmatrix} \begin{bmatrix} \cos(\theta) & 0 & \sin(\theta) \\ 0 & 1 & 0 \\ -\sin(\theta) & 0 & \cos(\theta) \end{bmatrix} \begin{bmatrix} 1 & 0 & 0 \\ 0 & \cos(\phi) & -\sin(\phi) \\ 0 & \sin(\phi) & \cos(\phi) \end{bmatrix} \quad \text{.........(1)}$$

$$= \begin{bmatrix} \cos\theta\cos\psi & \sin\phi\sin\theta\cos\psi - \cos\phi\sin\psi & \cos\phi\sin\theta\cos\psi + \sin\phi\sin\psi \\ \cos\theta\sin\psi & \sin\phi\sin\theta\sin\psi + \cos\phi\cos\psi & \cos\phi\sin\theta\sin\psi - \sin\phi\cos\psi \\ -\sin\theta & \sin\phi\cos\theta & \cos\phi\cos\theta \end{bmatrix}$$

Where R_{GS} is the rotational matrix which can be interpreted as components of the reference system of the sensor expressed in the global coordinate system and where ψ, θ, ϕ is the rotation of the sensor coordinate system around the Z, Y and X axis of the global coordinate system respectively.

The data was then processed using MATLAB (The MathWorks, Inc., USA) enabling the ROM for both sensors to be calculated.

5.7.1 Accuracy of the Measurements

Before carrying out the tests with any participant either healthy or with those having undergone posterior lumbar surgery performed, a pendulum with known movement values was used to check that the experimental set up and data processing were being performed correctly and accurately. In these tests a sensor named “L”, was attached to the movable arm of a pendulum while the other sensor, called “S”, was attached to the fixed base as shown in the Figure 5.7. During the tests, the rotation of the pendulum was measured with a goniometer.

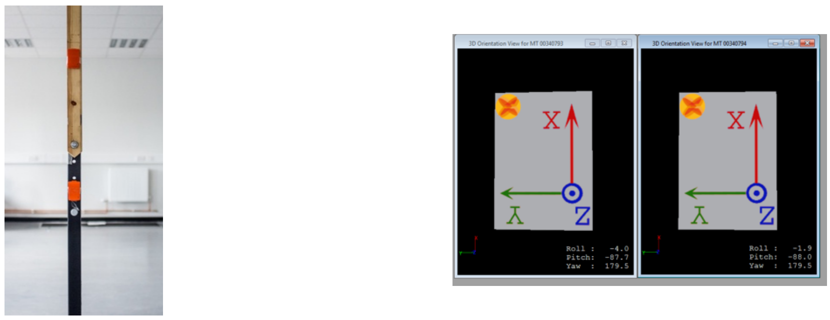

a) b)

Figure 5.7 a) Sensors attached to the pendulum b) Orientation of the sensors attached to the pendulum as seen in the computer

The same protocol was used for the forward bending motion in participants; the movable arm of the pendulum was rotated anticlockwise 90º during 5 seconds simulating the flexion motion. The movable arm was left in the 90º position for 5 seconds and then returned to the vertical position in another 5 seconds. The next figure shows the motion of the pendulum and the motion of the sensors.

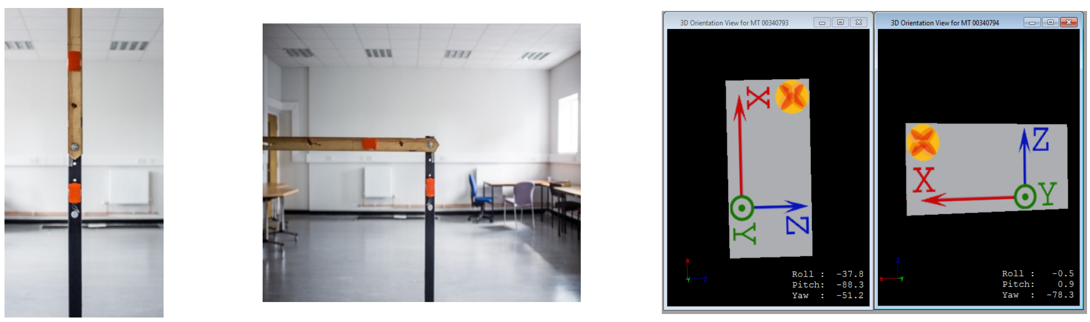

a) b) c)

Figure 5.8 a) Pendulum in the starting position b) Pendulum at 90°c) Orientation of the sensors attached to the pendulum as seen in the computer at 90

For the second test, the movable arm of the pendulum was rotated clockwise 45º on 5 seconds from the starting vertical position simulating the extension motion. The movable arm with the "L" sensor attached to it was left for 5 seconds in the 45º position and then returned to the initial position in another 5 seconds. The next figure shows the motion of the pendulum and the motion of the sensors simulating the extension movement.

a) b) c)

Figure 5.9 a) Pendulum in the starting position b) Pendulum at 45º c) Orientation of the sensors attached to the pendulum as seen in the computer at 45º

The results of these tests are shown in Figures 5.10 and 5.11. Figure 5.10 shows the data recorded from the trial of the pendulum simulating the flexion motion. It can be seen from the graph that the "L" sensor detected a 90º movement with respect to the vertical position, while the fixed segment did not record any motion.

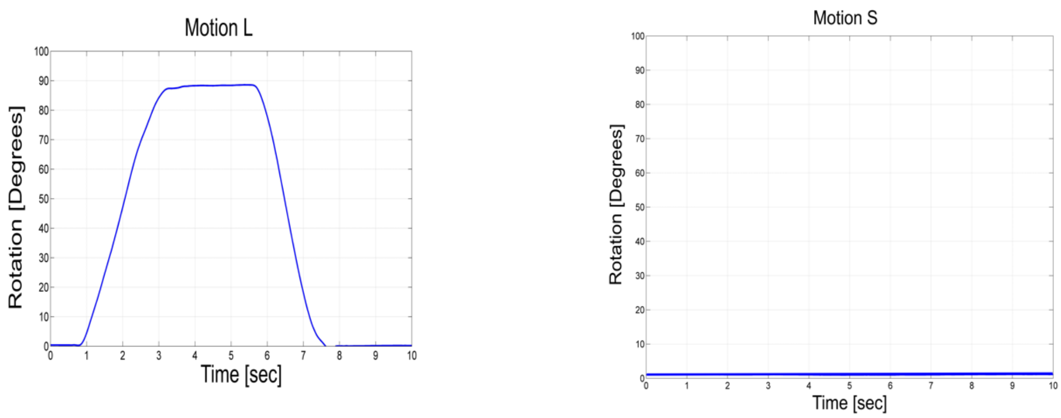

a) b)

Figure 5.10 Graphs showing data captured from the sensors for the 90º pendulum test a) Graph from the "L" sensor b) Graph for the "S" sensor

These tests were repeated 5 times for each motion. Table 5.3, shows the data recorded from the 5 pendulum tests that simulated the flexion motion. As can be seen upon inspection of this table, the values obtained were 90.4º±0.5º, which are in good agreement with the known pendulum values for this motion.

Table 5.3 - Flexion - Pendulum

Test	Motion-L [º]	Motion-S [º]	ROM [º]	Time[s]
Test-01	91.1	0.0	91.1	15
Test-02	89.54	0.0	89.54	15
Test-03	90.31	0.0	90.31	15
Test-04	90.74	0.0	90.74	15
Test-05	90.22	0.0	90.22	15
Average			**SD**	
90.4			.5	

For the extension movement 5 trials using the pendulum were also performed to test the accuracy of the instrumentation. Figure 5.11 shows the data recorded from one trial of the movement of the pendulum simulating the extension motion. It can be seen from this figure that the "L" sensor located on the movable arm moved 45º with respect to the vertical position, while the fixed segment did not record any motion.

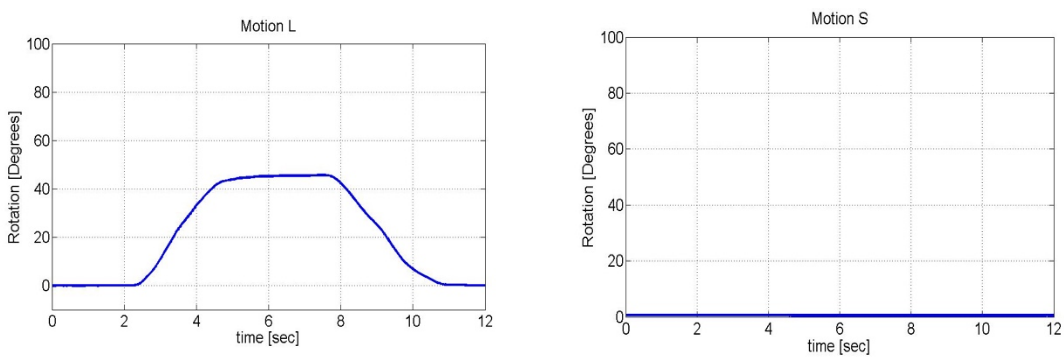

a) b)

Figure 5.11 Graphs showing data captured from the sensors for the 45º pendulum test a) Graph from the "L" sensor b) Graph for the "S" sensor

Table 5.4 shows the data recorded from the 5 pendulum tests that simulated the extension motion. From this table it can be seen that the ROM values for extension were 45.4º ±0.4º, a result, which is consistent with the actual value of the pendulum motion in these tests.

Table 5.4 - Extension – Pendulum

Test	Motion-L [º]	Motion-S [º]	ROM [º]	Time[s]
Test-01	45.2	0.0	45.2	15
Test-02	45.7	0.0	45.7	15
Test-03	44.7	0.0	44.7	15
Test-04	45.6	0.0	45.6	15
Test-05	45.9	0.0	45.9	15
Average			**SD**	
45.42			.42	

As can be seen from the previous two tables, the results obtained from the sensors attached to the pendulum were consistent with the actual values for the motion of this instrument. It can therefore be concluded that the procedure is a valid methodology for calculating the ROM of the lumbar spine for the *in-vivo* tests.

5.8 Results

In-vivo experiments using 10 subjects with no history of low back pain and 5 patients that had undergone PLIF surgery were performed to calculate the ROM of the lumbar spine in the sagittal plane. To obtain the ROM values two sensors were attached to each volunteer’s back. These sensors recorded the motions of the patients when they were asked to perform forward bending and backward bending motions.

5.8.1 Analysis of the Range of Motion of the Subjects with no History of Spine Problems

The range of motion for the flexed and extended spine was measured for the 10 healthy subjects. As explained previously, each subject performed five sets of each movement. Each trial was processed and analysed and the orientation for each sensor obtained. From these measurements the minimum, maximum, mean and the standard deviation of the ROM for each patient was calculated.

Figure 5.12 shows an example of the results obtained from the data from the sensors attached to one healthy subject during one of the forward bending motion trials. This figure shows the rotation of the L1 lumbar vertebra ("L" sensor) and S1 sacral bone (the "S" sensor) throughout one forward bending motion. Upon inspection of this figure it can be seen that although both sensors recorded changes from their initial positions, the "L" sensor (positioned over the L1 lumbar vertebra) registered a motion of 100º while the "S" sensor (positioned over the S1 sacral bone) moved just 40º from its original position. This general behaviour, where the sensor attached at the L1 location moved by a greater amount than the sensor located at the S1 level, was repeated for all the trials for this movement.

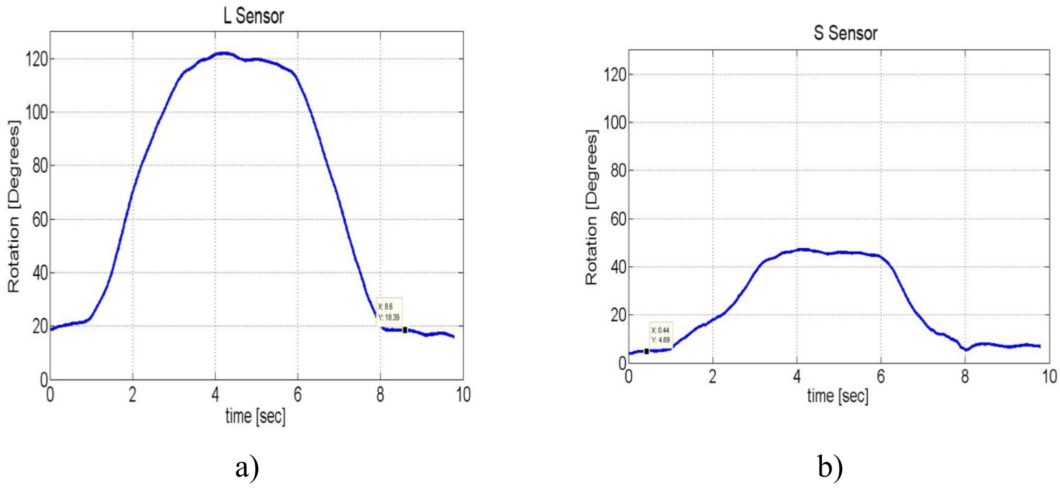

Figure 5.12 Graphs showing data captured from the sensors attached to a healthy volunteer while performing the flexion motion a) "L" sensor b) "S" sensor

Figure 5.13 shows an example of the results obtained from the data from the two sensors obtained for one of the backward bending motion (extension) trials undertaken by a healthy volunteer. This figure shows the rotation of the L1 lumbar vertebra (“L” sensor) and S1 sacral bone (the “S” sensor) throughout one backward bending motion. As for the flexion motion, the figure shows that both sensors registered changes in their orientation, with greater motion being registered by the “L” sensor than the “S” sensor. However, in this case the data obtained from the sensors showed that the difference in the orientation between the sensors was less than for the flexion motion.

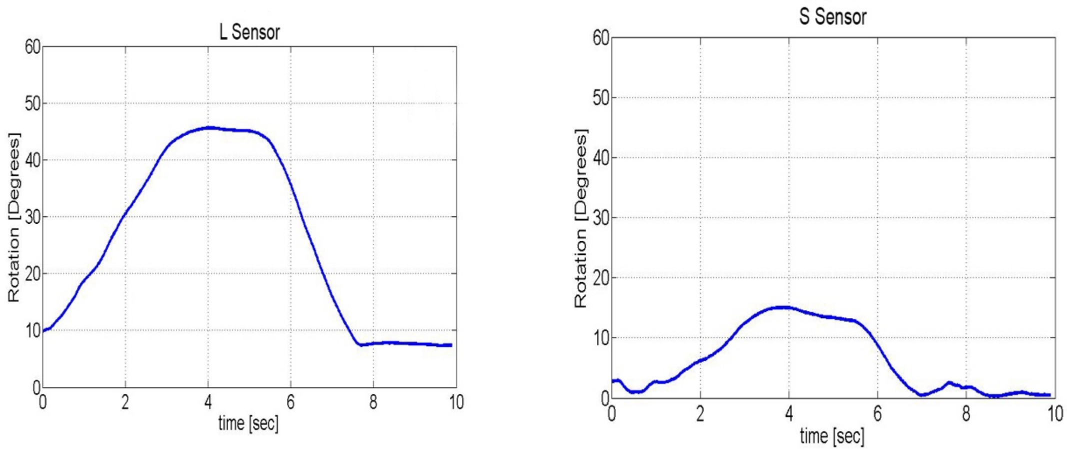

a) b)

Figure 5.13 Graphs showing data captured from the sensors attached to a healthy volunteer while performing the extension motion a) “L” sensor b) “S” sensor

Table 5.5 shows the average ROM results for the flexion and extension motions for each of the healthy patients as obtained and calculated from the trials. As can be seen from the table, subject H-07 was the most rigid volunteer for both motions, while subjects H-09 and H-08 were the more flexible volunteers for the flexion and extension motions respectively. Also given in this table is the overall average ROM for all subjects for both activities.

Table 5.5 Healthy Subjects

Participant	**Flexion Average [º]**	**Extension Average [º]**
H-01	59.9	26.38
H-02	46.42	16.84
H-03	48.78	30.36
H-04	52.42	24.06
H-05	53.5	22.9
H-06	50.26	20.88
H-07	42.26	16.1
H-08	52.26	31.56
H-09	62.22	16.54
H-10	51.62	16.74
Overall average	51.96	22.26

5.8.2 Analysis of the Range of Motion of the L4/5 PLIF Patients

The ROM for the flexed and extended spine was measured for the 5 participants who had previously undergone L4-5 lumbar fusion. Each subject performed five sets of flexion and extension motions while data was recorded from the two sensors attached to the volunteer. From this data the rotations of the L1 lumbar vertebra and the S1 sacral bone throughout the movements were obtained.

Figure 6.14 shows an example of the results obtained from the data from the sensors attached to one of the subjects who had previously undergone L4/5 PLIF during one flexion trial. It can be seen from this figure that at the L1 vertebra level ("L" sensor) more motion was recorded than at the S1 sacral bone level ("S" sensor). The same pattern of behaviour occurred in all the trials for the L4/5 PLIF subjects.

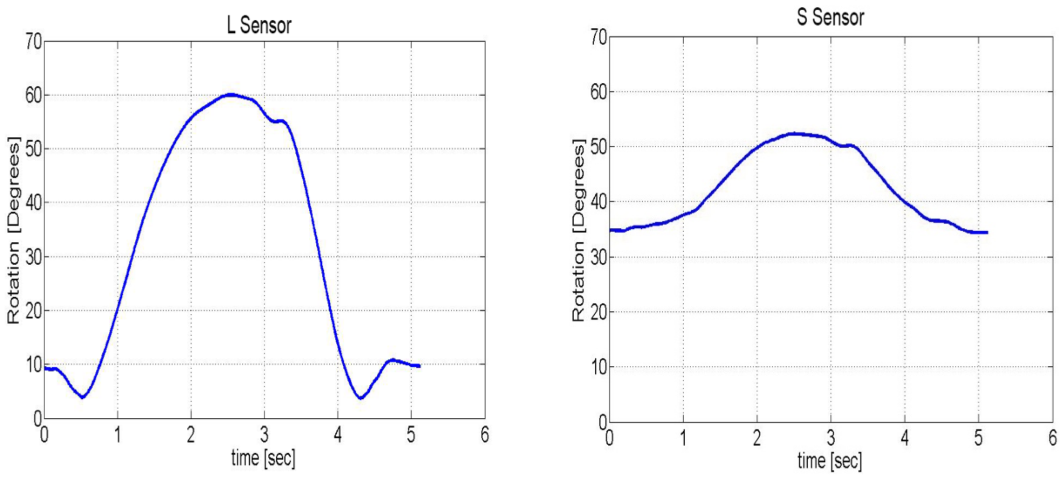

a) b)

Figure 5.14 Graphs showing data captured from the sensors attached to a L4/5 PLIF patient while performing the flexion motion a) "L" sensor b) "S" sensor

Figure 6.15 shows the changes in the orientation recorded by the L1 lumbar vertebra and S1 sacral bone sensors during an extension trial of one L4/5 PLIF subject. Upon inspection of this figure it can be seen that again, motion was greater at the L1 vertebra level ("L" sensor) than at the S1 sacral bone level ("S" sensor), a pattern that was repeated for all the L4/5 PLIF volunteers.

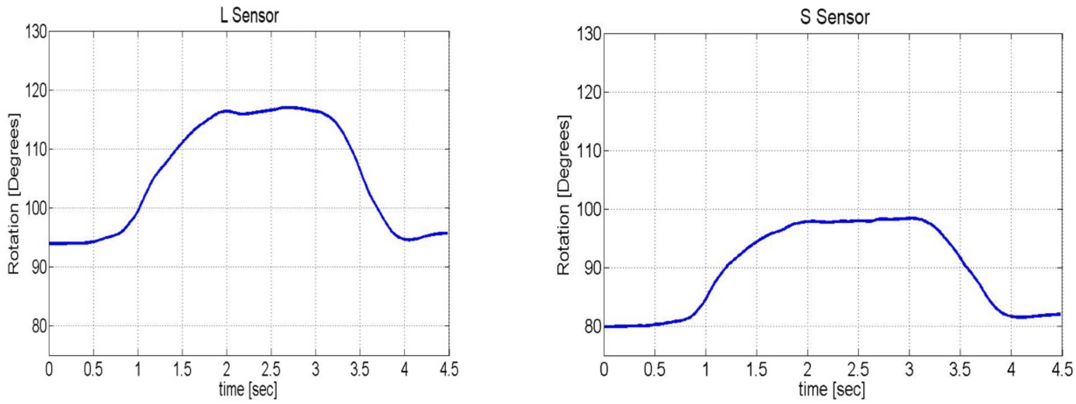

a) b)

Figure 5.15 Graphs showing data captured from the sensors attached to a L4/5 PLIF patient while performing the extension motion a) "L" sensor b) "S" sensor

Table 5.6 presents the average ROM results for the flexion and extension motions for the subjects that had undergone PLIF surgery as calculated from the trials. As can be seen from this table, subject P-04 was the participant who was able to perform less

ROM for both activities while subjects P-01 and P-02 were the most flexible volunteers from this group for the flexion and extension motions respectively.

Table 5.6 L4/5 PLIF Patients

Participant	Average of Flexion [º]	Average of Extension [º]
P-01	33.79	5.42
P-02	29.47	8.29
P-03	27.29	5.49
P-04	22.50	1.73
P-05	29.26	5.34
Overall Average	28.46	5.25

Different investigations have studied the motion of the lumbar spine as related to age*[160, 162, 177, 189, 190]*. These studies confirm a decreased in ROM of this part of the spine with advancing age. However, the results of these investigations show that the ROM registered for the subjects with a similar age of the subjects that had undergone PLIF surgery studied in this investigation, is greater. The next table shows the results of five investigations that studied the ROM on healthy subjects with more that 40 years old.

Table 5.7 L4/5 PLIF Patients

Study		Flexion [º]	Extension [º]
Wong et al.[189]	42 ± 8	61.9 ± 9.9	15.5 ± 7.4
Dvorak et al[162]	50 +	56.5 ± 5.8	20.4 ± 8.6
Herp et al[190]	50 - 59	58.1 ± 10.6	17.2 ± 7.2
Fitzgerald et al[177]	50 - 59	-	24.9 – 29.9
McGregor et al[160]	50 - 59	54.6 ± 11.8	18.3 ± 7.5

Comparing the results in Table 5.6 with the results of different investigations showed in Table 5.7, it is clear that the subjects that had undergone PLIF surgery have a reduced ROM compared to the subjects with no history of spine problems and low back pain.

Chapter V describes the *in-vivo* investigation used to analyze and compare the range of motion between patients that had and had not undergone L4/5 Interbody lumbar fusion. This chapter also presents a comparison of the ROM results between the two groups of participants in the study.

The next chapter will describe the process used to create the geometry of the Lumbo-Sacral Spine and the techniques used to simulate and analyse diverse motions of the spine in a finite element analysis.

Chapter VI Construction of the Finite Element Model

6.1 Introduction

As discussed in previous chapters, lumbar spinal fusion procedures are widely employed in the treatment of lower back disorders including spondylolysthesis and certain cases of degenerative disc disease. An understanding of the effect of a lumbar spinal fusion procedure on the adjacent spinal elements is essential for a successful clinical outcome. In order to investigate the effect of fusion procedures on the remaining spinal components, finite element analyses (FEA) were undertaken. As mentioned before, FEA is a tool that can be used to generate important information of use to surgeons and medical device manufacturers, information that *in-vivo* or *in-vitro* experiments may not provide. [115, 124, 134, 191-193]

Like many other engineering investigations that study the human body, the determination and modelling of the materials, components, loads and boundary conditions of the system is crucial to the creation of a realistic model. Nevertheless, the implementation of the boundary conditions in a biological system can be extremely challenging.

This chapter describes the development of a three-dimensional (3D) finite element model of the L1-S1 lumbar spine which was used to investigate the stresses and ROM in the adjacent spinal components following one-level spinal fusion of lumbar segment L4-L5. The creation of the finite element model is explained in detail, including the materials used for the different components, the loads used to simulate various movements in the spine and the creation of the representation of the instrumentation used to simulate the conditions of spinal fusion.[24, 139, 142].

For this investigation a Computer Tomography (CT) scan of a healthy lumbar spine from a twenty four year old male was used as the basis to create the following four models:

- Healthy Spine (HS)
- Posterolateral Fusion Model (PLF)
- Posterior Interbody Lumbar Fusion (0º and 4º)
- Posterior Interbody Lumbar Fusion following ossification (0º and 4º)

6.2. Construction of the Healthy Lumbar Model (L1-S1)

The model geometry of the lumbar spine of a young healthy patient was created from a Computed Tomography (CT) scan. Transverse CT scan slices at intervals of 0.625 mm (569 slices in total) were used to produce the geometry of the model.

The CT scan data were imported into the ScanIP® three-dimensional visualization software (ScanIP®, Simpleware Ltd). This software determines the density of the materials based on the grayscale values provided by the CT Scan information as seen in the Figure 6.1. From these data the ScanIP® software assigns different material properties to the different types of bone and soft tissue. For this study the software was used to differentiate the nucleus pulposus and the annulus fibrosus of the intervertebral discs and to recognize the cortical and trabecular bone of the vertebrae.

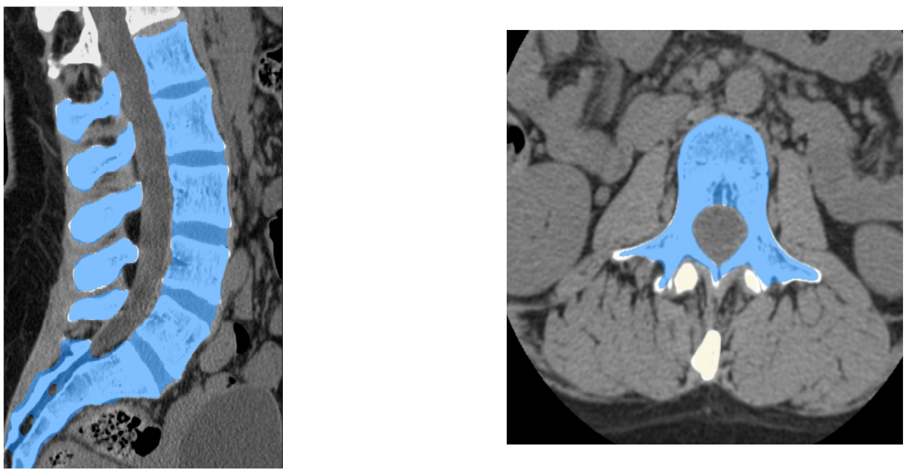

a) b)

Figure 6.1 Superior and lateral view of the CT Scans of the lumbosacral spine imported into the ScanIP Software

After the recognition of the different structures and materials in the lumbosacral spine, each component was assigned a colour mask to delimit the geometry of each part, as shown in Figure 6.2. and Figure 6.3 once each component was separated, filter tools were applied. These filter tools, such as the *Morphological Filter, the Noise Filter*, *or the Recursive Gaussian Filter* included in the ScanIP Software are used to delimit the external surface of the material, fill the unwanted spaces and smooth the surfaces in order to obtain a more accurate geometry of the vertebrae and the intervertebral discs.

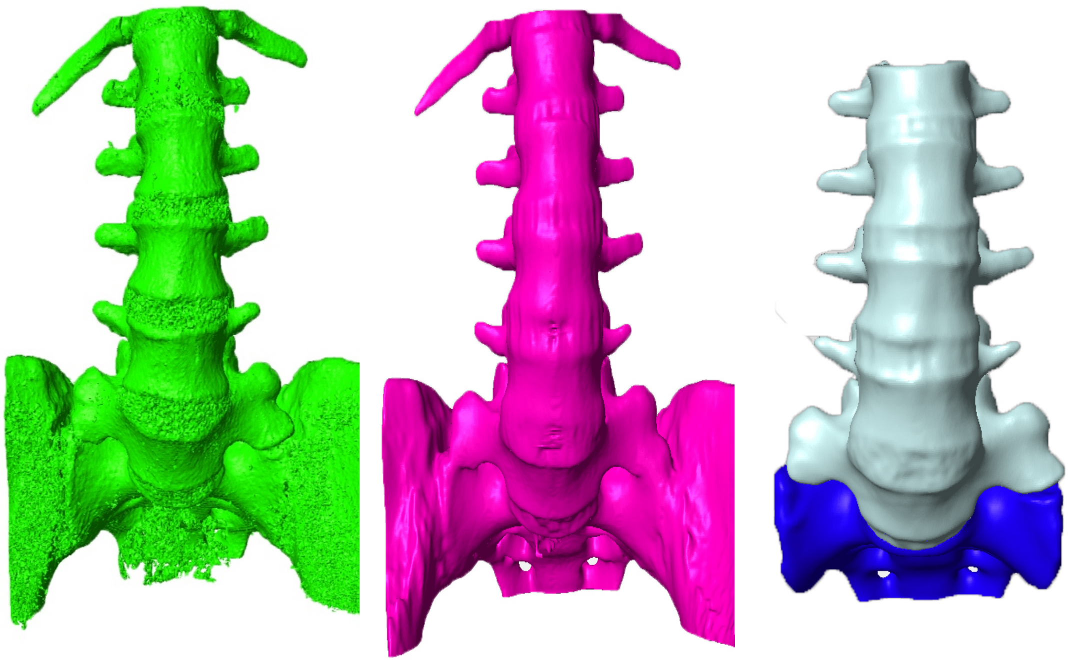

a) b) c)

Figure 6.2 Shape recognition of the Lumbosacral spine a) Imported data from CT scans b) Noise reduction of the imported data c) Geometry of the lumbosacral spine

Once the colour mask for each component was corrected, the surface information was exported as an Initial Graphics Exchange Specification (IGES) file from ScanIP into the Delcam PowerSHAPE Pro® software (Delcam plc, Birmingham, UK). In this software each component surface was converted into a solid model. The solid models were then saved as a parasolid format (.x_t) to enable the files to be imported into the Abaqus/CAE 6.10© finite element analysis software (Dassault Systèmes) where the assembly, the material properties assignation and the finite element analysis took place.

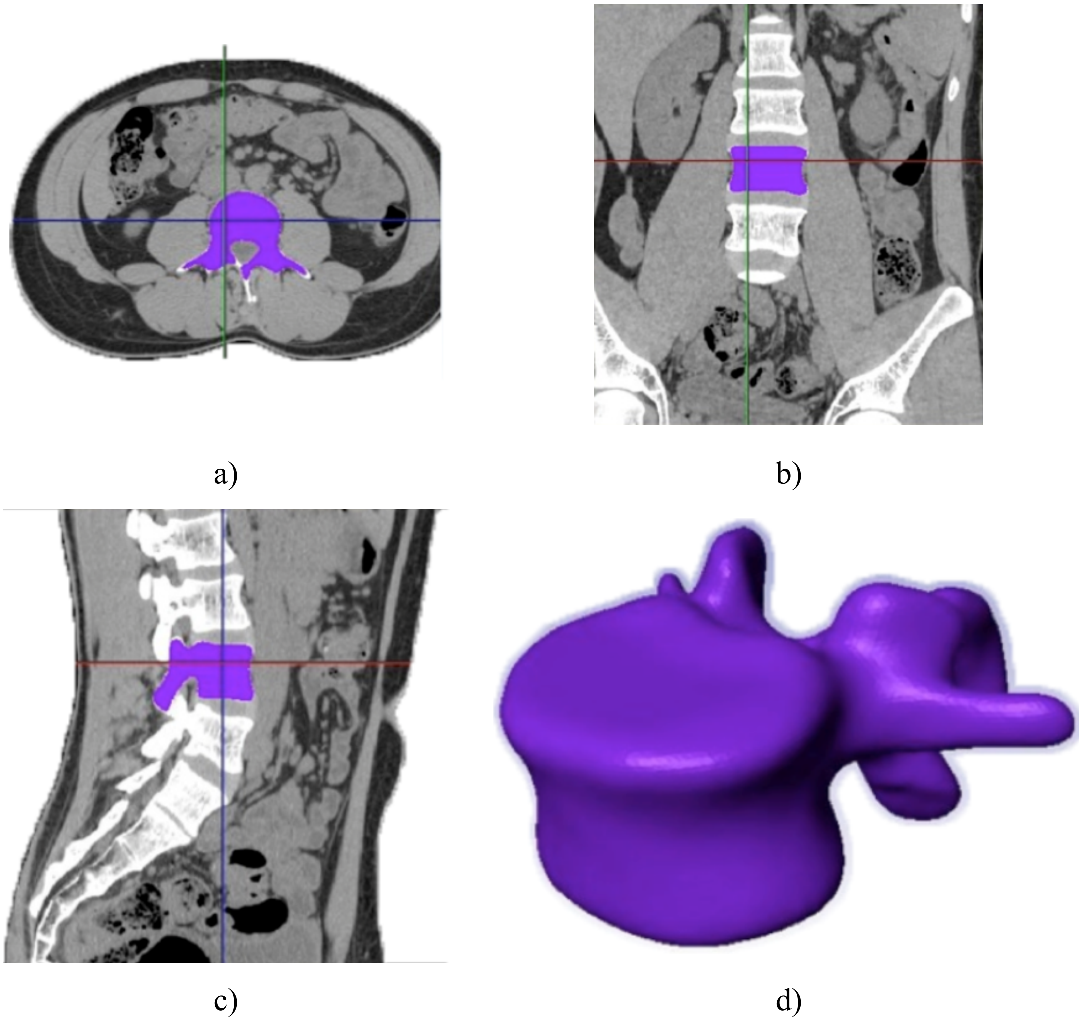

Figure 6.3 Different views of a vertebra mask in ScanIP Software once the mask and filters tools were applied.

Figure 6.4 illustrates the process explained above. In Delcam Software the triangular surfaces imported from ScanIP are repaired and patched to convert them into a solid model. Finally, the solid model of the vertebra is exported into the Abaqus/CAE 6.10© finite element analysis software.

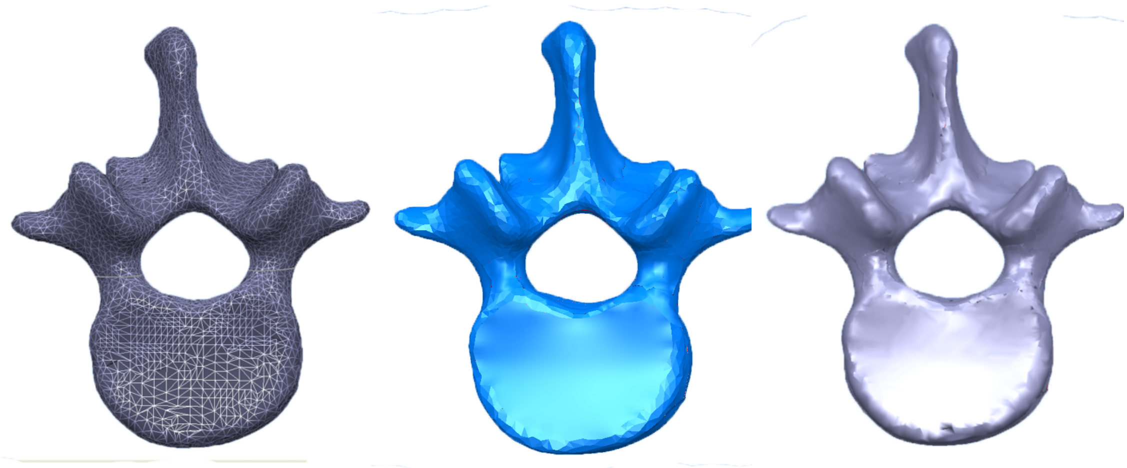

a) Triangular Surfaces b) Patched Surfaces c) Solid Model

Figure 6.4 Different steps to obtain the geometry of a vertebra.

6.3 Materials

The geometry, material properties, constraints and loading conditions are the main components required to recreate or generate an accurate model of the spine. However as Wilkox *et al*. and Zander *et al*. state in their studies of the spine, the determination of these properties in biological systems can be extremely challenging[24, 139]. The main difficulties mentioned are the complex geometry of the bones and the substantial differences in the material properties of the biological tissue and the loading conditions that vary within each individual. This section describes the material properties that were selected for the lumbar vertebrae, the sacral bone, and the soft tissue of the lumbosacral spine.

6.3.1 Vertebrae

All the bones at the macrostructure level can be divided into two sections; the cortical or compact bone and the trabecular or cancellous bone. The distribution of these types of osseous material depends on the geometry and the length of every bony structure.[31, 194]

As opposed to the femur, which is mainly formed by cortical bone in the middle and by trabecular bone surrounded by a cortical shell at the ends, vertebrae consist of a thin cortical shell that surrounds a matrix of cancellous bone in the vertebral body, and a combination of these two types of bone in the posterior elements where it is difficult to differentiate the bone types.[31]

As a consequence of this bone distribution several studies have divided the vertebrae into two or three sections depending on the anatomy of these bones. For this study the Sacrum was divided into the trabecular bone surrounded by a thin cortical shell whereas the Lumbar vertebrae were divided into three parts; the cortical bone, the trabecular bone and the posterior elements section. The figure 6.5 shows the different types of bone in one vertebra of the lumbosacral spine.

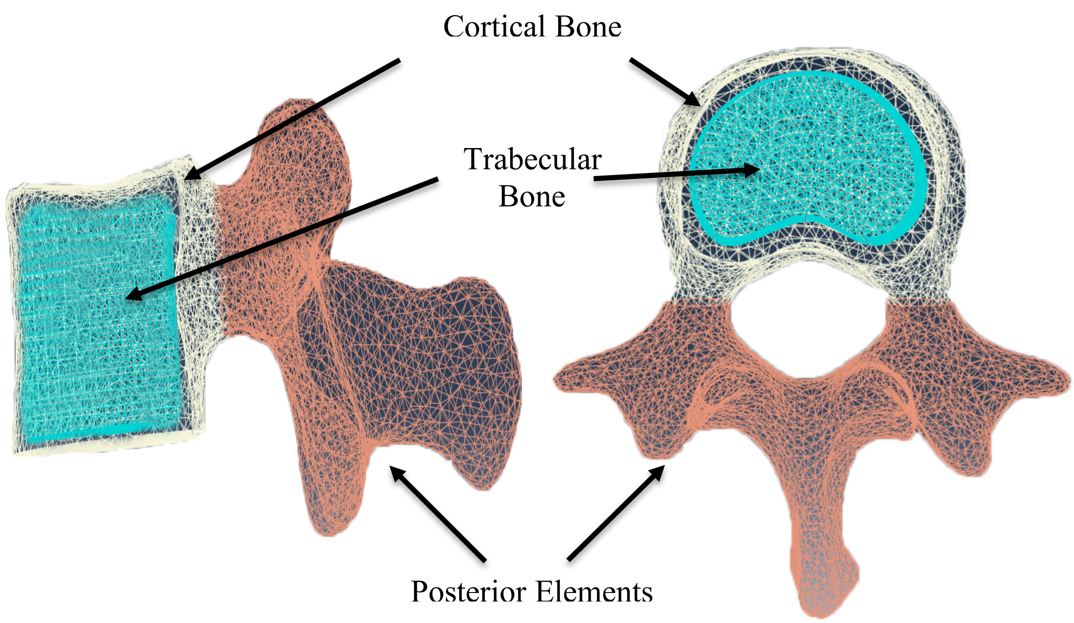

Figure 6.5 Parts and types of bones used in the vertebrae

The selection of the material properties of the vertebrae depends on the purpose of the investigation and the complexity of the problem. Whereas some investigations simulate the bones as an anisotropic structure or as a rigid body, most commonly the bone is represented as a homogeneous isotropic elastic material. In Table 6.1 the material properties used to simulate the different types of bone used for this study are presented. [50, 150, 194-196]

Table 6.1 Material properties used in the vertebrae elements [50, 150, 194-196]

Material	Young's Modulus [MPa]	Poison's Ratio	Behaviour
Cortical Bone	12,000	0.300	Homogeneous, Elastic, Isotropic
Trabecular Bone	100	0.200	Homogeneous, Elastic, Isotropic
Posterior Elements	3500	0.25	Homogeneous, Elastic, Isotropic

6.3.2 Intervertebral Discs

The Intervertebral Disc can be divided into three different parts; the Annulus Fibrosus, the Nucleus Pulposus and the Cartilage End Plates.

For the five intervertebral discs, the Nucleus Pulposus was considered as a homogeneous, isotropic material. As mentioned in the section 2.3 from chapter II, this part of the disc is mainly constituted of water, and so for this reason the center of the disc was simulated as an incompressible fluid with a Poisson Ratio of v=0.499 and a stiffness of 1MPa.[195, 197, 198]

There are different approaches to recreate the mechanical characteristics of the Annulus Fibrosus. Some studies replicate it as a Hyperelastic or Viscoelastic material. However, in other investigations and for this study, this structure was considered as a composite material formed by a ground substance reinforced with 8 concentric fibre layers.[142, 143, 199]

The ground substance of this element was simulated as a linear elastic material and the fibres were simulated using *Rebar elements* that functioned as reinforcement within the solid. The properties of these layers changed along the radial axis increasing stiffness from the centre to the outer surface of the disc. These layers were oriented at 30 and 150º relative to the cross-sectional area of the disc and defined as a "No Compression elements" in order to represent the correct behaviour of the

Annulus Fibrosus.[129, 195]. The next figure shows the structure of the nucleus pulposus and the annulus fibrosus with its fibre elements inserted into the ground substance.

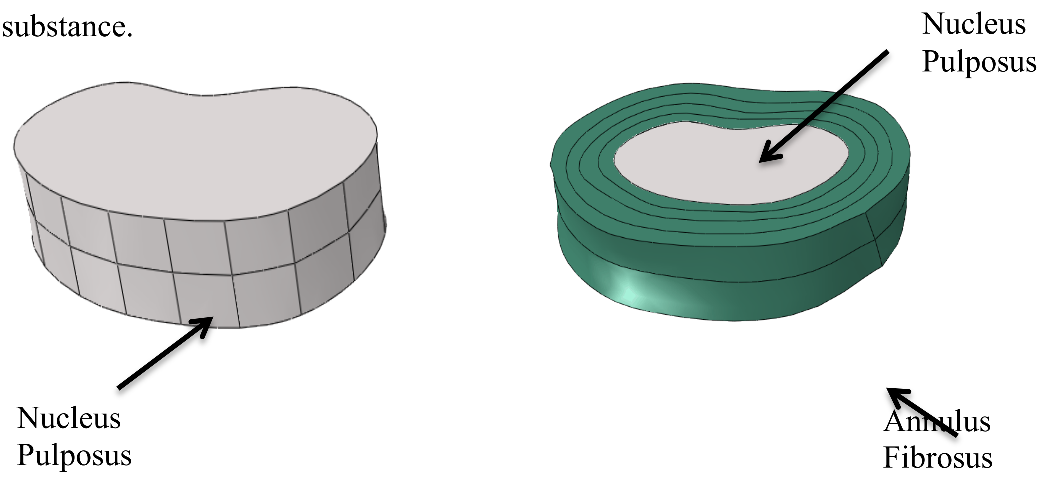

Figure 6.6 Nucleus and the Annulus Fibrosus of the Intervertebral Disc

The Cartilage Endplate serves as an interface between the intervertebral disc and the vertebra body. Several studies have measured this element obtaining a thickness between 0.5 mm and 1mm. For this study, the cartilage endplate was simulated as a homogeneous isotropic elastic material with a thickness of 0.5mm. The material properties of the Nucleus Pulposus, the ground substance of the Annulus Fibrosus, the Annulus Fibres and the Cartilage Endplates were obtained from the literature and are given in Table 6.2 [8, 134]

Table 6.2 Materials Properties used in the Intervertebral Disc [8, 134]

Material	**Young's Modulus [MPa]**	**Poison's Ratio**	**Behaviour**
Nucleus Pulposus	1	0.499	Homogeneous, Elastic, Isotropic
Annulus Fibrosus (Ground Substance)	3.15	0.45	Homogeneous, Elastic, Isotropic
Annulus Fibres	358 - 550	0.3	Uniaxial Reinforcement
Cartilage Endplates	24	0.4	Homogeneous, Elastic, Isotropic

6.3.3 Ligaments

The ligaments of the spine hold the vertebrae together providing support to the entire spinal column. As mentioned in Chapter 4, most of the studies that investigate the behaviour of the lumbar spine and the sacrum, a total of nine ligaments are used in the finite element model. These ligaments are the Anterior Longitudinal Ligament (ALL), the Posterior Longitudinal Ligament (PLL), Ligament Flavum (LF), Capsular Ligament (CL), Interspinous Ligament (ISL), Supraspinous Ligament (SSL), Intertransverse Ligament (ITL), Iliolumbar Ligament (ILL) and the Sacroiliac Ligament (SIL).[139-143]

Some studies simulated the spinal ligaments as three-dimensional structures or as cable elements that are active only in tension. For this investigation the ligaments were modelled as spring elements with stiffness characteristics during tension and without stiffness attributes during compression. The stiffness properties of these elements were assigned in the Abaqus/CAE 6.10© file, where a non linear behaviour was defined using the material properties showed in the Table 6.3. The point where the ligaments are inserted into the vertebra, the dimensions and the material properties of the tissues were simulated in accordance with the CT scan data and information available in the literature.

Table 6.3 Materials Properties used to simulate the Ligaments [49, 50, 115, 139, 143, 146, 196, 200-204]

Ligaments		**Stiffness (N/mm) (non-linear)**
Anterior Longitudinal Ligament	ALL	347-1864
Posterior Longitudinal Ligament	PLL	29.5-236
Ligament Flavum	LF	7.7-58.2
Capsular Ligament	CL	36-384
Inter Spinous Ligament	ISL	1.4-14.37
Supra Spinous Ligament	SSL	2.5-34
Intertransverse Ligament	ITL	0.3-10.7
Iliolumbar Ligament	IL	1000
Sacroiliac Ligament	SIL	5000

Once all the elements of the healthy lumbar spine were assigned material properties, they were assembled together for FEA. The position of each structure was based in the coordinates assigned by the CT Scan data software.

The next figure shows the assembly of the healthy lumbosacral spine. This assembly include the 5 lumbar vertebrae (L1-L5), the sacral bone, the five intervertebral discs including its cartilage endplates and the ligaments.

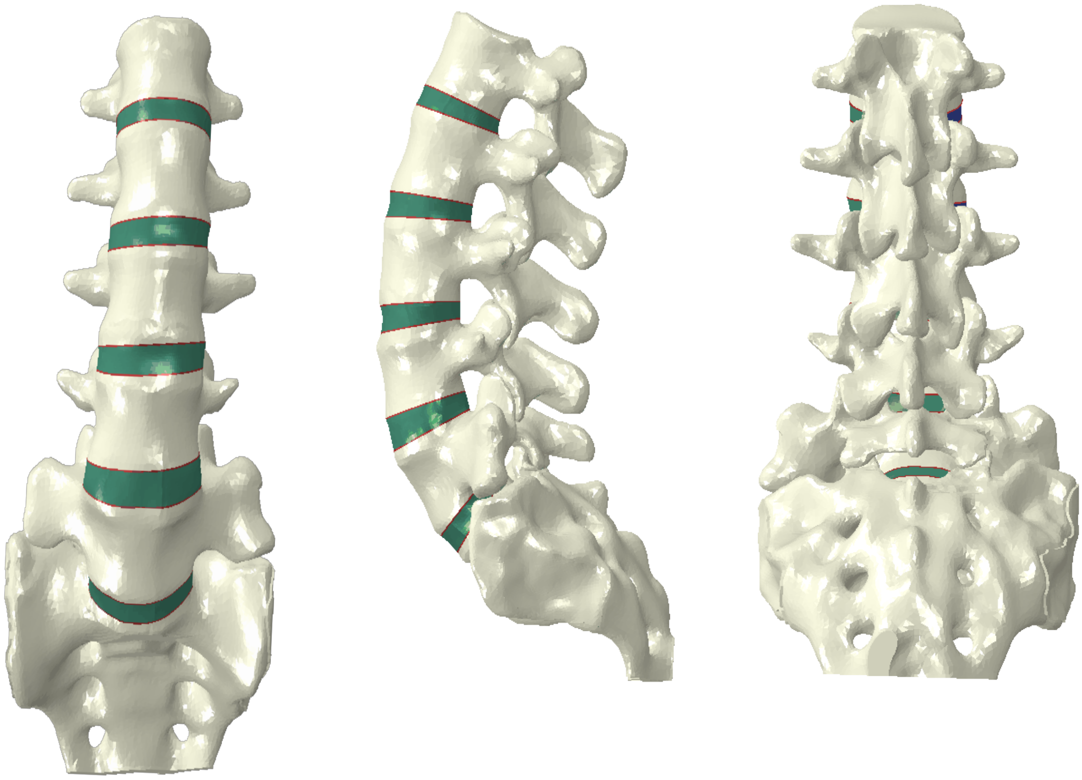

a) Frontal b) Lateral c) Posterior

Figure 6.7 Different views of the geometry of the Healthy Lumbosacral Model including the 5 lumbar vertebrae (L1-L5), the sacral bone, the five intervertebral discs including its cartilage endplates and the ligaments.

6.4 Instrumentation

In both posterolateral fusion and posterior interbody lumbar fusion techniques, the surgeon uses 4 titanium pedicular screws, 2 titanium rods and 2 intervertebral body cages of 0º or 4º of inclination. The geometry of these devices was created using as a base the screws, rods and cages provided by the surgeon and the material properties were obtained from the literature.[2, 152, 199]

The posterior instrumentation was simulated as a homogeneous elastic material with the properties of titanium. For the fusion surgeries at this part of the lumbar spine the recommended size of the pedicle screws is 6.5 mm in diameter with a length of 55 mm and for the rods a diameter of 6 mm.[199]

As in every device inserted in the human body the dimensions of the implants can change to match the size of the patient. For this study, the medical supervisors confirmed that the dimensions of the screws were correct for the proportions of the vertebrae.

The geometry of the screws and rods was created using the SolidWorks, Education Edition Software, (Dassault Systemes Corporation). In the case of the pedicular screws, the threads were ignored. This assumption, which will be explained below in the boundary condition section was based on the interaction between the bones and the screws, which was modelled as if there was no motion between these two structures. The next figure shows the dimension of the screws and rods and the geometry that was created for the simulation.

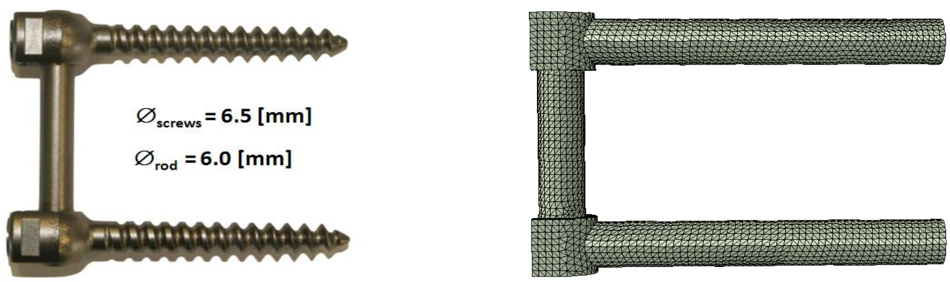

Figure 6.8 Rod and Pedicular Screws

To simulate the posterior lumbar fusion procedure, two PEEK interbody cages without inclination (0 Degree) and two PEEK interbody cages of dimension 7-9mm x 11 mm x 25mm (4 Degree) were created. The geometry of these cages was again created using SolidWorks, Education Edition Software.

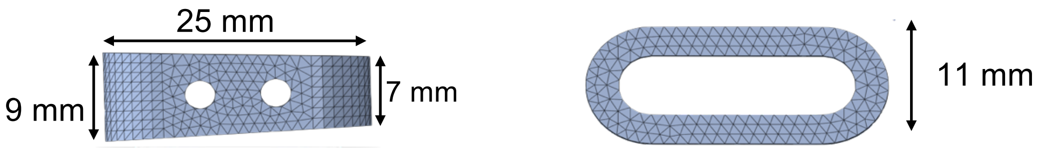

a) Lateral view b) Superior view

Figure 6.9. Dimensions of the intervertebral 4º PEEK cages

Once the geometry was built, these cages were imported into the Abaqus CAE software to assign the material properties and to assemble them into a Lumbar Fusion model. In order to recreate a reliable model that simulated the conditions of the surgeries, the location and the position of these devices was supervised and corrected by the surgeons.

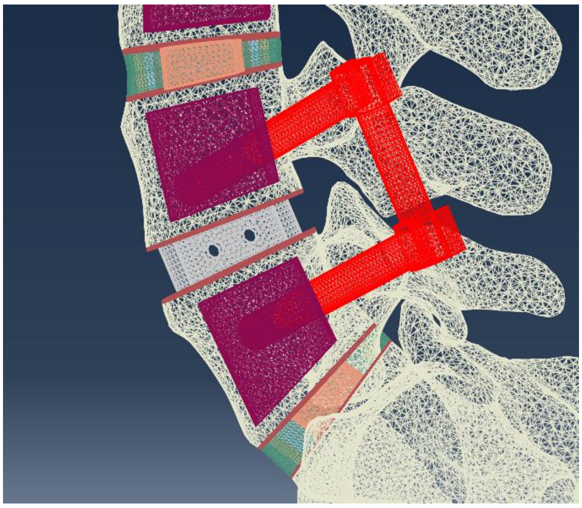

Figure 6.10. Lateral view of the screws and cages inserted at the L4/5 level

The next table presents the material properties, obtained from the literature, used to simulate the virtual instrumentation used to simulate the fusion techniques investigated in this study.

Table 6.4 Materials Properties used in instrumentation [2, 152, 199]

Material	Young's Modulus [MPa]	Poison's Ratio	Behaviour
Titanium Pedicle Screws	110,000	0.30	Homogeneous, Elastic plastic, isotropic
Titanium Rods	110,000	0.30	Homogeneous, Elastic plastic, isotropic
Peek Cages	3500	0.30	Homogeneous, Elastic plastic, isotropic

6.5 Development of the three fusion procedure models

In order to understand how the instrumentation affects the lumbar spine, the healthy lumbosacral model described above was used as the basis to create the structures that simulate the five different conditions investigated in this study. The modifications made to the healthy spine model are to understand the effects of the fixation system on the lumbar spine without the alterations that a pathological model could cause. These models are:

- Posterolateral Fusion Model
- Posterior Interbody Lumbar Fusion without Fusion (0 º)
- Posterior Interbody Lumbar Fusion following ossification (0 º)
- Posterior Interbody Lumbar Fusion without Fusion (4 º)
- Posterior Interbody Lumbar Fusion following ossification (4 º)

6.5.1 Posterolateral Fusion Model

To simulate the lumbar spine with the fixation system implanted, the healthy spine model was modified to include four pedicle titanium screws and two titanium rods. With the advice of the medical advisors, the screws were positioned on each side of the L4 and L5 vertebrae through the pedicles into both cortical bone and trabecular bone and linked together on both sides of the vertebrae by two titanium rods as seen in Figure 6.11. As mentioned before, these screws are assembled as if there was no motion between these two structures.

The insertion of the pedicle screws for this kind of surgery would only be used when the intervertebral disc at the damaged level has some kind of degeneration. However, for this investigation the L4/5 intervertebral disc wasn't degenerated for this study to have a clear comparison of the repercussions of the fixation system at the surgery level and at the adjacent intervertebral discs compared to the healthy intact spine.

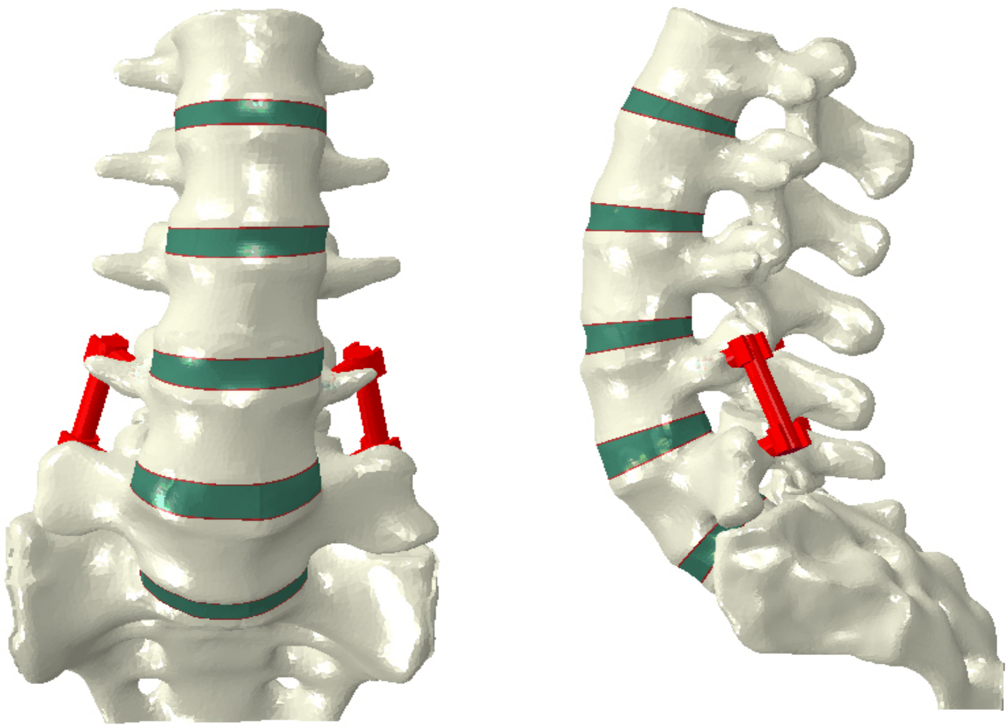

a) Frontal view　　　　b) Lateral view

Figure 6.11 Frontal and Lateral view of the Posterolateral Fusion Model

6.5.2 Posterior Interbody Lumbar Fusion (prior bone fusion)

To simulate the lumbar spine with the cages and the posterior instrumentation the healthy lumbosacral model was again modified to insert these devices. As same as the Posterolateral Model four pedicle titanium screws and two titanium rods were added on each side of the L4 and L5 vertebrae. For these models the L4-5 intevertebral disc was removed and two polyether ether ketone (PEEK) cages with 0^0 and 4^0 of inclination were positioned in the space previously occupied by the fourth interverbral lumbar disc. The positioning of the screws and cages was made by following the surgeon's instructions and was based on x-ray images of the completed surgery. The next figure shows the lateral and the posterior view of the implant in position.

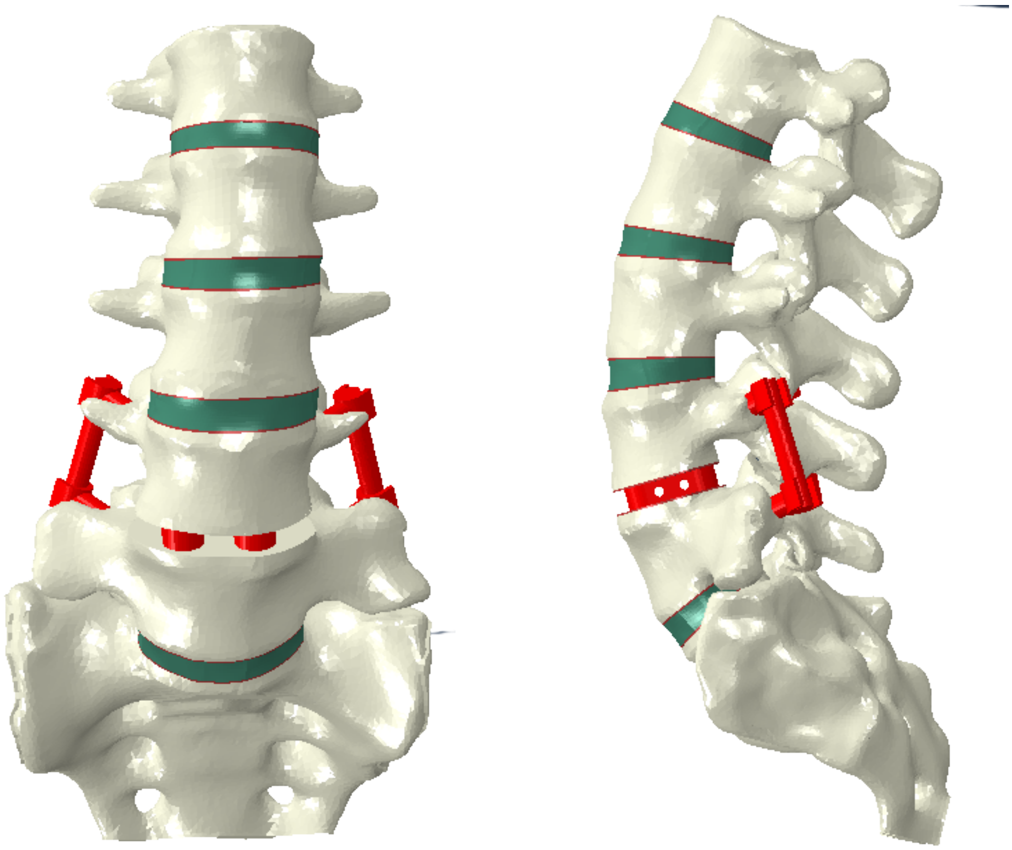

a) Frontal view   b) Lateral view

Figure 6.12 Frontal and Lateral view of the models with 0^o cages.

6.5.3 Posterior Interbody Lumbar Fusion (after ossification)

In order to simulate the bone growth between the L4 and L5 lumbar vertebrae the previous model was taken as a base. The screws, rods and the interbody cages remained in the same location and with the same boundary conditions. The modifications consisted of filling the voids inside and around the PEEK interbody cages, covering the space left by the intervertebral disc with a material that replicate the mechanical properties of the cortical bone. This model represents the ideal case of a perfect fusion between the vertebrae, and for this reason the boundary conditions were assigned as if there was no motion between the new bone and the vertebrae. The next figure shows different views of the model described.

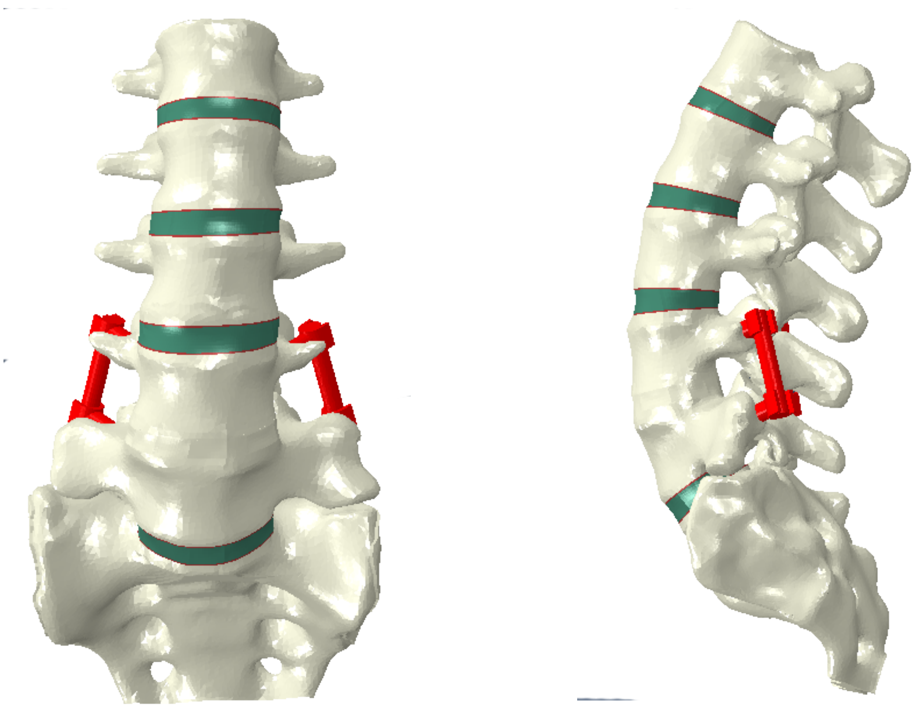

a) Frontal view b) Lateral view

Figure 6.13 Frontal and Lateral view of the PLIF models with 0^o of inclination

After the 6 different models were created, all the scenarios were simulated using the loads and boundary conditions described in section 6.6.

6.6 Loads, contacts and Boundary Conditions

The spine is a flexible structure that bears the weight of the upper body and carries loads derived from human activity. Like most structures in the body, the spine is composed of many different elements that affect its movement and respond to different loads. For this reason, it is necessary to consider the different physiological boundary conditions like the interactions with other bones, the effects of muscle forces, and the kinematic constraints. Unfortunately, modelling every component is often not achievable, and determining which components are critical is difficult.
This section will explain the loads applied to the lumbosacral model and the boundary conditions used in the model in order to simulate the interfaces between the vertebrae, soft tissues, ligaments and the devices.

6.6.1 Loads

For this study different load conditions were employed to analyse the compression, flexion, extension, torsion and lateral bending motions.

The lumbar spine by itself, without muscle support is an unstable structure, and so, if a load is applied in the axial direction at the top of the L1 vertebra without muscle support, the spine tends to buckle, as shown by Bresler and Lucas [205]. Additionally, Patwardhan *et al*. [206], undertook various experiments on cadaveric lumbar spines in which they tested the stability of the spine between a compressive vertical load applied at the top of the L1 vertebra and a compressive follower load that consisted of a compressive load that followed the path of the lordotic curve in this part of the spine.[207]

After this set of experiments, many other analytical and experimental investigations concluded that the follower load reproduced the effect of the muscles of the lower back, giving stability to the structure and showing that the follower load supported a greater load carrying capacity than the load applied in a vertical direction.[15, 146, 151, 199, 208, 209]

In this study, for the standing position, a follower load of 500N was applied. This load was simulated by attaching spring elements on each side of the vertebra as shown in Figure 6.14. These elements were assigned mechanical properties simulating a pretension of 250 N on each side of the lumbar spine following the lordotic curve of the spine, preventing any rotational movement between each segment.

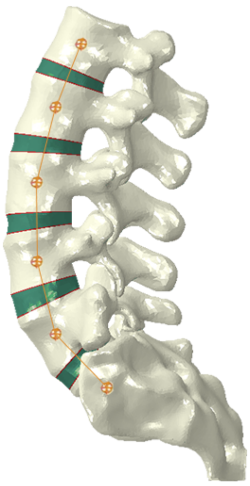

Figure 6.14 Follower load of 500N applied by attaching spring elements on each side of the vertebra (Abaqus/CAE 6.10).

In the case of the flexion, extension, lateral bending and rotational movements, in addition to the follower load, moments of 7.5 N.m was applied to a node, which was kinematic coupled to the top surface of the L1 vertebrae as shown in Figure 6.15.

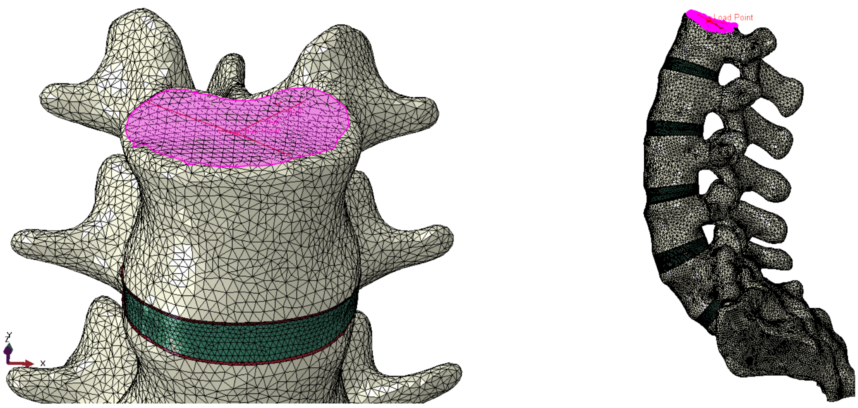

a) b)

Figure 6.15 Frontal and Lateral view of the models with 4 degree cages

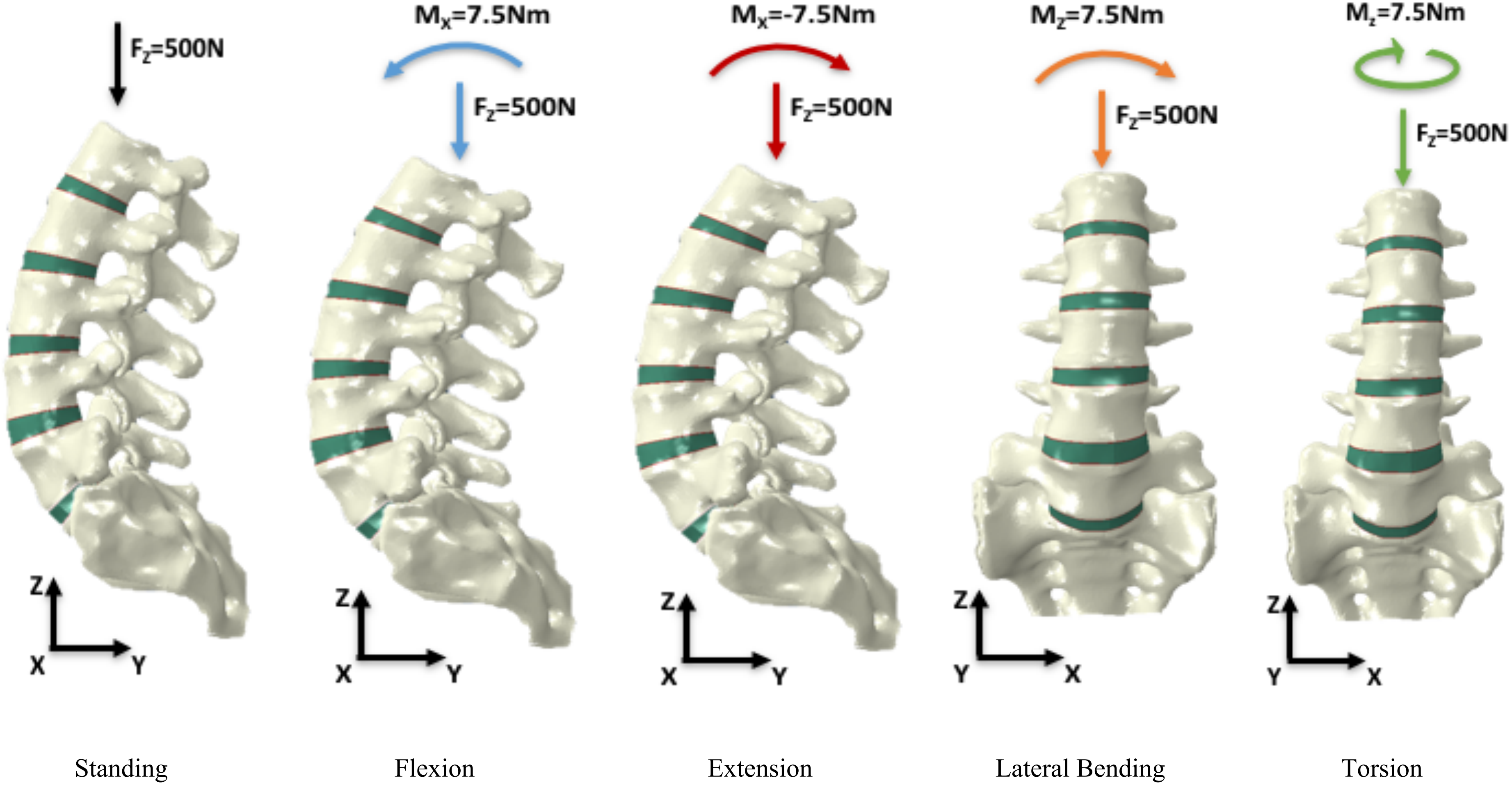

Figure 6.16 Five different movements in the lumbar spine.

6.6.2 Contacts and Boundary Conditions

After all the elements were assembled in the correct position with appropriate material properties assigned, the interaction between the various parts and the boundary conditions were defined.

To simulate the interfaces between the vertebral bodies, the Cartilage Endplates and the intervertebral disc, including the annulus fibrosus and the nucleous pulposus, a tie constraint boundary condition that ties the two surfaces in contact forming a contact pair together for the duration of the simulation was used to ensure that all the nodes considered under this boundary condition underwent the same displacement.

Similar to other studies in order to simulate the ideal postoperative bond between the vertebrae surfaces and the pedicular screws, a tie constraint boundary condition explained before was used to simulate all the model surfaces in contact with the fixation system.[146, 152, 197, 199, 210, 211]

For the case of the interaction between the PEEK interbody cages and the vertebral body, other investigations had simulated this interaction as a surface-surface contact problem simulating a high friction coefficient between these two elements. However, because this study does not investigate the motion of the cages or the stresses in these elements but rather how these elements affect the behaviour of the spinal components once inserted, a tie boundary condition was simulated that represented the conditions after a successful operation.[6, 15, 129]

For the models that simulated the intervertebral bone fusion, the interaction between the vertebrae and the new bone formed was simulated as if the bone was completely attached to the vertebrae. For this condition a tie constraint was also used between these elements.

To simulate the interaction between the ligament structures and the vertebrae a kinematic coupling constraint was used at the attachment points of the springs elements. A kinematic coupling constrains a group of slave nodes to the translation and rotation of a master node alleviating the local stress concentrations at one point and the localized deformations, which do not represent the correct behaviour of the ligaments.[49, 143, 212]

In order to have a correct representation of the behaviour of the sacro-lumbar spine the contact between the vertebrae facet joints must be accurately simulated. For this model this condition was simulated as a frictionless surface-surface contact interaction, where the elements only transmit forces perpendicular to the surface orientation.[51, 196]

For the inferior part of the spine segment the boundary condition used was to fix the auricular surfaces of the sacrum rigidly in all directions simulating the contact with the Ilium in order to generate similar conditions to the ones used in experimental studies. As shown in Figure 6.17, in this model, the auricular surface of the sacrum was fixed in all directions.[140, 141]

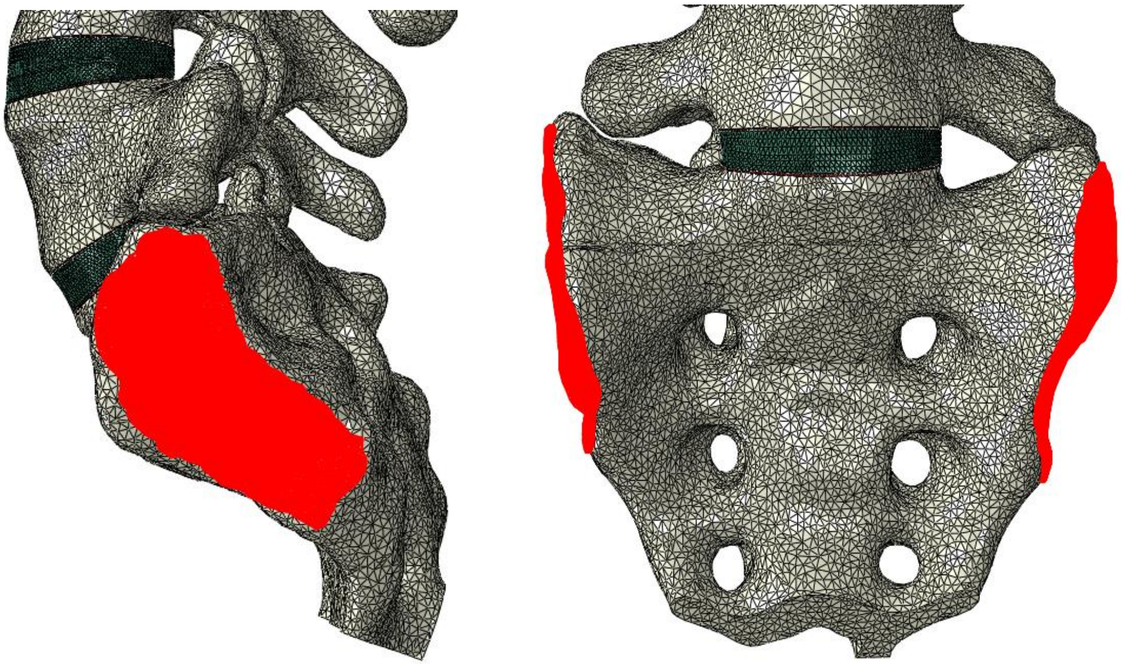

Figure 6.17 Fixed areas at the auricular surface of the sacral bone simulating the contact with the Ilium

6.7 Mesh Analysis

A mesh sensitivity analysis on the healthy lumbosacral model and on the instrumentation was undertaken to ensure the accuracy of the predictions of the models without excessive computational resources being required. To consider that a mesh is adequately refined for a finite element analysis some studies suggest that the results of the selected mesh cannot vary more than 5% with the predictions of a finer mesh. Because the complex geometry of the vertebrae, the soft tissue and the posterior implants, all the model parts, except for the ligaments, were meshed using four node linear tetrahedral elements.[24, 213]

In order to guarantee accurate predictions a mesh convergence study was performed using various mesh densities on the healthy spine model. For this analysis the model was loaded with the same loading and boundary conditions for all the tests and the variation in the von Mises stress and the ROM was calculated between the different meshes.

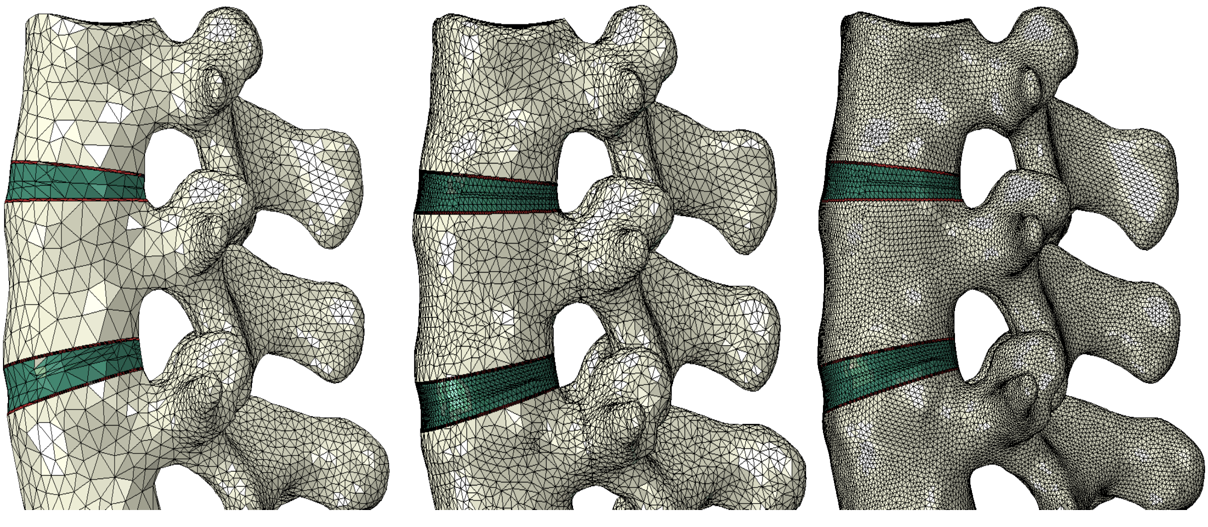

a) Coarse b) Regular c) Fine

Figure 6.18 Different Types of mesh used in the lumbosacral model mesh convergence analysis.

Due to the irregular geometry of the model, different points were evaluated as a part of the mesh convergence analysis to obtain the most appropriate mesh for the lumbosacral healthy model. The mesh that consist of 1,225,798 elements was chosen as the definitive mesh because the percentage change in the vertebral von Mises stress between this mesh and finer meshes was less than 4% and less than 3% for the ROM. This mesh was also used as the basis for creating the models employed in the investigation of the fusion techniques. Figure 6.19 shows the convergence analysis performed in a point located at the L1 vertebra, were the maximum von Mises stress was located in this part of the model.

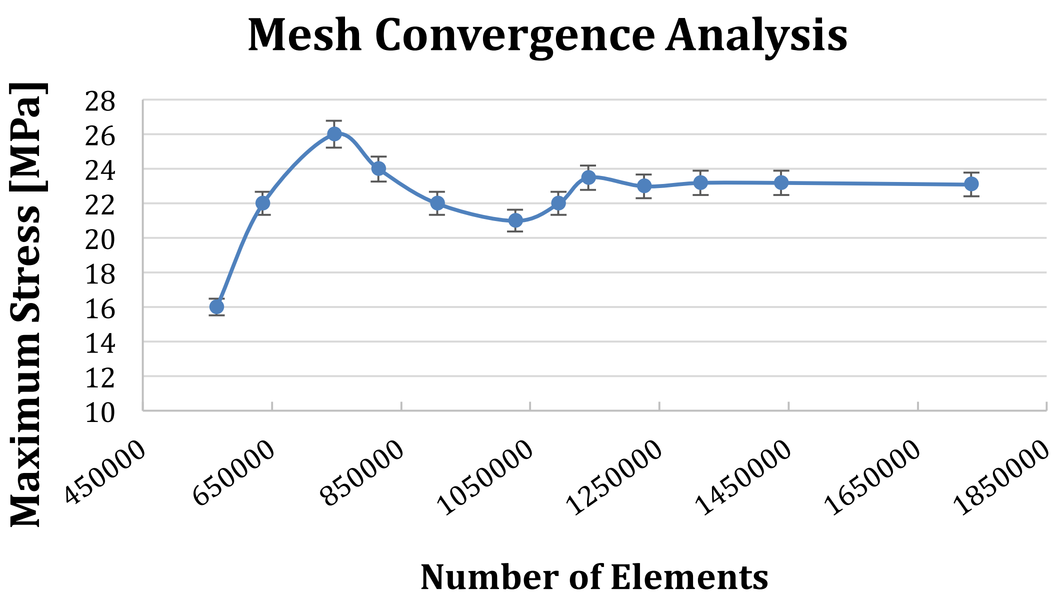

Figure 6.19 Mesh Convergence Analysis for the Lumbosacral healthy model

In the case of the pedicular screws, rods and PEEK interbody cages the same convergence analysis was done to every structure. The Figure 6.20 shows the different meshes used in the intervertebral body cages.

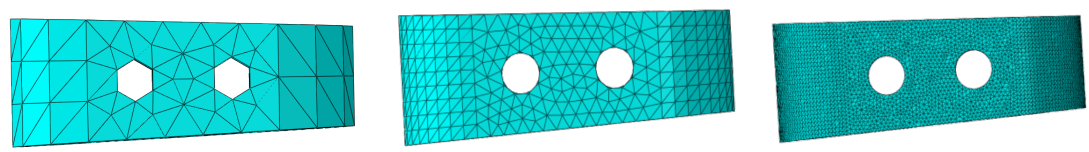

a) Coarse b) Regular c) Fine

Figure 6.20 Different Types of mesh used in the Intervertebral Cages mesh convergence analysis

6.8 Model Validation

The healthy spine model was validated against two cadaveric studies and two existing analytical investigations [25, 195, 214, 215]. The model validation consisted of comparing the ROM and intervertebral disc pressure predictions of the healthy lumbar spine model with results from the studies cited before. The mesh established by the mesh sensitivity analysis was used in the validation analysis.

To validate the ROM at each intervertebral disc level, output of the computational model was compared with the results from previous studies (Figure 6.21) using the same loading conditions applied by Yamamoto *et al*. [25]. The model constructed for this study predicted a total ROM of 32.7^{o} in flexion and 23.4º for lateral bending with the cadaveric studies reporting total ROM in the range 29.8^{o} – 38^{o} and 19.9º - 25.3º respectively for the same physiological conditions. In extension and torsion, the current study predicted total ROMs of 21.8^{o}, 8.9^{o} respectively both of which are above the upper values (2.2 ^{o} for Extension, 0.4 ^{o} for Torsion) of the corresponding ranges obtained from the cadaveric investigations.

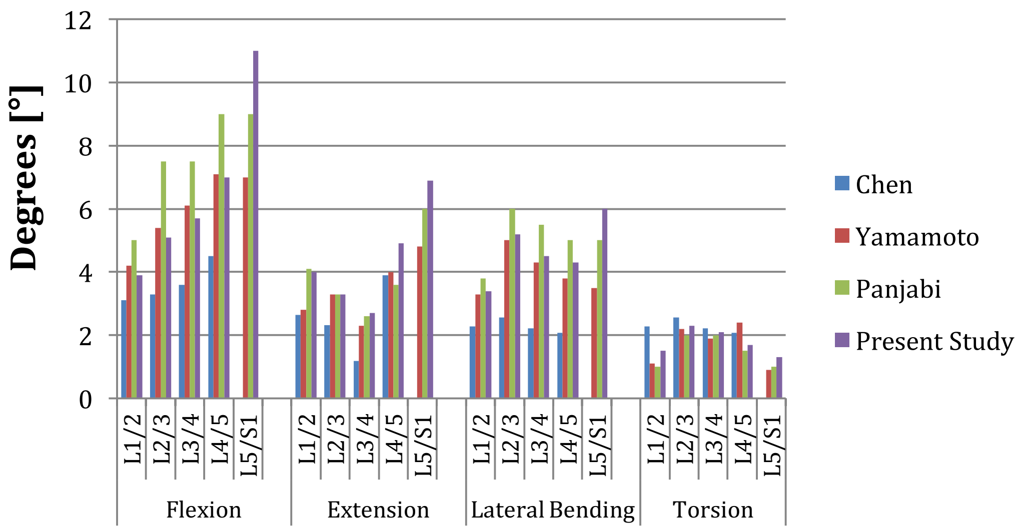

Figure 6.21 ROMs comparison for the five levels of the health lumbar spine model using the same loading conditions applied by Yamamoto et al.

Compared to the previous finite element investigation of a healthy spine undertaken by Chen *et al*. [195], our model predicted more flexible behaviour in flexion, extension and lateral bending but slightly stiffer behaviour in torsion. The model developed by Chen *et al*. considers only five levels, L1-L5, of the lumbar spine with the lower surface of the L5 vertebra being fixed. This will have had the effect of restricting motion at the intervertebral disc levels above, resulting in the generally stiffer behaviour exhibited in flexion, extension and lateral bending compared to both our model and the cadaveric studies.

For the intervertebral disc pressure validation, the results predicted on this investigation were compared against the results of an investigation that evaluated eight different validated finite element models of the healthy lumbar spine [214]. The geometry of these models, that include al least five lumbar vertebrae and four intervertebral discs, was obtained from CT scans of living subjects and cadaveric specimens. For this validation analysis the loading conditions were taken from FE studies by Rohlmann *et al*. [216] for the flexion and extension motions a by Dreischarf *et al*. [217]for the lateral bending and torsion motions.

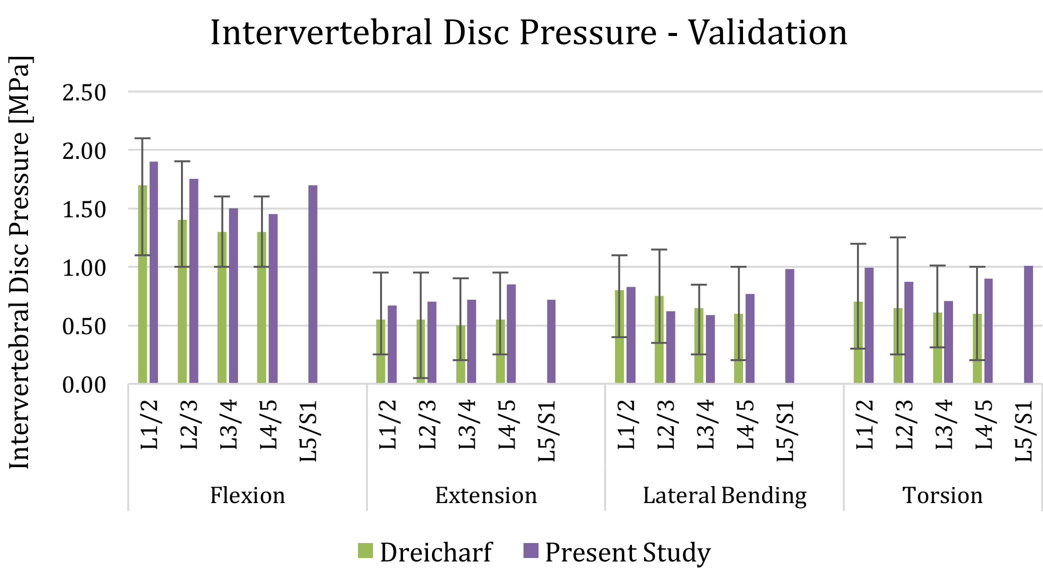

Figure 6.22 Intervertebral Disc Pressure calculated for the five Intervertebral Discs of the health spine model compared with previous finite element investigations.

The lumbosacral model created for this investigation predicted a higher Intervertebral Disc Pressure than the median value results of the eight models analysed in the Dreischarf study, for the four motions considered. However, the intervertebral disc pressure predicted for the model created for this investigation is within the range of the values presented as shown in Figure 6.22.

Having analysed model predictions and having compared them with the previous experimental trials detailed on figure 6.21 and figure 6.22 the lumbar spine model was considered to have been validated and as such could then be used as the basis for investigating the three fusion techniques.

Chapter VII Results

7.1 Introduction

The models developed were utilized to investigate three types of fusion techniques and two types of intervertebral PEEK cages in addition to the case of a healthy spine (HS). The fusion techniques considered were the spine with a pedicle screw fixation system implanted (PLF), the spine with a pedicle screw fixation system using two 0^0 interbody cages (PLIF0NF) and two 4^0 interbody cages (PLIF4NF), and the spine with a pedicle screw fixation system evaluating the 0^0 and 4^0 interbody cages implanted following fusion across L4-L5 vertebrae (PLIF0F and PLIF4F).

Standing, flexion, extension, lateral bending and torsion anatomical motions were simulated for the six models. In each case average von Mises stresses were calculated in the cortical bone of the L1 to the S1 vertebrae and in the intervertebral discs to study the behaviour of the hole structure after the insertion of the implants. Further analysis of the maximum von Mises stress in the vertebrae and the intervertebral discs was studied for the critical scenarios. Moreover, an analysis of the maximum von Mises stress for the fixation system is presented.

After the result analysis, a comparison between the use of 0º interbody cages and 4º interbody cages is presented. The comparison considers the effect on ROM and stresses in the adjacent vertebrae, intervertebral discs and fixation system for the five loading conditions.

In addition, ROM predictions from the 3D finite element model were compared with the results from the *in-vivo* investigation presented in chapter V.

7.2 Analysis of Average von Mises Stress in the L1 to S1 vertebrae

Table 7.1 and Figure 7.2 show the results of the average von Mises stresses in the L1 to S1 vertebra for the models representing the healthy spine and the fusion techniques (PLF, PLIF0NF, PLIF0F, PLIF4NF, PLIF4F) under the loading conditions simulating the five anatomical motions.

These results shows that the fusion procedures had no impact on average von Mises stress in the cortical bone of the L1, L2, L3 and the S1 vertebrae, with stress levels for the three fusion techniques considered being comparable to the healthy spine for the five motions investigated.

In the L4 vertebra the stress increased as a result of the fusion techniques for all five motions investigated. For each of the five motions, compression, flexion, extension, lateral bending and axial rotation, the maximum stress in L4 occurred in the PLF model, where the increase in stress for each of the five movements was 43%, 17%, 71%, 39% and 44% respectively compared to the healthy spine.

Once the L4/5 disc was replaced with the 0º PEEK intervertebral cages (PLIF0NF) the stresses in the L4 vertebra dropped compared to the PLF model but still remained higher compared to the healthy simulation by 19% on average. For the case where fusion was achieved (PLIF0F), the von Mises stress increased by 14% on average over the healthy model for all five anatomical motions.

When the L4/5 intervertebral disc was removed and the 4º PEEK cages were inserted (PLIF4NF) the stresses in the L4 vertebra dropped compared with the PLF model, however, they were still higher compared to the healthy model by 19% for compression, 1% for flexion, 48% for extension, 19% for lateral bending and 20% for axial rotation. Stress levels tended to reduce further following fusion using the same type of cages (PLIF4F), but still remained higher compared with the healthy model by up to 45%.

The effect of fusion on the L5 vertebra varied depending on the anatomical motion undertaken. Insertion of the pedicle fixation system (PLF) caused stresses to rise in the L5 vertebra by only 1% compared to the healthy model for the compression, flexion and axial rotation motions, but by 35% and 17% for the extension and the lateral bending motions respectively.

Table 7.1 Average von Mises Stress results in the vertebrae

	HS	PLF	PLIF4NF	PLIF0NF	PLIF4F	PLIF0F
Standing						
L1	1.45	1.45	1.45	1.45	1.46	1.45
L2	1.34	1.33	1.33	1.33	1.33	1.33
L3	1.20	1.18	1.19	1.18	1.19	1.18
L4	1.13	1.62	1.34	1.30	1.25	1.22
L5	1.31	1.32	1.35	1.30	1.33	1.3
S1	1.02	1.02	1.02	1.02	1.02	1.02
Flexion						
	HS	PLF	PLIF4NF	PLIF0NF	PLIF4F	PLIF0F
L1	1.64	1.64	1.64	1.64	1.66	1.64
L2	1.53	1.53	1.52	1.53	1.53	1.53
L3	1.37	1.35	1.36	1.35	1.36	1.35
L4	1.26	1.48	1.26	1.25	1.26	1.25
L5	1.48	1.48	1.57	1.50	1.56	1.49
S1	1.24	1.24	1.24	1.24	1.24	1.24
Extension						
	HS	PLF	PLIF4NF	PLIF0NF	PLIF4F	PLIF0F
L1	1.98	1.98	1.97	1.98	2	1.98
L2	1.25	1.24	1.24	1.24	1.21	1.24
L3	1.14	1.14	1.16	1.15	1.15	1.15
L4	1.12	1.92	1.66	1.63	1.62	1.61
L5	1.23	1.66	1.64	1.68	1.43	1.46
S1	0.90	0.90	0.90	0.90	0.90	0.90
Lateral Bending						
	HS	PLF	PLIF4NF	PLIF0NF	PLIF4F	PLIF0F
L1	1.80	1.81	1.81	1.81	1.81	1.81
L2	1.47	1.49	1.49	1.49	1.49	1.49
L3	1.35	1.38	1.38	1.38	1.38	1.38
L4	1.23	1.71	1.46	1.41	1.34	1.33
L5	1.37	1.6	1.58	1.53	1.44	1.38
S1	1.02	1.02	1.02	1.02	1.02	1.02
Torsion						
	HS	PLF	PLIF4NF	PLIF0NF	PLIF4F	PLIF0F
L1	1.72	1.72	1.72	1.7	1.72	1.7
L2	1.50	1.50	1.50	1.49	1.50	1.48
L3	1.35	1.32	1.34	1.31	1.33	1.31
L4	1.16	1.67	1.39	1.35	1.31	1.27
L5	1.33	1.34	1.35	1.35	1.35	1.35
S1	1.01	1.01	1.01	1.01	1.01	1.01

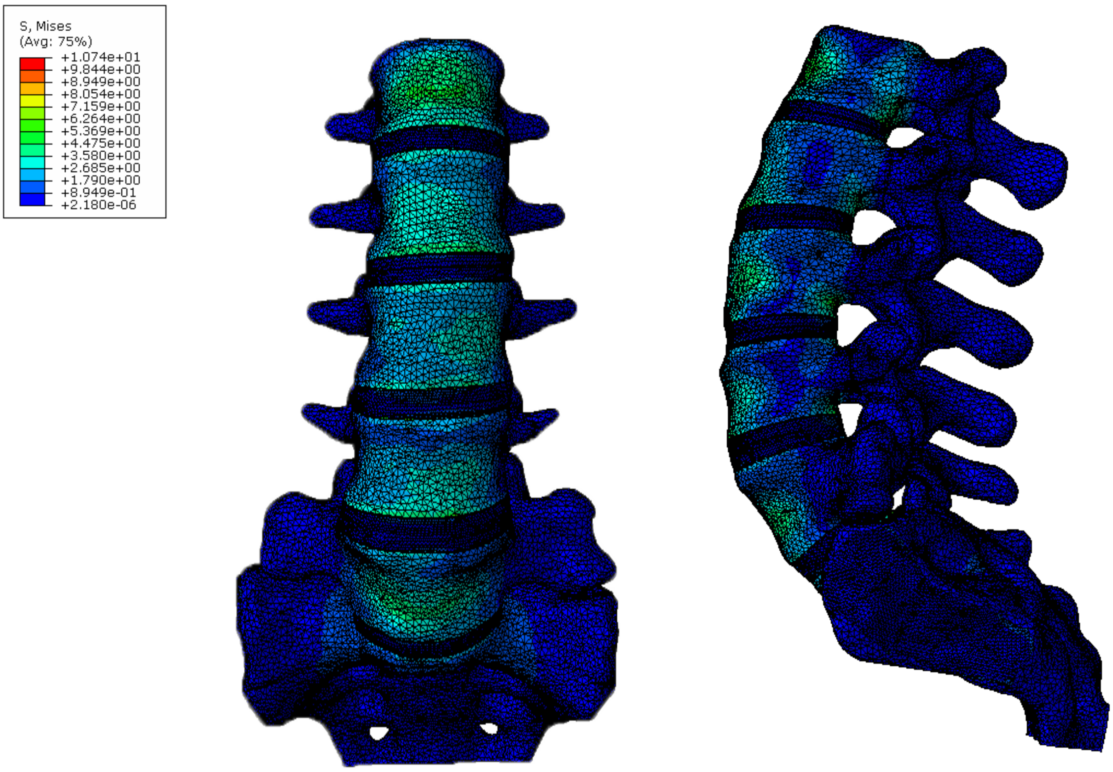

a) b)

Figure 7.1 Control plots of the lumbosacral spine a) Frontal view b) Lateral view

For the PLIF0NF and PLIF0F simulations the level of stress did not alter significantly for the L5 vertebra compared to the healthy spine for the standing position and the flexion and torsion motions (von Mises stress changed by less than 4% compared to the healthy spine). However, for the extension motion, the stress increased by up to 30% when the 0º cages were added and 15% when fusion was achieved compared to the healthy model.

The introduction of the 4º intervertebral cages at the L4-L5 level (PLIF4NF) only influenced stress levels to a relatively small degree in L5, causing stress to change by less than 5% in all cases compared to pedicle fixation alone (PLF). Following fusion, stress levels did not alter significantly for compression, flexion and axial rotation, but they reduced by 15% for extension and 8% for lateral bending compared with the model where the fusion has no yet been achieved as shown in Figure 7.2

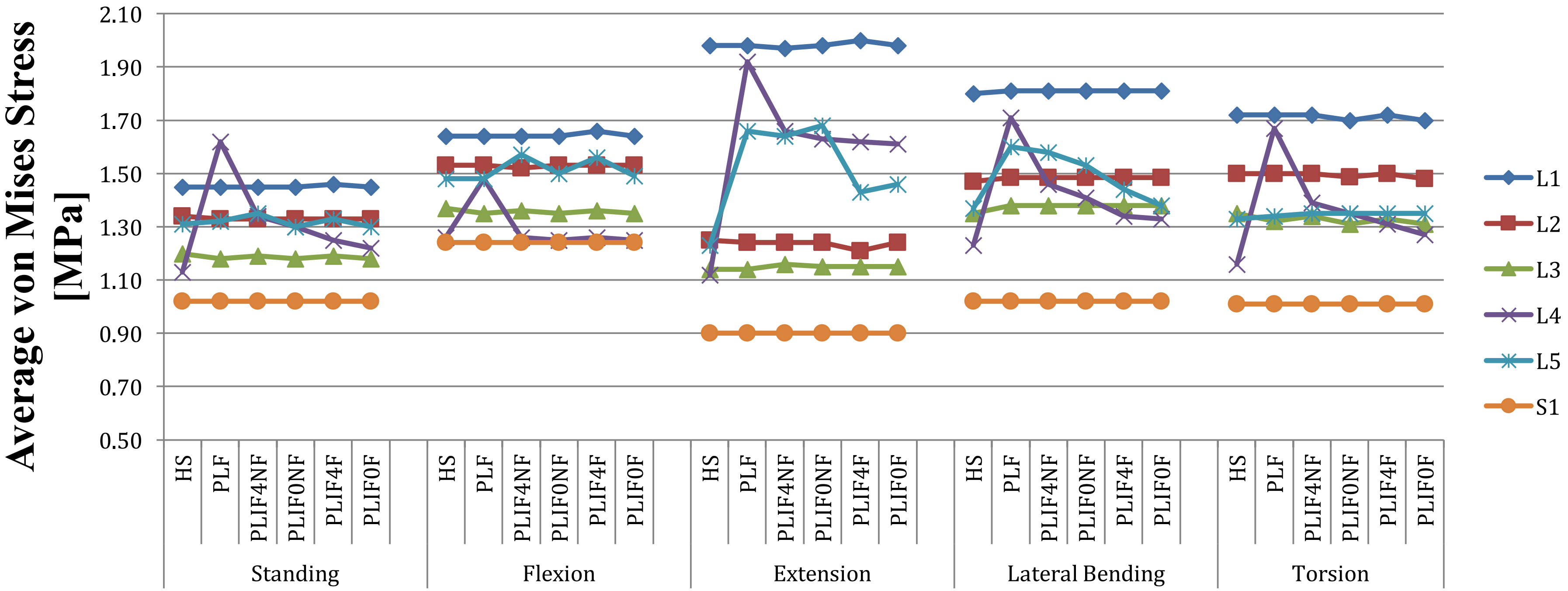

Figure 7.2 Results of average von Mises in cortical of the lumbar vertebrae for the standing, flexion, extension, lateral bending and torsion motions for the 4 models. HS-Healthy Spine, PLF-Posterolateral fusion PLIF#NF-Posterior Lumbar Interbody fusion using two 0^0 or 4^0 interbody cages prior fusion, PLIF#F-Posterior Lumbar Interbody fusion using two two 0^0 or 4^0 interbody cages following fusion across L4-L5 vertebrae level

7.3 Analysis of Maximum von Mises Stress in the L4 and the L5 Vertebrae

After the analysis of the average von Mises stress for the all the vertebrae in the lumbosacral spine, the maximum von Mises stress were calculated for the L4 and L5 vertebrae adjacent to the damaged intervertebral disc.

As it can be seen from Figure 7.3 the maximum von Mises stress for the L4 vertebra was registered when the pedicle screws were fixated without anterior supports when the extension motion was simulated. For this vertebra, situated above the damaged intervertebral disc, the highest level of stress (19.58 [MPa]), was located in the pedicle area bone/screw interface.

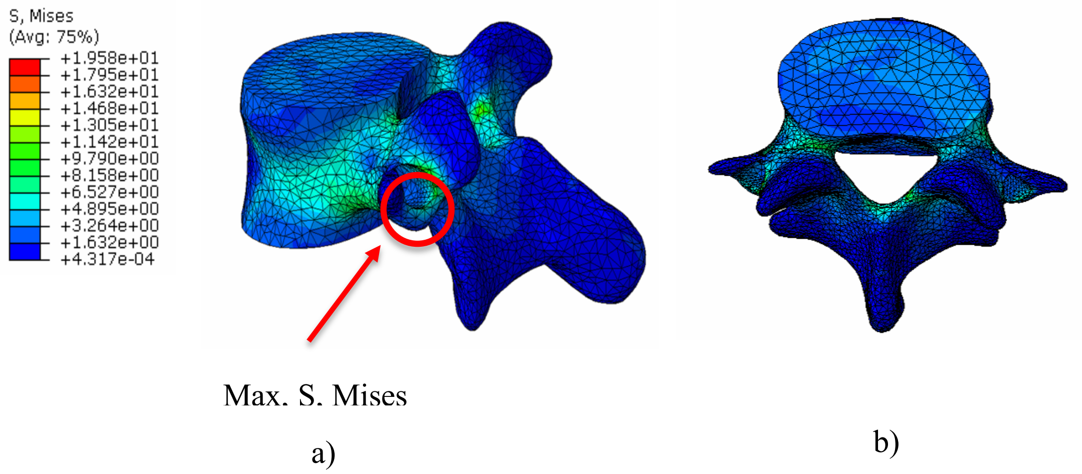

Figure 7.3 Two views of the Maximum von Mises stress registered for the L4 vertebrae a) Lateral view b) Inferior view

As same as the L4 vertebra, for the L5 vertebra, located below the damaged intervertebral disc, the maximum von Mises stress was registered in the model that simulated the extension motion in the scenario where the pedicle screws were fixated without anterior supports (PLF). For this vertebra the highest level of stress (14.14 [MPa]), was also situated in the bone/screw interface, in the location where the pedicle screw is inserted into the vertebra, as it can be seen in Figure 7.4

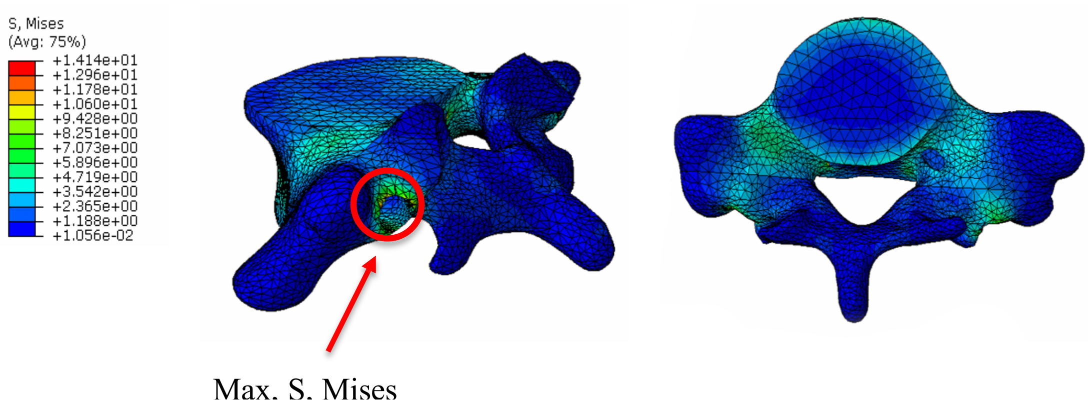

a) b)

Figure 7.4 Two views of the Maximum von Mises stress registered for the L5 vertebrae a) Lateral view b) Inferior view

The results obtained from the analysis of the maximum von Mises stress show that, although both vertebrae registered an increase in the level of stress as explained in section 7.2, the maximum level of stress in these structures are below the ultimate yield strength calculated for the lumbar vertebrae (100 - 138 [MPa]), avoiding the risk of a fracture in these elements.[218, 219]

7.4 Analysis of Average von Mises Stress in the intervertebral lumbar discs

Predicted average von Mises stress in the intervertebral disc for the six scenarios (HS, PLF, PLIF0NF, PLIF0F, PLIF4NF and PLIF4F models) and the five motions considered are shown in the Table 7.2 and the Figure 7.5.

Upon inspection of the predicted von Mises stresses presented in Table 7.2 it can be seen that the use of pedicle screw fixation, interbody cages in the spine and fusion of the L4-L5 vertebra (PLF, PLIF4NF, PLIF0NF, PLIF4F, PLIF0F scenarios) did not have a significant impact in terms of stress in the L1-2 and L2-3 intervertebral discs for the five motions considered. However, an increase in stress levels in the L3-4 and the L5-S1 intervertebral discs was observed.

Table 7.2 Average von Mises Stress results in the intervertebral discs

	HS	PLF	PLIF4NF	PLIF0NF	PLIF4F	PLIF0F
Standing						
	HS	PLF	PLIF4NF	PLIF0NF	PLIF4F	PLIF0F
L1/2	0.57	0.57	0.57	0.58	0.57	0.58
L2/3	0.71	0.73	0.73	0.71	0.73	0.71
L3/4	0.82	1.06	1.05	1.00	1.05	1.00
L4/5	1.10	0.24	-	-	-	-
L5/S1	1.19	1.35	1.42	1.42	1.42	1.42
Flexion						
	HS	PLF	PLIF4NF	PLIF0NF	PLIF4F	PLIF0F
L1/2	0.61	0.62	0.61	0.61	0.61	0.62
L2/3	0.61	0.62	0.63	0.65	0.63	0.65
L3/4	0.62	0.76	0.76	0.70	0.76	0.69
L4/5	1.08	0.38	-	-	-	-
L5/S1	1.21	1.42	1.61	1.65	1.68	1.69
Extension						
	HS	PLF	PLIF4NF	PLIF0NF	PLIF4F	PLIF0F
L1/2	0.88	0.88	0.88	0.88	0.88	0.90
L2/3	0.96	0.98	0.98	0.95	0.98	0.96
L3/4	1.01	1.35	1.34	1.29	1.34	1.30
L4/5	1.12	0.23	-	-	-	-
L5/S1	0.83	0.99	1.25	1.24	1.25	1.23
Lateral Bending						
	HS	PLF	PLIF4NF	PLIF0NF	PLIF4F	PLIF0F
L1/2	1.25	1.25	1.26	1.26	1.26	1.26
L2/3	1.01	1.02	1.02	0.99	1.02	0.99
L3/4	0.98	1.23	1.23	1.17	1.23	1.18
L4/5	1.11	0.23	-	-	-	-
L5/S1	1.38	1.54	1.62	1.51	1.62	1.51
Torsion						
	HS	PLF	PLIF4NF	PLIF0NF	PLIF4F	PLIF0F
L1/2	1.10	1.09	1.09	1.09	1.09	1.09
L2/3	0.92	0.91	0.91	0.91	0.91	0.91
L3/4	0.75	1.00	0.99	0.94	0.99	0.95
L4/5	0.93	0.22	-	-	-	-
L5/S1	1.24	1.47	1.49	1.47	1.48	1.47

For the disc above the surgical site, the insertion of the pedicle screws (PLF) caused an increase in the stress by up to 29% on average for the five motions considered compared to the healthy spine. The insertions of 4º cages and fusion using this type of cages reduced by 1% the level of stress on the L3/4 intervertebral disc compared with the PLF model. For this disc (L3/4), the insertion of the 0º cages and the achievement of fusion reduced the stress compared to the PLF model, however stresses still remained higher by up to 22% compared with the healthy lumbosacral model.

In intervertebral disc L5-S1, located below the surgical site, stresses were 16% higher on average for the case of pedicle fixation (PLF) compared to the healthy spine. Unlike the L3/4 disc, where the higher levels of stress were recorded when the model included the insertion of the screws, Figure 7.5 shows that for the L5/S1intervertebral disc the higher levels of stress were recorded in the cases where the cages were implanted and fusion was achieved.

The use of the 4º cages caused that the level of stress at the L5/S1 disc increase by 28% and and by 29% on average for the PLIF4NF and the PLIF4F scenarios respectively compared with the healthy model. The use of the 0º cages also caused also caused stresses to rise in the L5/S1 by 26% on average for the model with the cages inserted intervertebral disc (PLIF0NF) and by 27% when fusion was achieved (PLIF0F).

In the L4-5 intervertebral disc, the disc situated at the surgical site, stress levels decreased by an average of 75% compared to the healthy lumbar disc following insertion of the pedicle screws (PLF).

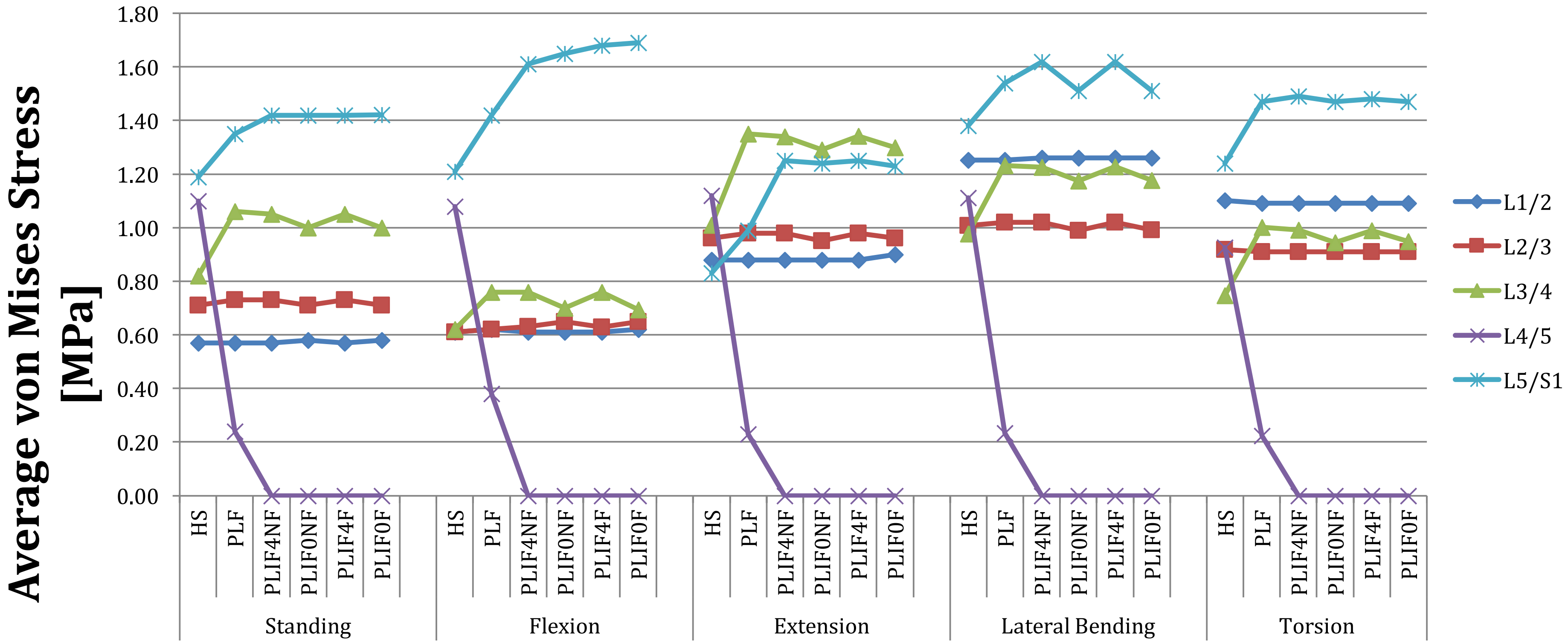

Figure 7.5 Results of average von Mises in the intervertebral discs for standing, flexion, extension, lateral bending and torsion for the 6 models. HS-Healthy Spine, PLF-Posterolateral fusion PLIF#NF-Posterior Lumbar Interbody fusion using two 0^0 or 4^0 interbody cages prior fusion, PLIF#F-Posterior Lumbar Interbody fusion using two 0^0 or 4^0 interbody cages following fusion across L4-L5 vertebrae level

7.5 Analysis of the Maximum von Mises Stress in the L3/4 and L5/S1 intervertebral discs

As same as the vertebrae, after the analysis of the average von Mises stress for all the intervertebral discs in the lumbosacral spine, the maximum von Mises stress for the intervertebral discs adjacent to the surgical site were calculated.

The highest level of stress for the L3/4 intervertebral discs (1.72 [MPa]), were registered in the model simulating the extension motion when the posterior fixation system was inserted without anterior column support. For this disc, situated above the surgical site, the maximum von Mises stress was located in the posterior part of the superior end of the intervertebral disc as it can be seen in Figure 7.6.

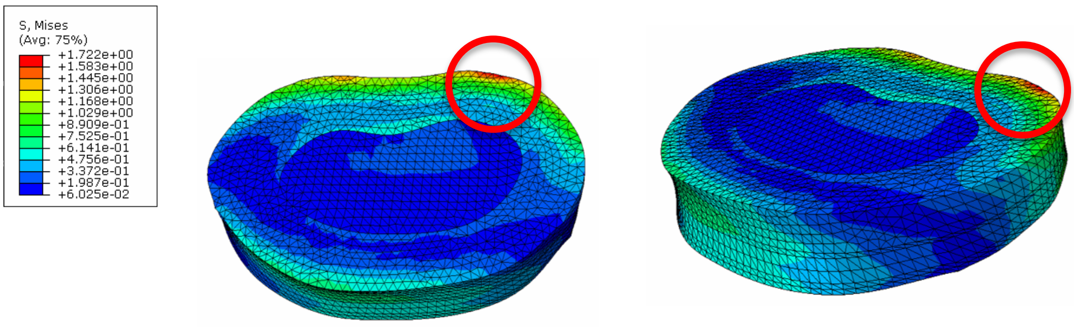

a) b)

Figure 7.6 Two views of the Maximum von Mises stress registered for the L3/4 Intervertebral disc a) Superior view b) Lateral view

Unlike the L3/4 intervertebral disc, for the disc L5/S1 located below the surgical site, the maximum von Mises (2.26 [MPa]) was registered when the flexion motion was simulated in the scenario where fusion was achieved using 0º PEEK interbody cages in addition to the posterior fixation system.

As it can be seen of Figure 7.7 that maximum von Mises stress for the L5/S1 intervertebral disc was located in the anterior part of the inferior side of the intervertebral disc.

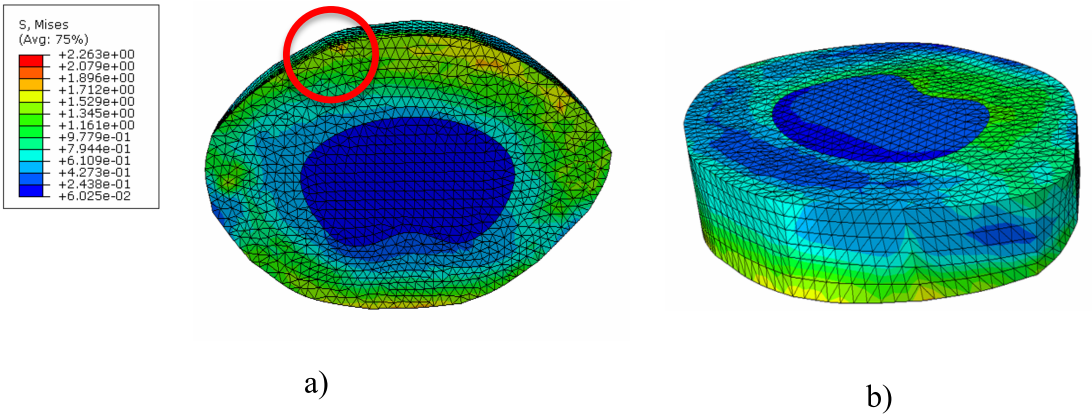

Figure 7.7 Two views of the Maximum von Mises stress registered for the L3/4 Intervertebral disc a) Inferior view b) Lateral view

Although the level of stress increased for the intervertebral discs above and below the surgical site after the insertion of the implants, the maximum von Mises stress registered for these structures are below the ultimate yield strength calculated in different investigations (3 - 7.2[MPa])[220, 221]. However, the increment in the level of stress in a degenerated intervertebral disc could cause instability in the adjacent segments as reported in different investigations. [220-222]

7.6 Performance of the fixation system

The performance of the pedicle fixation system in terms of stress levels was investigated for the five motions considered for the PLF, PLIF4NF, PLIF0NF, PLIF4F, PLIF0F scenarios. Maximum von Mises stresses were calculated and the critical location was established. The predicted maximum von Mises stresses for the scenarios and motions considered are given in Table 7.3

As shown in the table 7.3 the highest stress levels occurred in the PLF scenario, which is when the pedicular screw fixation system is inserted in the spine without anterior support. The results also show that for this model the critical case correspond to the flexion movement, which is the higher stress value, registered for this part of the study.

Table 7.3 Maximum von Mises stress results in the Pedicle Fixation System

	HS	PLF	PLIF4NF	PLIF0NF	PLIF4F	PLIF0F
Standing	-	116	68	57	49	35
Flexion	-	139	59	46	33	24
Extension	-	95	92	70	67	54
Lateral Bending	-	128	82	61	51	39
Torsion	-	108	74	54	50	37

When the 4º interbody cages were introduced the stress dropped sharply, by 34% on average, for the five motions compared. Following successful fusion using these same type of cages, stress dropped again, by another 34% on average compared with the model when fusion has not yet been achieved. Stress reduced by an average of 55% overall from when the pedicular screw fixation system was inserted (PLF) to when fusion was achieved, following the removal of the L4-5 intervertebral disc and the implanting of the 4º interbody cages (PLIF4F).

For the models using 0º interbody cages, once the intervertebral disc was removed and the intervertebral cages inserted, the level of stress dropped by at least 50% for all the motion considered except for the extension motion, which only drop 27% compared with the PLF model. This motion registered the higher stress value on the pedicle screws for the PLIF0NF model

Once the ossification between the L4 and the L5 vertebrae was achieved (PLIF0F), the stresses reduced further more by an average of 35% for all the motions considered, being the extension motion the critical case for this surgical procedure as shown in Figure 7.8.

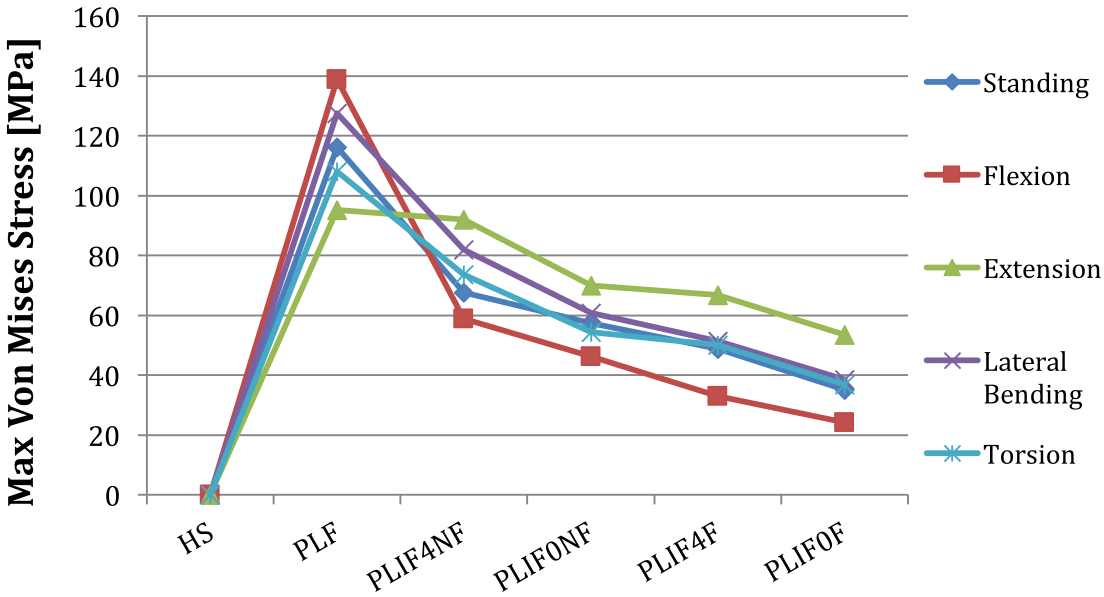

Figure 7.8 Maximum von Mises stress (MPa) results in the pedicular fixation for the 5 models and 5 motions studied .

The results obtained from our study for the pedicle fixation system merit comparison with the findings from the investigation undertaken by Chen *et al.* [79], who analysed 23 failed screws retrieved from patients who had previously undergone lumbar spine stabilisation procedures. Chen *et al.* used SEM fractography to analyse the fracture surface of the broken screws and utilised a FE model to undertake a stress analysis of posterolateral fusion.

Figure 7.9 shows that the location at the lower screw inserted in the L5 vertebra, towards the proximal end of the screw, close to the head, just inside the bone is where the maximum stress occurred for all the motion and models considered. The results obtained from the current study show that the highest maximum stress occurs in the screw inserted in the L5 vertebra which is also consistent with clinical studies which have reported that the majority of screw failures occur in the lower, caudal side screws [79, 223, 224].

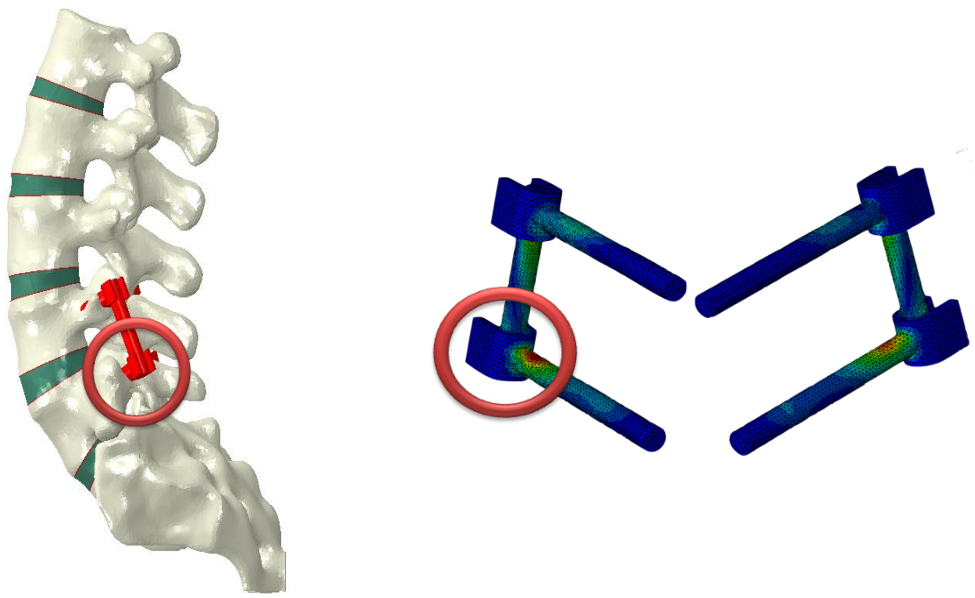

a) b)

Figure 7.9 Maximum von Mises stress in the pedicular fixation system. a) Location of maximum von Mises stress. b) Pedicular screw fixation system shown in-situ.

7.7 Comparison of the effects of 4º and a 0º degree interbody cages

In this section, the effect on the remaining spinal structures of L4-5 posterolateral fusion using 4º interbody cages is compared with that resulting from the use of 0º interbody cages. The comparison considers the effect on ROM and stresses in the adjacent vertebrae, intervertebral discs and fixation system for the five loading conditions considered previously, i.e. standing and spinal flexion, extension, lateral bending and torsion motions. In the previous analysis for both type of cages the results indicated that the insertion of the screws and the cages only affected the L4 and L5 vertebrae and the L3/4 and L5/S1 intervertebral discs. Therefore, in the analysis that follows only these structures are considered.

7.7.1 Analysis of Average von Mises Stress in the vertebrae

Figures 7.10 and 7.11 compare the average von Mises stress in the L4 and L5 vertebrae for the five loading scenarios considered when 4º and 0º interbody cages are employed. Upon inspection of the Figure 7.10 it can be seen that average von Mises stress was higher in the L4 vertebrae in the models containing 4º cages (PLIF4NF and PLIF4F) than in the models with the 0º cages implanted (PLIF0NF and PLIF0F) for all the motions considered.

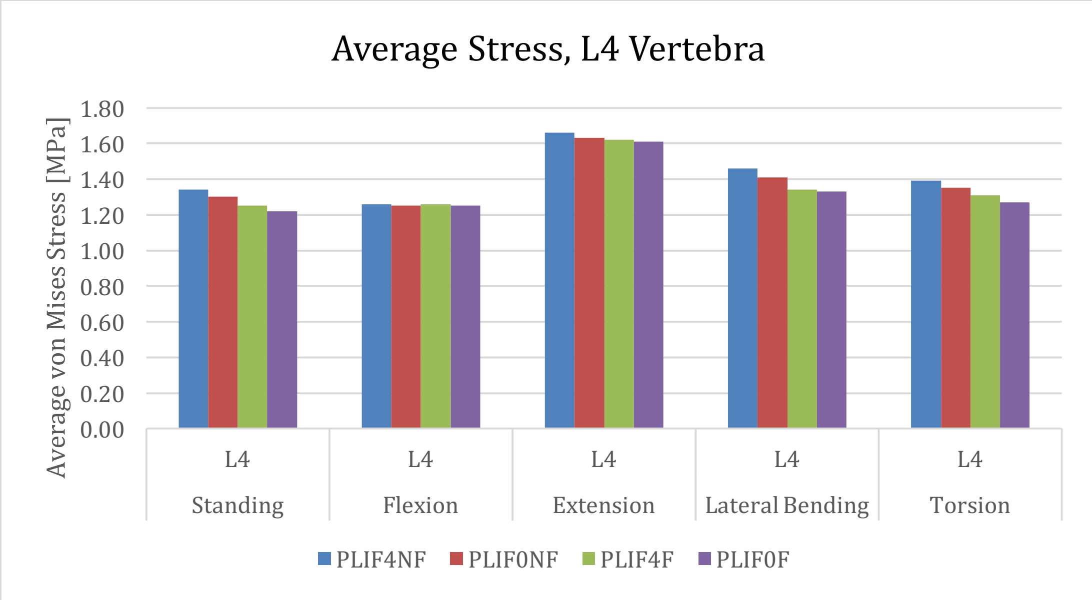

Figure 7.10 Comparison of the Average von Mises stress (MPa) results in the L4 Vertebrae when 4º and 0º interbody cages are employed

For the L4 vertebra, in the model that simulated posterior interbody fusion using the 0º cages when there is no ossification at L4/5 (PLIF0NF), average von Mises stress was 3%, 1%, 2%, 3%, and 3% less for the standing, flexion, extension, lateral bending and torsion motions respectively, compared to the corresponding 4º cage model (PLIF4NF). While for the 0º cage model that simulated complete ossification (PLIF0F) stresses were 2% lower for the standing position, 3% lower for the torsion motion and 1% lower for the flexion, extension and lateral bending movements compared to the equivalent 4º cage model (PLIF4F).

Unlike the L4 vertebra, the levels of stress at L5 were not higher in the 4º cage models compared to the 0º cage cases in all the motions considered. Lower levels of stress were registered for the 0º cage model for the standing, flexion and lateral bending motions whilst in the extension and torsion motions, stress was equivalent to or higher than that recorded for the 4º cage model.

For the L5 vertebra, stresses were lower by 4%, 4% and 3% in the PLIF0NF model for the standing, flexion and lateral bending motions respectively compared to the PLIF4NF model, whilst for the extension movement stress was 2% higher than in the PLIF4NF model. In the 0º cage model where complete ossification was simulated (PLIF0F) stress levels were 2% lower for the standing position and 4% lower for the flexion and lateral bending motions compared to the corresponding 4º cage model (PLIF4F). For the extension movement, stress was 2% higher for the PLIF0F model compared to the equivalent 4ºcage model. For the torsion motion, the level of stress was approximately the same for both types of cages.

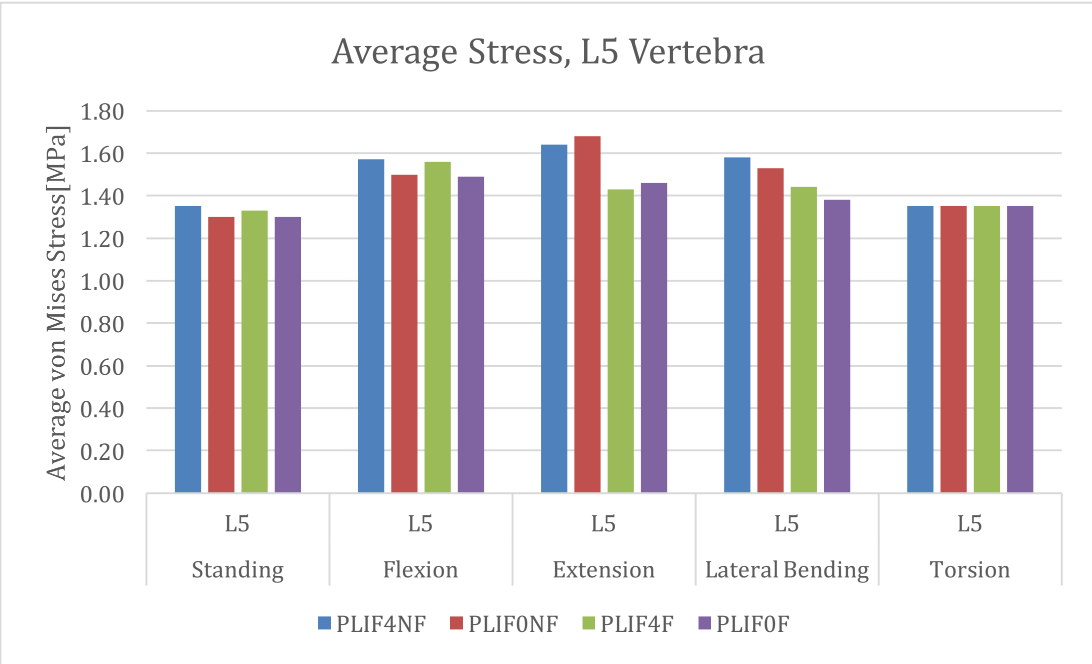

Figure 7.11 Comparison of the Average von Mises stress (MPa) results in the L5 Vertebrae when 4º and 0º interbody cages are employed.

7.7.2 Intervertebral Discs

Figure 7.12 and 7.13 compares average von Mises stress in the L3/4 and L5/S1 intervertebral discs for the five loading scenarios considered when 4º and 0º interbody cages are employed. The results presented in Figure 7.9 show that stresses in the L3/4 intervertebral disc, situated above the fusion site, were higher when 4 º cages were employed compared to when 0º cages were used for all the motions considered.

At this level, in the 0º cage model simulating the case prior to ossification (PLIF0NF), stresses were 5% lower for the standing and torsion motions, 4% lower for the extension and lateral bending movements and 8% lower for the flexion motion compared to the corresponding 4º cage model (PLIF4NF).

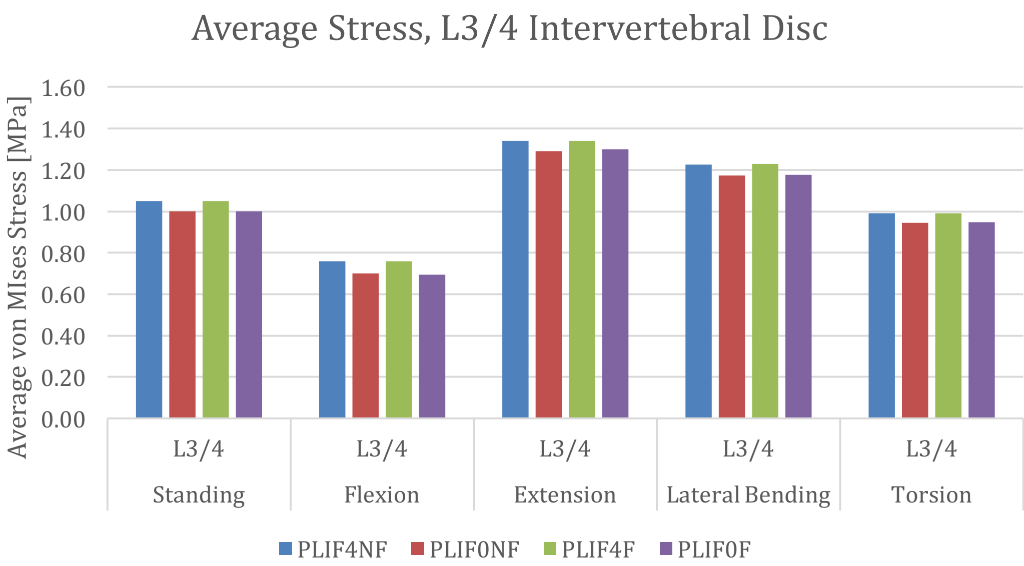

Figure 7.12 Average von Mises stress (MPa) results in the L3/4 Intervertebral Discs

Following ossification, the use of 0º cages also resulted in lower stress levels in the L3/4 intervertebral disc compared to when 4º cages were used. For the standing, flexion and lateral bending positions stress levels were lower in the 0º cage model compared to the 4º cage model by the same amounts as in the cases prior to ossification (by 5%, 8%, 4% respectively). In the case of the extension and torsion motions, stresses in the L3/4 intervertebral disc were 3% and 4% lower respectively in the PLIF0F model compared to the PLIF4F model.

Stresses in the L5/S1 intervertebral disc were higher when 4º cages were used compared to 0º cages for the extension, lateral bending and torsion motions for the cases representing prior to, and following ossification. However, for the flexion motion, stress levels were slightly higher for the 0º cage model compared with the 4º cage model. Stress levels were equivalent in the 0º and 4º cage models for the standing position scenario.

At the L5/S1 intervertebral disc level, stress in the PLIF0NF model was 1% lower for the extension and torsion movements and 7% lower for lateral bending compared to the PLIF4NF model. For the flexion motion, the stresses in the PLIF0NF model were 3% higher than in the PLIF4NF model while there was no difference in stress level for the standing position case. Following ossification, stresses in the 0º cage model were lower than in the 4º cage model by 3%, 4% and 1% for the extension, lateral bending and torsion movements respectively, whilst for the flexion motion stresses in the L5/S1 intervertebral disc were 1% higher when 0º cages were used (PLIF0F) compared to when 4º cages were employed (PLIF4F). Following ossification, stress levels were the same for the standing position regardless of whether 0º or 4º cages were used.

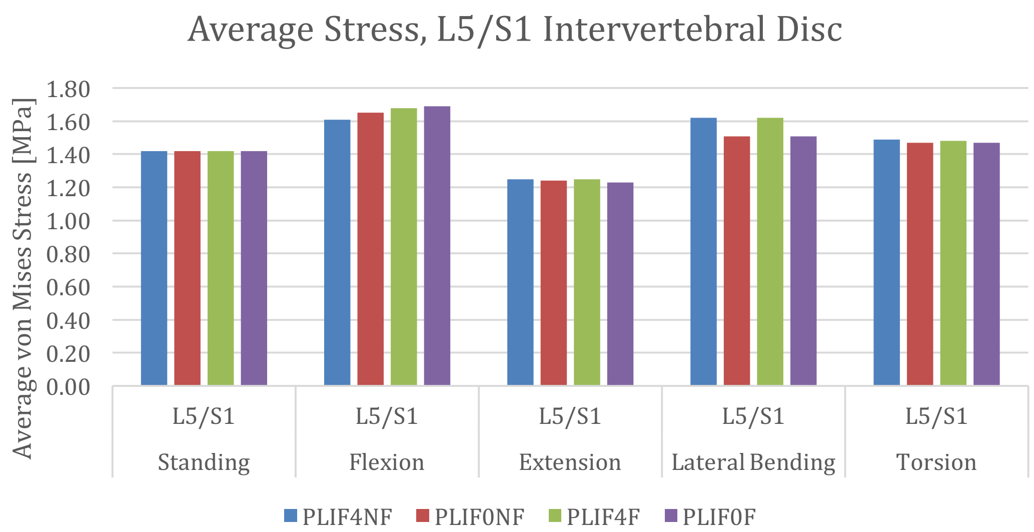

Figure 7.13 Average von Mises stress (MPa) results in the L5/S1 Intervertebral Disc

7.7.3 Analysis of Maximum von Mises Stress in the Screws

Figure 7.14 shows the maximum von Mises stresses calculated in the screws of the pedicular fixation system for the five loading scenarios considered when 4º and 0º interbody cages are employed. As mentioned previously, the highest levels of stresses developed when the screws were inserted without anterior support (PLF). Once the intervertebral cages were inserted, the level of stress in the fixation system decreases. Unlike the PLF model, where the maximum level of stress was recorded when the spine was flexed, once the cages were added the higher stresses were recorded in the extension motion.

As can be seen upon inspection of Figure 7.14, the stresses decreased on average by 34% when the 4º cages were added and 49% when the 0º cages were used compared with the PLF model for all the motions considered. The highest level of stress was recorded in the extension motion where the insertion of the 4º cages resulted in a reduction of 3% in stress from that recorded for the PLF model. For the case where 0º cages were used, stress was 26% lower compared to the PLF model for the extension motion case.

Stress levels were also lower for the 0º cage model compared to the 4º cage model for the other 4 motions: stresses in the PLIF0NF model were 15% lower for the standing position, 21% for flexion and 26% for the lateral bending and torsion motions compared to the PLIF4NF model.

Following ossification at the L4/5 level, stresses in the fixation system were higher in the 4º model than in the 0º cage model. Compared to the PLF model, the stresses in the screws were 56% lower on average following ossification when the 4º cages were used. Moreover, when 0º cages were inserted and fusion was achieved the stresses reduced further, to a level that was 67% lower on average for all the motions considered compared to the PLF model.

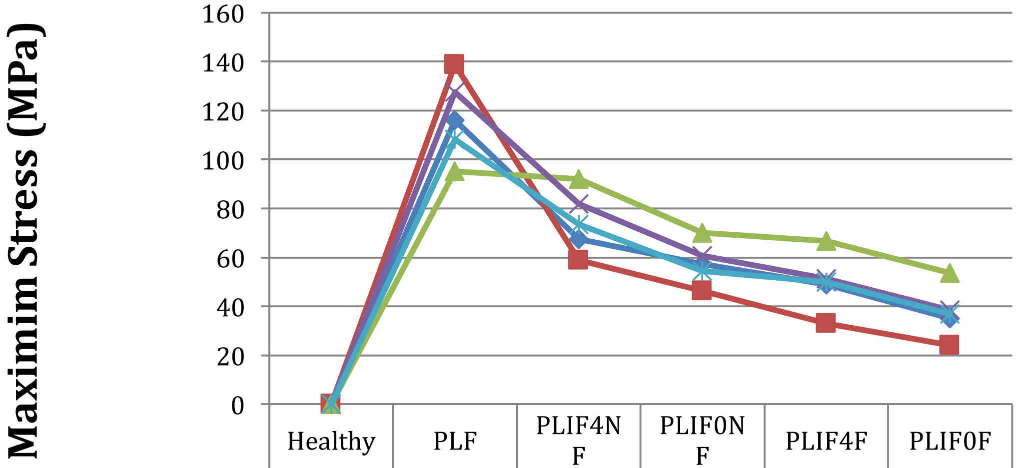

	Healthy	PLF	PLIF4NF	PLIF0NF	PLIF4F	PLIF0F
Compression	0	116	68	57	49	35
Flexion	0	139	59	46	33	24
Extension	0	95	92	70	67	54
Lateral Bending	0	128	82	61	51	39
Torsion	0	108	74	54	50	37

Figure 7.14 Maximum von Mises stress (MPa) results in the pedicular fixation system.

7.7.4 Analysis of Range of Motion between the 0° and the 4° cages

Figure 7.15 shows the ROM calculated at the different levels of the lumbosacral spine for the cases of the healthy spine and the spine instrumented with 4º and 0º interbody cages for flexion, extension, lateral bending and torsion movements.

Upon inspection of Figure 7.15 it can be seen that insertion of the pedicle screws and the interbody cages does not affect the ROM in the superior part of the lumbosacral spine. The L1/2 and L2/3 levels maintained the same ROM once the posterior instrumentation and the interbody cages were inserted, whereas at the L3/4, L4/5 and L5/S1 levels instrumentation resulted in an alteration of the ROM.

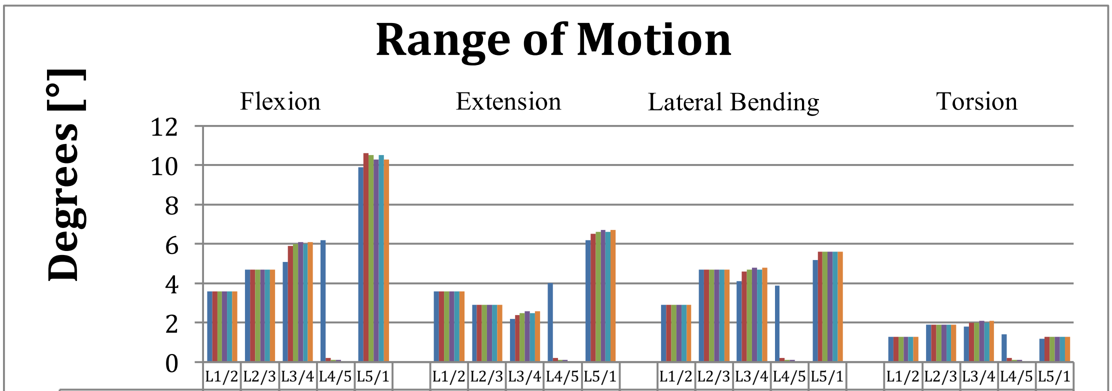

	Flexion L1/2	Flexion L2/3	Flexion L3/4	Flexion L4/5	Flexion L5/1	Extension L1/2	Extension L2/3	Extension L3/4	Extension L4/5	Extension L5/1	Lateral Bending L1/2	Lateral Bending L2/3	Lateral Bending L3/4	Lateral Bending L4/5	Lateral Bending L5/1	Torsion L1/2	Torsion L2/3	Torsion L3/4	Torsion L4/5	Torsion L5/1
Healthy	3.6	4.7	5.1	6.2	9.9	3.6	2.9	2.2	4	6.2	2.9	4.7	4.1	3.9	5.2	1.3	1.9	1.8	1.4	1.2
Screws with Disc	3.6	4.7	5.9	0.20	10.6	3.6	2.9	2.4	0.20	6.5	2.9	4.7	4.6	0.20	5.6	1.3	1.9	2	0.20	1.3
4 Cages	3.6	4.7	6	0.10	10.5	3.6	2.9	2.5	0.10	6.6	2.9	4.7	4.7	0.10	5.6	1.3	1.9	2	0.10	1.3
0 Cages	3.6	4.7	6.1	0.10	10.3	3.6	2.9	2.6	0.10	6.7	2.9	4.7	4.8	0.10	5.6	1.3	1.9	2.1	0.10	1.3
4 Fusion	3.6	4.7	6	0.00	10.5	3.6	2.9	2.5	0.00	6.6	2.9	4.7	4.7	0.00	5.6	1.3	1.9	2	0.00	1.3
0 Fusion	3.6	4.7	6.1	0.00	10.3	3.6	2.9	2.6	0.00	6.7	2.9	4.7	4.8	0.00	5.6	1.3	1.9	2.1	0.00	1.3

Figure 7.15 Range of Motion (degrees) for the 6 models created and 4 motions studied.

For the L3/4 and L5/S1 levels, the insertion of the pedicle screws and the interbody cages resulted in an increase in the ROM at both levels for both types of cages and for all motions considered.

Figure 7.16 shows the ROM calculated at the L3/4 level of the lumbosacral spine for the cases of the healthy spine and the spine instrumented with 4º and 0º interbody cages for flexion, extension, lateral bending and torsion movements. From the results shown in Figure 7.16 it can be seen that the ROM at L3/4 increased by 18%, 15%, 15% and 13% for all the fusion techniques on average for the flexion, extension, lateral bending and torsion motions respectively. At this level, the ROM was an average of 12% greater for the PLF model compared to the healthy spine model for the 5 motions considered. ROM increased compared with the PLF procedure following insertion of the cages and ossification. When the 4º interbody cages were inserted the ROM increased by 14% on average for all the motions considered compared with the healthy model results.

The greatest ROM at the L3/4 level was obtained when the 0º cages were inserted. Compared with the healthy model, insertion of these cages resulted in an increase of 18% in ROM. Ossification did not result in a change in ROM for both type of cages.

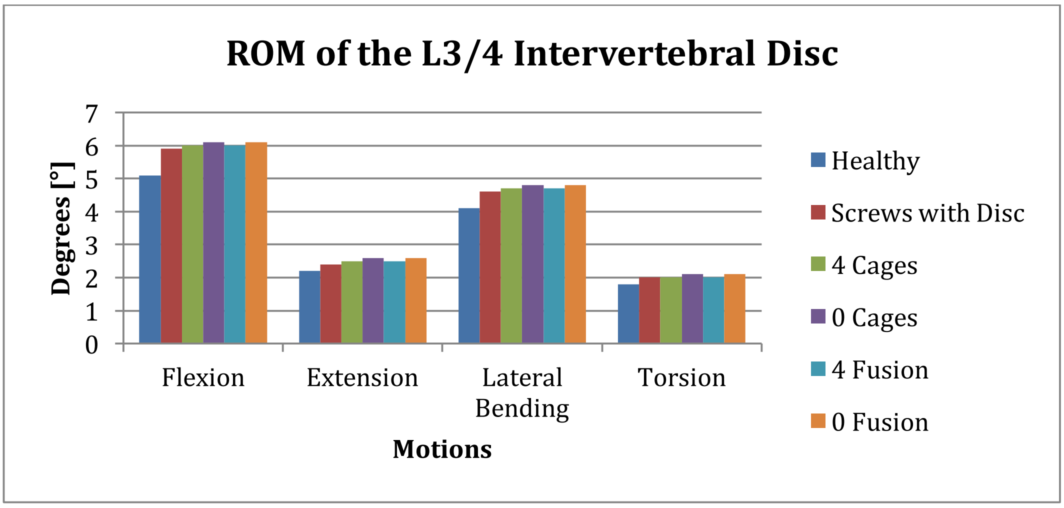

Figure 7.16 Range of Motion of the L3/4 Intervertebral disc

At the surgical level (L4/5), ROM decreased drastically as a result of instrumentation. The insertion of the pedicle screws resulted in a reduction in ROM of 93%, on average, compared with the healthy spine. The insertion of the 0º and 4º cages as well as the successful fusion of the L4 and the L5 vertebrae resulted in ROM being completely constrained at this level.

As was the case for the L3/4 level, ROM between the fifth vertebra and the sacrum (L5/S1 level) also increased as a result of instrumentation for all motions considered. As can be deduced from Figure 7.17, ROM increased by an average of 7% following instrumentation compared to the healthy spine for all the motions considered.

At this level, instrumentation resulted in ROM increasing by 5% for flexion, 7% for extension and 8% for torsion and lateral bending motions on average compared with the healthy model.

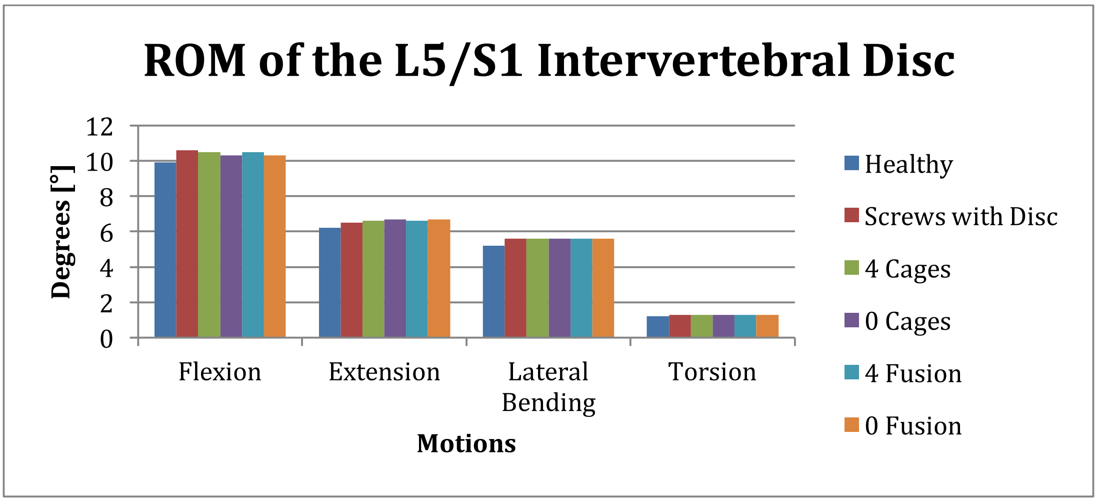

Figure 7.17 Range of Motion of the L5/S1 Intervertebral disc

Although there is not a major increase in the ROM for both levels adjacent to the surgical site, the hypermobility caused by the insertion of the pedicle screws and the intervertebral cages combined with the increase in the level of stress may lead to an accelerated degeneration in these structures according to different studies.[225, 226]

7.8 Comparison between the in-vivo Motion Analysis and the Finite Element Method

This section presents a comparison between the ROM of the *in-vivo* Motion Analysis and the results predicted by the Finite Element Method.

7.8.1 Comparison of the Trial Results for Subjects with no History of Spine Problems with the Finite Element Model Predictions

Figure 7.18 presents a comparison of the *in-vivo* data obtained from the *in-vivo* trials with data obtained from the finite element model. In this figure, the average ROM obtained for the participants in the experimental flexion and extension trials is shown alongside the corresponding prediction obtained from the computation model. As can be seen upon inspection of this figure, the FEA model predicts greater ROM in both flexion and extension than obtained in the *in-vivo* investigation. For the flexion motion, the finite element model was just 1.2° more flexible than the *in-vivo* measurements while for the extension motion the computational model registered 3.6º more motion than the experimental trials.

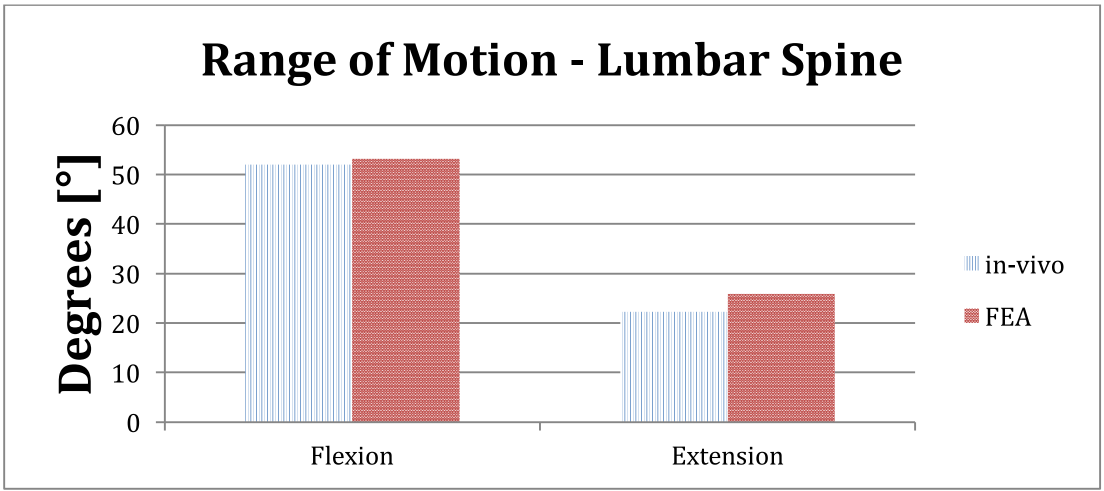

Figure 7.18 Range of motion of the non instrumented spine

Figure 7.19 shows the initial and final positions of the spine as predicted by the finite element model for the flexion and extension motions. As can be seen in the figure, the ROM for flexion motion is clearly greater than in extension, which is as expected due to the anatomy of the spine. The finite element analysis model predicted a ROM of 53.2 º for the flexion motion whereas for the extension motion the predicted ROM was 25.9º.

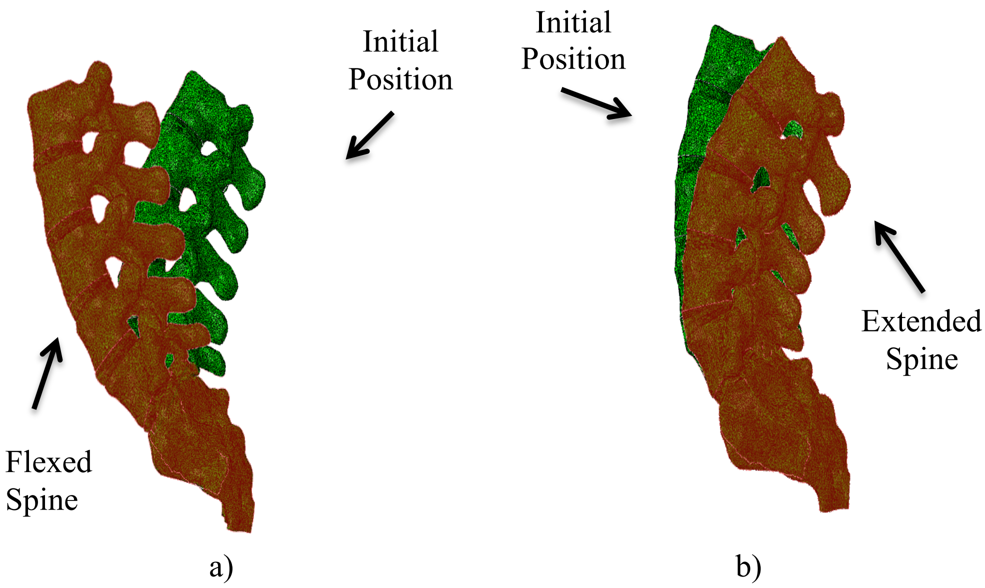

Figure 7.19 Healthy Spine–Finite Element Study. a) Flexion Motion b) Extension motion

7.8.2 Comparison of the ROM of the L4/5 PLIF Patients and the PLIF4N FEA Model

In this section, the ROM results obtained from the *in-vivo* trials undertaken on subjects that had undergone L4/5 PLIF surgery are compared with the predictions from the finite element model developed to model this scenario (PLIF4F model).

An important consideration when modelling an instrumented spine is the possibility of degeneration of the remaining discs. This is more likely to be an important factor in older patients [40, 227]. In addition, it has been argued that instrumentation of the spine can lead to accelerated degeneration at levels adjacent to the surgical site[117, 228]. The average age of the L4/5 PLIF volunteers who took part in the trials was 55±9 years, so it is likely that these subjects would have had some level of degeneration in their remaining intervertebral discs, accelerated as a result of them having undergone fusion surgery. With this in mind, the PLIF4F finite element model was run with material properties modified to simulate two degrees of degeneration of the remaining intervertebral discs in addition to the non degeneration case.

An approach commonly used to simulate intervertebral disc degeneration was employed in this study [42, 229]. This entailed decreasing the Poisson's ratio and the Young's modulus of the nucleus pulposus accompanied by the stiffening of the Young's modulus of the annulus fibrosus to simulate mild and moderate degeneration of the remaining intervertebral discs. The material properties used in the computational model to simulate two degrees of degeneration of the intevertebral discs are shown in Table 6.7 alongside those used for the non-degeneration case.[42, 229, 230]

Table 7.4 Material properties used in the intervertebral disc to simulate two different stages of degeneration in the lumbar spine

Part	Element	Young Modulus [MPa]	Poisson's Ratio
Non Degenerated Intervertebral Disc	Nucleus Pulposus	1	0.499
	Annulus Fibrosus	3.15	0.45
Mild Degenerated (25%) Intervertebral Disc	Nucleus Pulposus	1.5	0.48
	Annulus Fibrosus	3.9	0.45
Moderate Degenerate (50%) Intervertebral Disc	Nucleus Pulposus	2.1	0.47
	Annulus Fibrosus	4.7	0.45

Figure 7.20 presents a comparison of the results from the data obtained from the *in-vivo* experimental tests for the patients that had undergone PLIF surgery with the predictions obtained from the PLIF4F finite element model with material properties used to simulate no, mild (25%) and moderate (50%) degeneration of the remaining intervertebral discs.

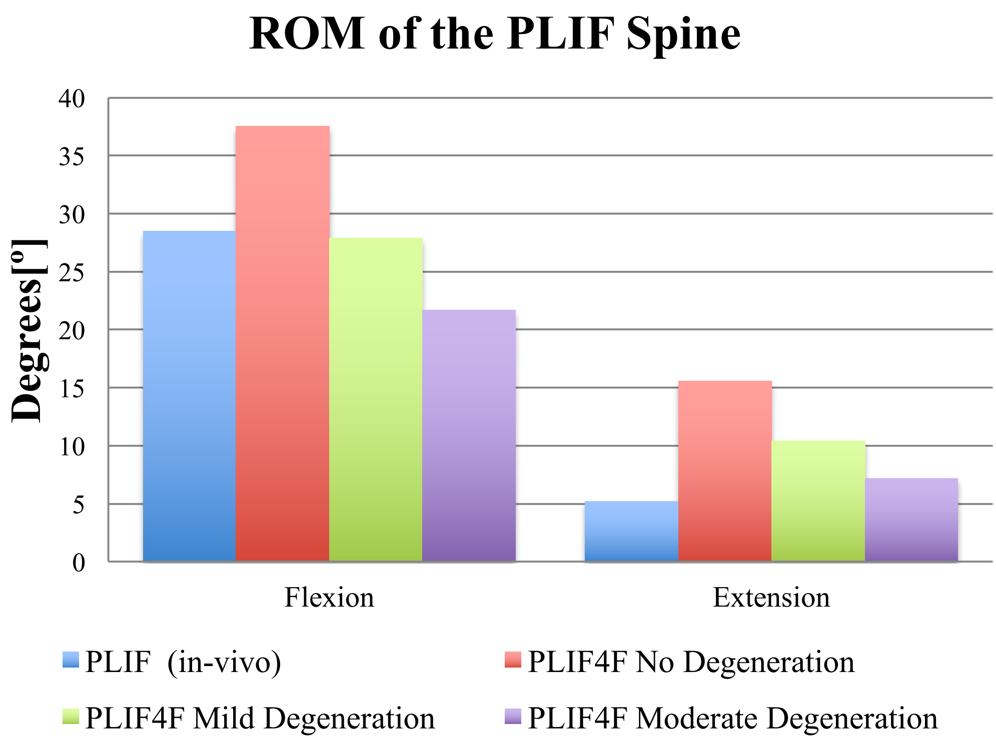

Figure 7.20 ROM instrumented spine and degenerative models mild

Upon inspection of Figure 7.20 it can be seen that, when no degeneration was simulated in the remaining intervertebral discs, the computational model (PLIF4F No Degeneration) predicted a ROM that was greater in both flexion and extension compared to that obtained from the *in-vivo* trials. In flexion, the model predicted a ROM that was 31% greater than the *in-vivo* results, whereas in extension, it predicted ROM was almost 200% greater.

The computational models used to simulate mild (PLIF4F Mild) and moderate (PLIF4F Moderate) disc degeneration predicted ROMs in both flexion and extension that were less than those predicted when no degeneration was considered (PLIF4F No Degeneration) and closer to the *in-vivo* results.

The mild disc degeneration model predicted a ROM of 27.9º for the flexion motion, which was just 2% (0.6º) less than that obtained from the experimental trials, while the ROM predicted by the moderate disc degeneration model was 21.7º, or 24% (6.8º) less than the *in-vivo*.

For the extension motion the 2 numerical models simulating disc degeneration predicted lower ROM than the no disc degeneration model. The mild disc degeneration model predicted a ROM of 10.4º in extension, which was 99% (5.17º) greater than the *in-vivo* test while the moderate disc degeneration model predicted a ROM of 7.2º, which was 37% (1.97º) higher.

Figure 7.21 shows the initial and final position of the flexed and extended instrumented spine as predicted by the computational model using material properties chosen to simulate mild degeneration of the remaining intervertebral discs (PLIF4F Mild model)

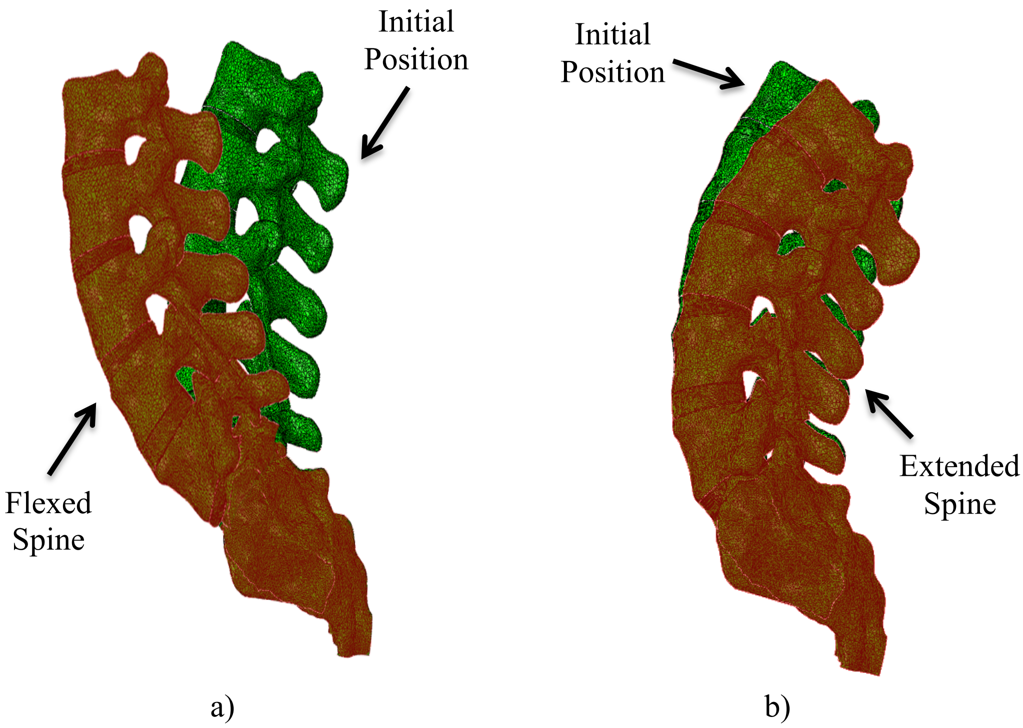

Figure 7.21 PLIF4F Mild Model – Finite Element Study a) Flexion Motion b) Extension motion

The analytical models created for this investigation do not take into consideration the muscles that surround the lumbar spine due to the applied follower load, as mentioned in section 6.6.1. However, it can be seen from the results that the degeneration in the intervertebral discs has a major effect in the mobility of this region, where it can be seen that the ROM for both motions is reduced when compared with the non degenerated model.

Chapter VIII Conclusions and Future Work

Posterolateral Fusion and Posterior Lumbar Interbody Fusion are two of the most used surgical procedures for treating lumbar intervertebral disc disease. These procedures are commonly used and performed successfully, however the effects of these surgeries in the intervertebral discs and vertebrae bodies adjacent to the surgical site and the consequences of these procedures on the reduction of the Range of Motion of the lower back has not been exhaustively investigated.

Many investigations have developed models to study the biomechanical behaviour of various aspects of lumbar spinal fusion procedures, however many of the studies model less than five levels in the lumbar spine and concentrate on reporting the ROM at the surgical site and in the immediately adjacent segments.

The aim of the research described in this thesis was to investigate and compare the performance of the Posterolateral Fusion and Posterior Lumbar Interbody Fusion surgical techniques undertaken on the L4/5 lumbar segment. In addition, this investigation evaluated how the changes in the sagittal plane when using 0° or 4° PEEK intervertebral cages affect the biomechanics of the lumbar spine

For this investigation six models simulating the healthy spine, and two different fusion procedures (PLF, PLIF) were created. The impact of these procedures at the surgical site and at adjacent vertebral structures was analysed for five anatomical motions. In addition, an innovative clinical study was undertaken that entailed comparing the range of motion from subjects that had undergone a L4/5 PLIF using 4º intervertebral cages and subjects who had no history of low back pain.

8.1 Conclusions

8.2.1 Vertebrae

In a patient whose sagittal profile is close to being compromised due to degenerative processes of the spine, a relatively small change resulting from a loss of position of the fixation from the one desired by the surgeon can significantly affect the outcome of the surgery. In cases where lumbar fusion is being considered, an understanding of the stresses, such as provided by the current analysis, is important when selecting the type of surgery required for the patient.

The results from the computational analysis indicated that the fusion procedures across intervertebral disc L4/5 did not cause an increase in average von Mises stresses in the L1, L2, L3 and the S1 vertebrae, however the L4 and L5 vertebrae were clearly affected by these surgical procedures.

The largest change in the average stress in the affected L4 vertebra occurred when the pedicle screw fixation system was introduced with no anterior column support (PLF). When intervertebral cages were introduced instead of the damaged disc, the level of stress in this vertebra reduced for all motions considered. It can be concluded from this analysis that the insertion of anterior support is an important mechanism that contributes to reduce the level of stress in this vertebra, reducing the risk of fracture at this structure.

In the L5 vertebrae the maximum stress registered was located in the interface between the bone and the screw. For these vertebra the use of anterior support is also recommended as the use of these devices reduced the stress level in this part of the vertebrae.

8.2.2 Intervertebral Discs

The results obtained from computational analysis predictions indicated that the fusion procedures at the L4-5 level did not cause an increase in average von Mises stresses in the upper intervertebral discs (L1/2, L2/3), however as a consequence of these surgical procedures the stress levels rose in the adjacent L3/4 and L5/S1 intervertebral discs situated above and below the surgical level.

Unlike the vertebrae, the insertion of intervertebral cages did not reduce the level of stress in the intervertebral disc, indicating that the use of anterior column support does not reduce the risk of adjacent degenerative disc disease.

For both adjacent intervertebral discs, the highest stresses were reported when the extension motion was simulated. These results suggest that this motion could be the hardest anatomical movement that a patient can perform after a posterolateral or a posterior interbody fusion.

In summary, it has been demonstrated using a 3D finite element model of the L1-S1 lumbar spine that instrumentation causes the stress levels in adjacent intervertebral discs to rise. This is significant as it reinforces the view that fusion may lead to accelerated degeneration of the intervertebral discs adjacent to the instrumentation.[231]

These results also predict an increased risk of post-operative degeneration following fusion procedures, a likelihood that may increase if some degree of degeneration pre-exists in the adjacent discs[14].

8.2.3 Pedicle Screws

In terms of the performance of the pedicle screw fixation system, the PLF scenario resulted in the highest maximum stress for all motions considered. These results indicate that the use of anterior column support is beneficial for the patient as the insertion of intervertebral cages reduce the stress levels in the pedicle screws, reducing the risk of screw breakage.

This analysis also demonstrated that a successful fusion between the L4 and L5 vertebrae reduce the risk of screw loosening due to the decrease in the level of stress in the posterior fixation implants in comparison with the non fused models.

The maximum stress values in the posterior fixation system registered (139 MPa) are well below the yield strength of the aluminium alloy, Ti-6Al-4V, from which the screws and rods of the pedicle fixation system are manufactured, which is typically in the range 795-869 MPa[232], suggesting that the fixation system elements will not fail in yield.

Also, from the analysis of the stresses in the fixation system elements it was determined that screw failure was likely to occur towards the thread end in the screws in the lower section of the fixation system through fatigue. This is backed up by the fracture analyses performed by Chen *et al.* [79] and Griza *et al.* [233], the findings from which suggested that metal fatigue was the primary cause of fracture in the broken screws retrieved from patients.

8.2.4 Comparison 0 vs 4

This investigation also presented a comparison of the effect on the adjacent spinal structures of employing L4/5 posterolateral fusion using 4º interbody cages with that resulting from the use of 0º interbody cages. Stresses and ROM at adjacent segment levels were analysed in addition to the stresses in the pedicular fixation system for the five loading scenarios (motions) considered.

The results from the analysis demonstrated that in general stress levels in the L4 and the L5 vertebrae and in the intervertebral disc L3/4 and L5/S1 were lower when the 0º interbody cages were employed compared to when the 4º cages were used for the cases both prior to and following ossification at L4/5. Furthermore, stress levels in the pedicle fixation system were also lower on average when 0º interbody cages were employed compared to when 4º cages were used prior to and following ossification.
Analysing these results, it can be concluded that the use of 0º interbody cages reduce the risk of screw breakage or screw loosening compared to when 4º interbody cages were used. However, after the stress analysis in the intervertebral discs, there is not a clear difference of the convenience of using a 0º or a 4º cages, as the use of both intervertebral cages increase the possibilities of degeneration in these structures.

The introduction of interbody cages had no effect on the ROM of the superior part of the lumbosacral spine, however, the range of motion of the segments adjacent to the surgical site were altered. At the L3/4 intervertebral disc level, the use of 0º interbody cages resulted in an increase in the ROM compared when the 4º cages were used. At the L5/S1 level, below the surgical site, both intervertebral cages increased the ROM in the same proportion on average.

This investigation demonstrated that as the motion at the surgical site level was effectively constrained when instrumentation was employed, the ROM at adjacent levels increased in order to compensate for this constraining effect during the motions undertaken. After the analysis it can be concluded that the 0º caused more hypermobility compared to the 4º cages. These increase in ROM at levels directly above and below the surgical site, accompanied by increased levels of stress, adds weight to the theory that spinal fusion using 0º interbody cages may lead to a more accelerated degeneration of the intervertebral discs at adjacent levels compared to when the 4º cages are used.

8.2.5 Motion Capture Analysis

In addition, this investigation described an innovative *in-vivo* investigation that determined the ROM for subjects that had undergone L4/5 posterior lumbar interbody fusion (PLIF) and for subjects who had no history of low back pain conditions and who had not undergone fusion surgery.

The results from the *in-vivo* investigation, when compared with the predictions of the finite element analysis and the studies performed in healthy adult subjects *[160, 162, 177, 189, 190]*, clearly demonstrated that L4/5 posterior lumbar interbody fusion (PLIF) causes a significant reduction in the ROM of the spine following surgery.

From these results, it appears that the patients that had undergone posterior lumbar surgery had more trouble undertaking the extension motion, achieving less ROM than that obtained from the computational model, even taking into consideration potential degeneration of the remaining intervertebral discs. This may be due to the nature of the movement, with subjects feeling less confident in performing the full ROM possible in extension, moving the spine in a backward motion, as a result of having undergone the fusion surgery.

8.3 Limitations of the Study and Future Work

The models created provide stress levels in the spinal structures and fixation system, information that can assist a surgeon in assessing the effects of fixation choice on adjacent spinal structures, effects that can include accelerated degeneration of the intevertebral discs at adjacent levels. In addition, the models can aid in assessing the likelihood of the loss of position or failure of the construct. However, as with all numerical studies, limitations exist arising from various sources including material property and behavior assumptions, boundary and loading conditions and approximations in the geometric representation of the anatomical structures analyzed.

Moreover, the models developed here were based on a healthy spine, which by definition, would not normally require a spinal fusion procedure. If a more realistic degenerated disc was employed, then this would likely affect the results obtained to an extent which would depend upon the degree of degeneration assumed. For example, a moderately degenerated disc is likely to cause only relatively small changes in intersegmental rotation and facet joint forces at the implant and adjacent levels but a more significant reduction in intradiscal pressure under certain loading conditions [36]. A more degenerative disc is likely to have a larger effect on these variables. Our model also assumes no degree of degeneration exists in the adjacent disc levels, which may not be the case in practice. Given these limitations, it is probably safe to assume that our model would slightly underestimate the effect of the fusion procedures on adjacent levels of the spine.

Considering all the limitations mentioned a further study in this area would require a model that simulates a degree of degeneration in the intervertebral disc at the surgical level and in the adjacent levels.

This investigation evaluated the effect of using 0º or 4º interbody cages in a PLIF procedure. Although these types of cages are the most common used to stabilize the damaged lumbar spine, other cages such as the 8º interbody cage or the cage used for a Transforaminal Lumbar Interbody Fusion (TLIF) could also be studied and compared against the cages analyzed in this investigation.

In reference to the *in-vivo* investigation only 5 patients that had undergone a L4/5 posterior lumbar interbody fusion using 4º cages participated in this study. Therefore, a posterior investigation in this area needs to evaluate additional patients that had undergone this surgery with this type of cage and also include patients with 0º cages implanted. In addition, this investigation studied just the change in the ROM for the flexion and extension motions. Therefore, a posterior study needs to evaluate the change in the ROM for the torsion and lateral bending motions.

References

1. Xu, H.-Z., et al., *Biomechanical evaluation of a dynamic pedicle screw fixation device.* Clinical biomechanics (Bristol, Avon), 2006. **21**(4): p. 330-6.
2. Gornet, M.F., et al., *Biomechanical assessment of a PEEK rod system for semi-rigid fixation of lumbar fusion constructs.* J Biomech Eng, 2011. **133**(8): p. 081009.
3. Vadapalli, S., et al., *Biomechanical rationale for using polyetheretherketone (PEEK) spacers for lumbar interbody fusion-A finite element study.* Spine, 2006. **31**(26): p. E992-8.
4. Zhong, Z.C., S.H. Chen, and C.H. Hung, *Load- and displacement-controlled finite element analyses on fusion and non-fusion spinal implants.* Proceedings of the Institution of Mechanical Engineers Part H, Journal of engineering in medicine, 2009. **223**(2): p. 143-57.
5. Kim, H.-J., et al., *The quantitative assessment of risk factors to overstress at adjacent segments after lumbar fusion: removal of posterior ligaments and pedicle screws.* Spine, 2011. **36**(17): p. 1367-73.
6. Fantigrossi, A., et al., *Biomechanical analysis of cages for posterior lumbar interbody fusion.* Med Eng Phys, 2007. **29**(1): p. 101-9.
7. Rohlmann, A., et al., *Effect of an internal fixator and a bone graft on intersegmental spinal motion and intradiscal pressure in the adjacent regions.* European spine journal : official publication of the European Spine Society, the European Spinal Deformity Society, and the European Section of the Cervical Spine Research Society, 2001. **10**(4): p. 301-8.
8. Chen, S.-H., et al., *Biomechanical comparison of a new stand-alone anterior lumbar interbody fusion cage with established fixation techniques - a three-dimensional finite element analysis.* BMC musculoskeletal disorders, 2008. **9**: p. 88.
9. Polikeit, A., et al., *Factors influencing stresses in the lumbar spine after the insertion of intervertebral cages: finite element analysis.* European spine journal : official publication of the European Spine Society, the European Spinal Deformity Society, and the European Section of the Cervical Spine Research Society, 2003. **12**(4): p. 413-20.
10. Chuah, H.G., I. Abd Rahim, and M.I. Yusof, *Topology optimisation of spinal interbody cage for reducing stress shielding effect.* Computer methods in biomechanics and biomedical engineering, 2010. **13**(3): p. 319-26.
11. Chen, S.-H., et al., *Biomechanical comparison between lumbar disc arthroplasty and fusion.* Medical engineering & physics, 2009. **31**(2): p. 244-53.
12. Rohlmann, A., et al., *Comparison of the effects of bilateral posterior dynamic and rigid fixation devices on the loads in the lumbar spine: a finite element analysis.* European spine journal : official publication of the European Spine Society, the European Spinal Deformity Society, and the

European Section of the Cervical Spine Research Society, 2007. **16**(8): p. 1223-31.

13. Chen, B.L., et al., *Adjacent segment degeneration after single-segment PLIF: the risk factor for degeneration and its impact on clinical outcomes.* Eur Spine J, 2011. **20**(11): p. 1946-50.
14. Yan, J.Z., et al., *Finite element analysis in adjacent segment degeneration after lumbar fusion.* Int J Med Robot, 2011. **7**(1): p. 96-100.
15. Zhong, Z.-C., et al., *Finite element analysis of the lumbar spine with a new cage using a topology optimization method.* Medical engineering & physics, 2006. **28**(1): p. 90-8.
16. Gao, S.G., et al., *Biomechanical comparison of lumbar total disc arthroplasty, discectomy, and fusion: effect on adjacent-level disc pressure and facet joint force.* J Neurosurg Spine, 2011. **15**(5): p. 507-14.
17. Cunningham, B.W., et al., *The effect of spinal destabilization and instrumentation on lumbar intradiscal pressure: an in vitro biomechanical analysis.* Spine (Phila Pa 1976), 1997. **22**(22): p. 2655-63.
18. Zhong, Z.C., et al., *Finite element analysis of the lumbar spine with a new cage using a topology optimization method.* Med Eng Phys, 2006. **28**(1): p. 90-8.
19. Adam, C., M. Pearcy, and P. McCombe, *Stress analysis of interbody fusion--finite element modelling of intervertebral implant and vertebral body.* Clinical biomechanics (Bristol, Avon), 2003. **18**(4): p. 265-72.
20. White, A.A., 3rd, *Clinical biomechanics of cervical spine implants.* Spine (Phila Pa 1976), 1989. **14**(10): p. 1040-5.
21. Kowalski, R.J.a.F., L. A. and Benzel,E. C., *Biomechanics of the spine.* Neurosurgery Quarterly, 2005. **15**(1): p. 42-59.
22. Ferguson, S.J. and T. Steffen, *Biomechanics of the aging spine.* Eur Spine J, 2003. **12 Suppl 2**: p. S97-S103.
23. Panjabi, M.M. and A.A. White, 3rd, *Basic biomechanics of the spine.* Neurosurgery, 1980. **7**(1): p. 76-93.
24. Jones, A.C. and R.K. Wilcox, *Finite element analysis of the spine: towards a framework of verification, validation and sensitivity analysis.* Med Eng Phys, 2008. **30**(10): p. 1287-304.
25. Yamamoto, I., et al., *Three-dimensional movements of the whole lumbar spine and lumbosacral joint.* Spine (Phila Pa 1976), 1989. **14**(11): p. 1256-60.
26. Kim, K. and Y.H. Kim, *Role of trunk muscles in generating follower load in the lumbar spine of neutral standing posture.* J Biomech Eng, 2008. **130**(4): p. 041005.
27. White, A.A. and M.M. Panjabi, *Clinical biomechanics of the spine*. 1990, Philadelphia: Lippincott. xxiii, 722 p.
28. 3D4Medical, *Spine Pro III.* Mobile application Software, 2013(Version 3.7).
29. Paiva, K.B. and J.M. Granjeiro, *Bone tissue remodeling and development: Focus on matrix metalloproteinase functions.* Arch Biochem Biophys, 2014.
30. Clarke, B., *Normal bone anatomy and physiology.* Clin J Am Soc Nephrol, 2008. **3 Suppl 3**: p. S131-9.

31. Rho, J.Y., L. Kuhn-Spearing, and P. Zioupos, *Mechanical properties and the hierarchical structure of bone.* Med Eng Phys, 1998. **20**(2): p. 92-102.
32. Iyo, T., et al., *Anisotropic viscoelastic properties of cortical bone.* J Biomech, 2004. **37**(9): p. 1433-7.
33. Novitskaya, E., et al., *Anisotropy in the compressive mechanical properties of bovine cortical bone and the mineral and protein constituents.* Acta Biomater, 2011. **7**(8): p. 3170-7.
34. Carter, D.R. and D.M. Spengler, *Mechanical properties and composition of cortical bone.* Clin Orthop Relat Res, 1978(135): p. 192-217.
35. Wirtz, D.C., et al., *Critical evaluation of known bone material properties to realize anisotropic FE-simulation of the proximal femur.* J Biomech, 2000. **33**(10): p. 1325-30.
36. Gupta, H.S. and P. Zioupos, *Fracture of bone tissue: The 'hows' and the 'whys'.* Med Eng Phys, 2008. **30**(10): p. 1209-26.
37. Marcus, R., et al., *Fundamentals of Osteoporosis*. 2009: Elsevier Science.
38. Nordin, M. and V.H. Frankel, *Basic Biomechanics of the Musculoskeletal System*. 2001: Lippincott Williams & Wilkins.
39. Humzah, M.D. and R.W. Soames, *Human intervertebral disc: structure and function.* The Anatomical record, 1988. **220**(4): p. 337-56.
40. Prescher, A., *Anatomy and pathology of the aging spine.* Eur J Radiol, 1998. **27**(3): p. 181-95.
41. Zhu, D., et al., *Micro-structure and mechanical properties of annulus fibrous of the L4-5 and L5-S1 intervertebral discs.* Clinical biomechanics (Bristol, Avon), 2008. **23 Suppl 1**: p. S74-82.
42. Rohlmann, A., et al., *Analysis of the influence of disc degeneration on the mechanical behaviour of a lumbar motion segment using the finite element method.* J Biomech, 2006. **39**(13): p. 2484-90.
43. Koeller, W., et al., *Biomechanical properties of human intervertebral discs subjected to axial dynamic compression--influence of age and degeneration.* Journal of Biomechanics, 1986. **19**(10): p. 807-16.
44. Shapiro, I.M. and M.V. Risbud, *The Intervertebral Disc: Molecular and Structural Studies of the Disc in Health and Disease*. 2013: Springer Vienna.
45. Orca Health, I., *Spine Decide.* Mobile application Software, 2014(Version 4.0.5).
46. Kurtz, S.M. and A.A. Edidin, *Spine technology handbook*. 2006, Amsterdam ; London: Elsevier Academic Press. xiv, 535.
47. Schultz, D.S., et al., *Mechanical profiling of intervertebral discs.* Journal of Biomechanics, 2009. **42**(8): p. 1154-7.
48. Best, B.A., et al., *Compressive mechanical properties of the human anulus fibrosus and their relationship to biochemical composition.* Spine, 1994. **19**(2): p. 212-21.
49. Bellini, C.M., et al., *Biomechanics of the lumbar spine after dynamic stabilization.* J Spinal Disord Tech, 2007. **20**(6): p. 423-9.
50. Zander, T., A. Rohlmann, and G. Bergmann, *Influence of different artificial disc kinematics on spine biomechanics.* Clin Biomech (Bristol, Avon), 2009. **24**(2): p. 135-42.
51. Zhang, L., et al., *The biomechanical effects of osteoporosis vertebral augmentation with cancellous bone granules or bone cement on treated*

and adjacent non-treated vertebral bodies: a finite element evaluation. Clin Biomech (Bristol, Avon), 2010. **25**(2): p. 166-72.
52. 3D4Medical, *The muscle System Pro III.* Mobile application Software, 2013(Version 3.7).
53. Skinner, H. and P.J. McMahon, *CURRENT Diagnosis & Treatment in Orthopedics, Fifth Edition*. 2013: McGraw-Hill Education.
54. White, A.A., 3rd and M.M. Panjabi, *The basic kinematics of the human spine. A review of past and current knowledge.* Spine (Phila Pa 1976), 1978. **3**(1): p. 12-20.
55. Gardner-Morse, M.G. and I.A. Stokes, *Structural behavior of human lumbar spinal motion segments.* J Biomech, 2004. **37**(2): p. 205-12.
56. Hansen, L., et al., *Anatomy and biomechanics of the back muscles in the lumbar spine with reference to biomechanical modeling.* Spine (Phila Pa 1976), 2006. **31**(17): p. 1888-99.
57. Nordin, M., et al., *Basic biomechanics of the musculoskeletal system*. 1989, Philadelphia ; London: Lea & Febiger. xxiii,323p.
58. Nachemson, A.L., A.B. Schultz, and M.H. Berkson, *Mechanical properties of human lumbar spine motion segments. Influence of age, sex, disc level, and degeneration.* Spine (Phila Pa 1976), 1979. **4**(1): p. 1-8.
59. Swartz, E.E., R.T. Floyd, and M. Cendoma, *Cervical spine functional anatomy and the biomechanics of injury due to compressive loading.* J Athl Train, 2005. **40**(3): p. 155-61.
60. Bogduk, N. and S. Mercer, *Biomechanics of the cervical spine. I: Normal kinematics.* Clin Biomech (Bristol, Avon), 2000. **15**(9): p. 633-48.
61. Ahmadi, A., et al., *Kinematic analysis of dynamic lumbar motion in patients with lumbar segmental instability using digital videofluoroscopy.* Eur Spine J, 2009. **18**(11): p. 1677-85.
62. Taylor, V.M., et al., *Low back pain hospitalization. Recent United States trends and regional variations.* Spine (Phila Pa 1976), 1994. **19**(11): p. 1207-12; discussion 13.
63. Andersson, G.B., *Epidemiological features of chronic low-back pain.* Lancet, 1999. **354**(9178): p. 581-5.
64. Kelsey, J.L. and A.A. White, 3rd, *Epidemiology and impact of low-back pain.* Spine (Phila Pa 1976), 1980. **5**(2): p. 133-42.
65. Szpalski, M., et al., *The aging of the population: a growing concern for spine care in the twenty-first century.* Eur Spine J, 2003. **12 Suppl 2**: p. S81-3.
66. Bothmann, M., et al., *Dynesys fixation for lumbar spine degeneration.* Neurosurg Rev, 2008. **31**(2): p. 189-96.
67. Powell, M.C., et al., *Prevalence of lumbar disc degeneration observed by magnetic resonance in symptomless women.* Lancet, 1986. **2**(8520): p. 1366-7.
68. Kirkaldy-Willis, W.H., et al., *Pathology and pathogenesis of lumbar spondylosis and stenosis.* Spine (Phila Pa 1976), 1978. **3**(4): p. 319-28.
69. Roberts, S., et al., *Histology and pathology of the human intervertebral disc.* J Bone Joint Surg Am, 2006. **88 Suppl 2**: p. 10-4.
70. Masaryk, T.J., et al., *High-resolution MR imaging of sequestered lumbar intervertebral disks.* AJR Am J Roentgenol, 1988. **150**(5): p. 1155-62.

71. Boos, N. and M. Aebi, *Spinal Disorders: Fundamentals of Diagnosis and Treatment*. 2008: Springer.
72. Chen, Z., et al., *Surgical treatment of recurrent lumbar disc herniation by transforaminal lumbar interbody fusion.* Int Orthop, 2009. **33**(1): p. 197-201.
73. Mroz, T.E., et al., *Differences in the surgical treatment of recurrent lumbar disc herniation among spine surgeons in the United States.* Spine J, 2014.
74. Wiltse, L.L., P.H. Newman, and I. Macnab, *Classification of spondylolisis and spondylolisthesis.* Clin Orthop Relat Res, 1976(117): p. 23-9.
75. Rosenberg, N.J., *Degenerative spondylolisthesis. Predisposing factors.* J Bone Joint Surg Am, 1975. **57**(4): p. 467-74.
76. Cho, W., S.K. Cho, and C. Wu, *The biomechanics of pedicle screw-based instrumentation.* J Bone Joint Surg Br, 2010. **92**(8): p. 1061-5.
77. Rohlmann, A., et al., *Effect of a pedicle-screw-based motion preservation system on lumbar spine biomechanics: A probabilistic finite element study with subsequent sensitivity analysis.* J Biomech, 2010.
78. Kim, J.-S., D.-H. Kim, and S.-H. Lee, *Comparison between instrumented mini-TLIF and instrumented circumferential fusion in adult low-grade lytic spondylolisthesis: can mini-TLIF with PPF replace circumferential fusion?* Journal of Korean Neurosurgical Society, 2009. **45**(2): p. 74-80.
79. Chen, C.S., et al., *Failure analysis of broken pedicle screws on spinal instrumentation.* Med Eng Phys, 2005. **27**(6): p. 487-96.
80. Lin, L.C., H.H. Chen, and S.P. Sun, *A biomechanical study of the cortex-anchorage vertebral screw.* Clin Biomech (Bristol, Avon), 2003. **18**(6): p. S25-32.
81. Okuyama, K., et al., *Can insertional torque predict screw loosening and related failures? An in vivo study of pedicle screw fixation augmenting posterior lumbar interbody fusion.* Spine, 2000. **25**(7): p. 858-64.
82. Kramer, D.L., W.B. Rodgers, and F.L. Mansfield, *Transpedicular instrumentation and short-segment fusion of thoracolumbar fractures: a prospective study using a single instrumentation system.* J Orthop Trauma, 1995. **9**(6): p. 499-506.
83. Kim, D.-H., S.-T. Jeong, and S.-S. Lee, *Posterior lumbar interbody fusion using a unilateral single cage and a local morselized bone graft in the degenerative lumbar spine.* Clinics in orthopedic surgery, 2009. **1**(4): p. 214-221.
84. Vadapalli, S., et al., *Biomechanical rationale for using polyetheretherketone (PEEK) spacers for lumbar interbody fusion-A finite element study.* Spine (Phila Pa 1976), 2006. **31**(26): p. E992-8.
85. Lau, S. and K.S. Lam, *(iv) Lumbar stabilisation techniques.* Current Orthopaedics, 2007. **21**(1).
86. Spruit, M., et al., *The in vitro stabilising effect of polyetheretherketone cages versus a titanium cage of similar design for anterior lumbar interbody fusion.* Eur Spine J, 2005. **14**(8): p. 752-8.
87. Liao, J.C., et al., *Polyetheretherketone (PEEK) cage filled with cancellous allograft in anterior cervical discectomy and fusion.* Int Orthop, 2008. **32**(5): p. 643-8.
88. Bauer, T.W. and G.F. Muschler, *Bone graft materials. An overview of the basic science.* Clin Orthop Relat Res, 2000(371): p. 10-27.

89. Finkemeier, C.G., *Bone-grafting and bone-graft substitutes.* J Bone Joint Surg Am, 2002. **84-A**(3): p. 454-64.
90. Patel, V.V., et al., *Spine Surgery Basics*. 2013: Springer.
91. Kim, K.T., et al., *Clinical outcomes of 3 fusion methods through the posterior approach in the lumbar spine.* Spine (Phila Pa 1976), 2006. **31**(12): p. 1351-7; discussion 1358.
92. Schmoelz, W., et al., *Non-fusion instrumentation of the lumbar spine with a hinged pedicle screw rod system: an in vitro experiment.* Eur Spine J, 2009. **18**(10): p. 1478-85.
93. Humphreys, S.C., et al., *Comparison of posterior and transforaminal approaches to lumbar interbody fusion.* Spine (Phila Pa 1976), 2001. **26**(5): p. 567-71.
94. Wu, Y., et al., *Outcome of posterior lumbar interbody fusion versus posterolateral fusion in lumbar degenerative disease.* J Clin Neurosci, 2011. **18**(6): p. 780-3.
95. Rutherford, E.E., et al., *Lumbar spine fusion and stabilization: hardware, techniques, and imaging appearances.* Radiographics, 2007. **27**(6): p. 1737-49.
96. Cloward, R.B., *The treatment of ruptured lumbar intervertebral disc by vertebral body fusion. III. Method of use of banked bone.* Ann Surg, 1952. **136**(6): p. 987-92.
97. Watkins, M.B., *Posterolateral fusion of the lumbar and lumbosacral spine.* J Bone Joint Surg Am, 1953. **35-A**(4): p. 1014-8.
98. Tajima, N., E. Chosa, and S. Watanabe, *Posterolateral lumbar fusion.* J Orthop Sci, 2004. **9**(3): p. 327-33.
99. Cloward, R.B., *The treatment of ruptured lumbar intervertebral discs by vertebral body fusion. I. Indications, operative technique, after care.* J Neurosurg, 1953. **10**(2): p. 154-68.
100. Wang, J.L., A. Shirazi-Adl, and M. Parnianpour, *Search for critical loading condition of the spine--a meta analysis of a nonlinear viscoelastic finite element model.* Comput Methods Biomech Biomed Engin, 2005. **8**(5): p. 323-30.
101. Totoribe, K., E. Chosa, and N. Tajima, *A biomechanical study of lumbar fusion based on a three-dimensional nonlinear finite element method.* Journal of spinal disorders & techniques, 2004. **17**(2): p. 147-53.
102. Patil, S.S., et al., *Outcome of single level instrumented posterior lumbar interbody fusion using corticocancellous laminectomy bone chips.* Indian J Orthop, 2011. **45**(6): p. 500-3.
103. Cloward, R.B., *Lesions of the intervertebral disks and their treatment by interbody fusion methods. The painful disk.* Clin Orthop Relat Res, 1963. **27**: p. 51-77.
104. Chrastil, J. and A.A. Patel, *Complications associated with posterior and transforaminal lumbar interbody fusion.* J Am Acad Orthop Surg, 2012. **20**(5): p. 283-91.
105. Chen, L., H. Yang, and T. Tang, *Cage migration in spondylolisthesis treated with posterior lumbar interbody fusion using BAK cages.* Spine (Phila Pa 1976), 2005. **30**(19): p. 2171-5.

106. Smith, A.J., et al., *Increased incidence of cage migration and nonunion in instrumented transforaminal lumbar interbody fusion with bioabsorbable cages.* J Neurosurg Spine, 2010. **13**(3): p. 388-93.
107. Chen, Y., et al., *Subsidence of titanium mesh cage: a study based on 300 cases.* J Spinal Disord Tech, 2008. **21**(7): p. 489-92.
108. Choi, J.Y. and K.H. Sung, *Subsidence after anterior lumbar interbody fusion using paired stand-alone rectangular cages.* Eur Spine J, 2006. **15**(1): p. 16-22.
109. Steffen, T., A. Tsantrizos, and M. Aebi, *Effect of implant design and endplate preparation on the compressive strength of interbody fusion constructs.* Spine (Phila Pa 1976), 2000. **25**(9): p. 1077-84.
110. Jutte, P.C. and R.M. Castelein, *Complications of pedicle screws in lumbar and lumbosacral fusions in 105 consecutive primary operations.* Eur Spine J, 2002. **11**(6): p. 594-8.
111. Kumar, M.N., A. Baklanov, and D. Chopin, *Correlation between sagittal plane changes and adjacent segment degeneration following lumbar spine fusion.* Eur Spine J, 2001. **10**(4): p. 314-9.
112. Okuda, S., et al., *Risk factors for adjacent segment degeneration after PLIF.* Spine (Phila Pa 1976), 2004. **29**(14): p. 1535-40.
113. Ruberte, L.M., R.N. Natarajan, and G.B. Andersson, *Influence of single-level lumbar degenerative disc disease on the behavior of the adjacent segments--a finite element model study.* J Biomech, 2009. **42**(3): p. 341-8.
114. Schoenfeld, A.J., *Adjacent segment degeneration after lumbar spinal fusion: risk factors and implications for clinical practice.* Spine J, 2011. **11**(1): p. 21-3.
115. Fagan, M.J., S. Julian, and A.M. Mohsen, *Finite element analysis in spine research.* Proc Inst Mech Eng H, 2002. **216**(5): p. 281-98.
116. Lee, C.S., et al., *Risk factors for adjacent segment disease after lumbar fusion.* Eur Spine J, 2009. **18**(11): p. 1637-43.
117. Chou, W.Y., et al., *Adjacent segment degeneration after lumbar spinal posterolateral fusion with instrumentation in elderly patients.* Arch Orthop Trauma Surg, 2002. **122**(1): p. 39-43.
118. Hilibrand, A.S. and M. Robbins, *Adjacent segment degeneration and adjacent segment disease: the consequences of spinal fusion?* Spine J, 2004. **4**(6 Suppl): p. 190S-194S.
119. Anandjiwala, J., et al., *Adjacent segment degeneration after instrumented posterolateral lumbar fusion: a prospective cohort study with a minimum five-year follow-up.* Eur Spine J, 2011. **20**(11): p. 1951-60.
120. Gupta, K.K. and J.L. Meek, *A brief history of the beginning of the finite element method.* International Journal for Numerical Methods in Engineering, 1996. **39**(22): p. 3761-3774.
121. Turner, M.J., et al., *Stiffness and Deflection Analysis of Complex Structures.* Journal of the Aeronautical Sciences, 1956. **23**(9): p. 805-&.
122. Brekelmans, W.A., H.W. Poort, and T.J. Slooff, *A new method to analyse the mechanical behaviour of skeletal parts.* Acta Orthop Scand, 1972. **43**(5): p. 301-17.
123. Simula, D.S., *Abaqus/CAE 6.10 Analysis Users's Manual.* User Manual
124. Belytschko, T., et al., *Finite element stress analysis of an intervertebral disc.* J Biomech, 1974. **7**(3): p. 277-85.

125. Goto, M., et al., *Buckling and bone modeling as factors in the development of idiopathic scoliosis.* Spine (Phila Pa 1976), 2003. **28**(4): p. 364-70; discussion 371.
126. Villarraga, M.L., et al., *The biomechanical effects of kyphoplasty on treated and adjacent nontreated vertebral bodies.* J Spinal Disord Tech, 2005. **18**(1): p. 84-91.
127. Overaker, D.W., N.A. Langrana, and A.M. Cuitino, *Finite element analysis of vertebral body mechanics with a nonlinear microstructural model for the trabecular core.* J Biomech Eng, 1999. **121**(5): p. 542-50.
128. Higgins, K.B., et al., *Biomechanical alterations in intact osteoporotic spine due to synthetic augmentation: finite element investigation.* J Biomech Eng, 2007. **129**(4): p. 575-85.
129. Polikeit, A., et al., *Factors influencing stresses in the lumbar spine after the insertion of intervertebral cages: finite element analysis.* Eur Spine J, 2003. **12**(4): p. 413-20.
130. Crawford, R.P., C.E. Cann, and T.M. Keaveny, *Finite element models predict in vitro vertebral body compressive strength better than quantitative computed tomography.* Bone, 2003. **33**(4): p. 744-50.
131. Buckley, J.M., K. Loo, and J. Motherway, *Comparison of quantitative computed tomography-based measures in predicting vertebral compressive strength.* Bone, 2007. **40**(3): p. 767-74.
132. Shirazi-Adl, A., *Analysis of large compression loads on lumbar spine in flexion and in torsion using a novel wrapping element.* J Biomech, 2006. **39**(2): p. 267-75.
133. Han, K.S., et al., *Lumbar spinal loads vary with body height and weight.* Med Eng Phys, 2013. **35**(7): p. 969-77.
134. Moramarco, V., et al., *An accurate validation of a computational model of a human lumbosacral segment.* Journal of Biomechanics, 2010. **43**(2): p. 334-42.
135. Ferguson, S.J., K. Ito, and L.P. Nolte, *Fluid flow and convective transport of solutes within the intervertebral disc.* J Biomech, 2004. **37**(2): p. 213-21.
136. Espino, D.M., et al., *Stochastic finite element analysis of biological systems: comparison of a simple intervertebral disc model with experimental results.* Comput Methods Biomech Biomed Engin, 2003. **6**(4): p. 243-8.
137. Schroeder, Y., et al., *Osmoviscoelastic finite element model of the intervertebral disc.* Eur Spine J, 2006. **15 Suppl 3**: p. S361-71.
138. Du, C., et al., *Biomechanical investigation of thoracolumbar spine in different postures during ejection using a combined finite element and multi-body approach.* Int J Numer Method Biomed Eng, 2014. **30**(11): p. 1121-31.
139. Zander, T., et al., *Estimation of muscle forces in the lumbar spine during upper-body inclination.* Clin Biomech (Bristol, Avon), 2001. **16 Suppl 1**: p. S73-80.
140. Hao, Z., et al., *The effect of boundary condition on the biomechanics of a human pelvic joint under an axial compressive load: a three-dimensional finite element model.* J Biomech Eng, 2011. **133**(10): p. 101006.
141. Zhu, R., et al., *Comparison of four reconstruction methods after total sacrectomy: a finite element study.* Clin Biomech (Bristol, Avon), 2012. **27**(8): p. 771-6.

142. Schmidt, H., et al., *Application of a new calibration method for a three-dimensional finite element model of a human lumbar annulus fibrosus.* Clin Biomech (Bristol, Avon), 2006. **21**(4): p. 337-44.
143. Rohlmann, A., et al., *Determination of trunk muscle forces for flexion and extension by using a validated finite element model of the lumbar spine and measured in vivo data.* J Biomech, 2006. **39**(6): p. 981-9.
144. El-Rich, M., et al., *Finite element investigation of the loading rate effect on the spinal load-sharing changes under impact conditions.* Journal of Biomechanics, 2009. **42**(9): p. 1252-62.
145. Wagnac, E., et al., *Finite element analysis of the influence of loading rate on a model of the full lumbar spine under dynamic loading conditions.* Med Biol Eng Comput, 2012. **50**(9): p. 903-15.
146. Rohlmann, A., et al., *Comparison of the effects of bilateral posterior dynamic and rigid fixation devices on the loads in the lumbar spine: a finite element analysis.* Eur Spine J, 2007. **16**(8): p. 1223-31.
147. Tsuang, Y.H., et al., *Comparison of cage application modality in posterior lumbar interbody fusion with posterior instrumentation--a finite element study.* Med Eng Phys, 2009. **31**(5): p. 565-70.
148. Zander, T., et al., *Estimation of muscle forces in the lumbar spine during upper-body inclination.* Clinical Biomechanics, 2001. **16**: p. S73-S80.
149. Han, K.S., et al., *Spinal muscles can create compressive follower loads in the lumbar spine in a neutral standing posture.* Med Eng Phys, 2011. **33**(4): p. 472-8.
150. Rohlmann, A., T. Zander, and G. Bergmann, *Spinal loads after osteoporotic vertebral fractures treated by vertebroplasty or kyphoplasty.* Eur Spine J, 2006. **15**(8): p. 1255-64.
151. Renner, S.M., et al., *Novel model to analyze the effect of a large compressive follower pre-load on range of motions in a lumbar spine.* J Biomech, 2007. **40**(6): p. 1326-32.
152. Liu, C.L., et al., *Influence of Dynesys system screw profile on adjacent segment and screw.* J Spinal Disord Tech, 2010. **23**(6): p. 410-7.
153. Dvorak, J., et al., *Functional radiographic diagnosis of the lumbar spine. Flexion-extension and lateral bending.* Spine (Phila Pa 1976), 1991. **16**(5): p. 562-71.
154. Boden, S.D. and S.W. Wiesel, *Lumbosacral segmental motion in normal individuals. Have we been measuring instability properly?* Spine (Phila Pa 1976), 1990. **15**(6): p. 571-6.
155. Pearcy, M., I. Portek, and J. Shepherd, *Three-dimensional x-ray analysis of normal movement in the lumbar spine.* Spine (Phila Pa 1976), 1984. **9**(3): p. 294-7.
156. O'Sullivan, K., et al., *Validation of a novel spinal posture monitor: comparison with digital videofluoroscopy.* Eur Spine J, 2012. **21**(12): p. 2633-9.
157. Okawa, A., et al., *Dynamic motion study of the whole lumbar spine by videofluoroscopy.* Spine (Phila Pa 1976), 1998. **23**(16): p. 1743-9.
158. Edmondston, S.J., et al., *MRI evaluation of lumbar spine flexion and extension in asymptomatic individuals.* Man Ther, 2000. **5**(3): p. 158-64.

159. Battie, M.C., et al., *1991 Volvo Award in clinical sciences. Smoking and lumbar intervertebral disc degeneration: an MRI study of identical twins.* Spine (Phila Pa 1976), 1991. **16**(9): p. 1015-21.
160. McGregor, A.H., I.D. McCarthy, and S.P. Hughes, *Motion characteristics of the lumbar spine in the normal population.* Spine (Phila Pa 1976), 1995. **20**(22): p. 2421-8.
161. Troke, M., et al., *A normative database of lumbar spine ranges of motion.* Man Ther, 2005. **10**(3): p. 198-206.
162. Dvorak, J., et al., *Normal motion of the lumbar spine as related to age and gender.* Eur Spine J, 1995. **4**(1): p. 18-23.
163. O'Sullivan, K., et al., *The between-day and inter-rater reliability of a novel wireless system to analyse lumbar spine posture.* Ergonomics, 2011. **54**(1): p. 82-90.
164. Consmuller, T., et al., *Comparative evaluation of a novel measurement tool to assess lumbar spine posture and range of motion.* Eur Spine J, 2012. **21**(11): p. 2170-80.
165. Goodvin, C., et al., *Development of a real-time three-dimensional spinal motion measurement system for clinical practice.* Med Biol Eng Comput, 2006. **44**(12): p. 1061-75.
166. Ha, T.H., et al., *Measurement of lumbar spine range of movement and coupled motion using inertial sensors - a protocol validity study.* Man Ther, 2013. **18**(1): p. 87-91.
167. Lee, J.K., et al., *A portable inertial sensing-based spinal motion measurement system for low back pain assessment.* Conf Proc IEEE Eng Med Biol Soc, 2011. **2011**: p. 4737-40.
168. Tojima, M., et al., *Novel 3-dimensional motion analysis method for measuring the lumbar spine range of motion: repeatability and reliability compared with an electrogoniometer.* Spine (Phila Pa 1976), 2013. **38**(21): p. E1327-33.
169. Lee, M.J., et al., *The effect of bilateral laminotomy versus laminectomy on the motion and stiffness of the human lumbar spine: a biomechanical comparison.* Spine (Phila Pa 1976), 2010. **35**(19): p. 1789-93.
170. Vismara, L., et al., *Effect of obesity and low back pain on spinal mobility: a cross sectional study in women.* J Neuroeng Rehabil, 2010. **7**: p. 3.
171. Wai-Yin, W. and W. Man-Sang, *Measurement of Postural Change in Trunk Movements Using Three Sensor Modules.* Instrumentation and Measurement, IEEE Transactions on, 2009. **58**(8): p. 2737-2742.
172. Lee, J.H., et al., *Effect of intraoperative position used in posterior lumbar interbody fusion on the maintenance of lumbar lordosis.* J Neurosurg Spine, 2008. **8**(3): p. 263-70.
173. Godde, S., et al., *Influence of cage geometry on sagittal alignment in instrumented posterior lumbar interbody fusion.* Spine (Phila Pa 1976), 2003. **28**(15): p. 1693-9.
174. Panjabi, M.M., et al., *On the understanding of clinical instability.* Spine (Phila Pa 1976), 1994. **19**(23): p. 2642-50.
175. Li, G., et al., *Segmental in vivo vertebral motion during functional human lumbar spine activities.* Eur Spine J, 2009. **18**(7): p. 1013-21.

176. Gracovetsky, S.A., *Range of normality versus range of motion: A functional measure for the prevention and management of low back injury.* J Bodyw Mov Ther, 2010. **14**(1): p. 40-9.
177. Fitzgerald, G.K., et al., *Objective assessment with establishment of normal values for lumbar spinal range of motion.* Phys Ther, 1983. **63**(11): p. 1776-81.
178. W-K, C., et al., *A non-invasive protocol for the determination of lumbar spine mobility.* Clin Biomech (Bristol, Avon), 1996. **11**(8): p. 474-480.
179. Ochia, R.S., et al., *Three-dimensional in vivo measurement of lumbar spine segmental motion.* Spine (Phila Pa 1976), 2006. **31**(18): p. 2073-8.
180. Gracovetsky, S., et al., *A database for estimating normal spinal motion derived from noninvasive measurements.* Spine (Phila Pa 1976), 1995. **20**(9): p. 1036-46.
181. Morl, F. and R. Blickhan, *Three-dimensional relation of skin markers to lumbar vertebrae of healthy subjects in different postures measured by open MRI.* Eur Spine J, 2006. **15**(6): p. 742-51.
182. Cerveri, P., A. Pedotti, and G. Ferrigno, *Non-invasive approach towards the in vivo estimation of 3D inter-vertebral movements: methods and preliminary results.* Med Eng Phys, 2004. **26**(10): p. 841-53.
183. Rozumalski, A., et al., *The in vivo three-dimensional motion of the human lumbar spine during gait.* Gait & posture, 2008. **28**(3): p. 378-84.
184. Yang, Z., et al., *Error analysis on spinal motion measurement using skin mounted sensors.* Conf Proc IEEE Eng Med Biol Soc, 2008. **2008**: p. 4740-3.
185. Y-H, L., et al., *Predictive model of intersegmental mobility of lumbar spine in the sagittal plane from skin markers.* Clin Biomech (Bristol, Avon), 1995. **10**(8): p. 413-420.
186. Wong, W.Y. and M.S. Wong, *Trunk posture monitoring with inertial sensors.* Eur Spine J, 2008. **17**(5): p. 743-53.
187. Taylor, W.R., T. Consmuller, and A. Rohlmann, *A novel system for the dynamic assessment of back shape.* Med Eng Phys, 2010. **32**(9): p. 1080-3.
188. Xsense, T., *MTw User Manual.* Equipment User Manual p. http://www.xsens.com.
189. Wong, T.K. and R.Y. Lee, *Effects of low back pain on the relationship between the movements of the lumbar spine and hip.* Hum Mov Sci, 2004. **23**(1): p. 21-34.
190. Van Herp, G., et al., *Three-dimensional lumbar spinal kinematics: a study of range of movement in 100 healthy subjects aged 20 to 60+ years.* Rheumatology (Oxford), 2000. **39**(12): p. 1337-40.
191. Ayturk, U.M. and C.M. Puttlitz, *Parametric convergence sensitivity and validation of a finite element model of the human lumbar spine.* Comput Methods Biomech Biomed Engin, 2011. **14**(8): p. 695-705.
192. Le Huec, J.C., et al., *Validated finite element analysis of the maverick total disc prosthesis.* J Spinal Disord Tech, 2010. **23**(4): p. 249-57.
193. Adams, M.A. and P. Dolan, *Spine biomechanics.* J Biomech, 2005. **38**(10): p. 1972-83.
194. Goto, K., et al., *Effects of lumbar spinal fusion on the other lumbar intervertebral levels (three-dimensional finite element analysis).* J Orthop Sci, 2003. **8**(4): p. 577-84.

195. Chen, C.S., et al., *Stress analysis of the disc adjacent to interbody fusion in lumbar spine.* Med Eng Phys, 2001. **23**(7): p. 483-91.
196. Qiu, T.X., E.C. Teo, and Q.H. Zhang, *Effect of bilateral facetectomy of thoracolumbar spine T11-L1 on spinal stability.* Med Biol Eng Comput, 2006. **44**(5): p. 363-70.
197. Galbusera, F., et al., *Rigid and flexible spinal stabilization devices: a biomechanical comparison.* Med Eng Phys, 2011. **33**(4): p. 490-6.
198. Shin, D.S., K. Lee, and D. Kim, *Biomechanical study of lumbar spine with dynamic stabilization device using finite element method.* Computer-Aided Design, 2007. **39**(7): p. 559-567.
199. Kim, H.J., et al., *The biomechanical effect of pedicle screws' insertion angle and position on the superior adjacent segment in 1 segment lumbar fusion.* Spine (Phila Pa 1976), 2012. **37**(19): p. 1637-44.
200. El-Rich, M., et al., *Finite element investigation of the loading rate effect on the spinal load-sharing changes under impact conditions.* J Biomech, 2009. **42**(9): p. 1252-62.
201. Teo, E.C. and H.W. Ng, *Evaluation of the role of ligaments, facets and disc nucleus in lower cervical spine under compression and sagittal moments using finite element method.* Med Eng Phys, 2001. **23**(3): p. 155-64.
202. Laville, A., S. Laporte, and W. Skalli, *Parametric and subject-specific finite element modelling of the lower cervical spine. Influence of geometrical parameters on the motion patterns.* J Biomech, 2009. **42**(10): p. 1409-15.
203. Schmidt, H., F. Heuer, and H.-J. Wilke, *Which axial and bending stiffnesses of posterior implants are required to design a flexible lumbar stabilization system?* Journal of Biomechanics, 2009. **42**(1): p. 48-54.
204. Yoganandan, N., S. Kumaresan, and F.A. Pintar, *Biomechanics of the cervical spine Part 2. Cervical spine soft tissue responses and biomechanical modeling.* Clinical biomechanics (Bristol, Avon), 2001. **16**(1): p. 1-27.
205. Lucas, D.B. and B. Bresler, *Stability of the ligamentous spine*. 1961: Biomechanics Laboratory, University of California.
206. Patwardhan, A.G., et al., *A follower load increases the load-carrying capacity of the lumbar spine in compression.* Spine (Phila Pa 1976), 1999. **24**(10): p. 1003-9.
207. Rohlmann, A., et al., *Influence of a follower load on intradiscal pressure and intersegmental rotation of the lumbar spine.* Spine (Phila Pa 1976), 2001. **26**(24): p. E557-61.
208. Kim, K., et al., *Stress analysis in a pedicle screw fixation system with flexible rods in the lumbar spine.* Proc Inst Mech Eng H, 2010. **224**(3): p. 477-85.
209. Schmidt, H., et al., *Effect of multilevel lumbar disc arthroplasty on spine kinematics and facet joint loads in flexion and extension: a finite element analysis.* Eur Spine J, 2012. **21 Suppl 5**: p. S663-74.
210. Ivanov, A.A., et al., *Lumbar fusion leads to increases in angular motion and stress across sacroiliac joint: a finite element study.* Spine (Phila Pa 1976), 2009. **34**(5): p. E162-9.
211. Zhao, Y., et al., *Comparison of stability of two kinds of sacro-iliac screws in the fixation of bilateral sacral fractures in a finite element model.* Injury, 2012. **43**(4): p. 490-4.

212. Rohlmann, A., et al., *Effect of an artificial disc on lumbar spine biomechanics: a probabilistic finite element study.* Eur Spine J, 2009. **18**(1): p. 89-97.
213. Mizrahi, J., M.J. Silva, and W.C. Hayes, *Finite element stress analysis of simulated metastatic lesions in the lumbar vertebral body.* J Biomed Eng, 1992. **14**(6): p. 467-75.
214. Dreischarf, M., et al., *Comparison of eight published static finite element models of the intact lumbar spine: predictive power of models improves when combined together.* J Biomech, 2014. **47**(8): p. 1757-66.
215. Panjabi, M.M., et al., *Mechanical behavior of the human lumbar and lumbosacral spine as shown by three-dimensional load-displacement curves.* J Bone Joint Surg Am, 1994. **76**(3): p. 413-24.
216. Rohlmann, A., et al., *Realistic loading conditions for upper body bending.* J Biomech, 2009. **42**(7): p. 884-90.
217. Dreischarf, M., et al., *Optimised in vitro applicable loads for the simulation of lateral bending in the lumbar spine.* Med Eng Phys, 2012. **34**(6): p. 777-80.
218. Zhang, Q.H., S.H. Tan, and S.M. Chou, *Effects of bone materials on the screw pull-out strength in human spine.* Med Eng Phys, 2006. **28**(8): p. 795-801.
219. Goel, V.K., et al., *An analytical investigation of the mechanics of spinal instrumentation.* Spine (Phila Pa 1976), 1988. **13**(9): p. 1003-11.
220. Stemper, B.D., et al., *Mechanical yield of the lumbar annulus: a possible contributor to instability: Laboratory investigation.* J Neurosurg Spine, 2014. **21**(4): p. 608-13.
221. Green, T.P., M.A. Adams, and P. Dolan, *Tensile properties of the annulus fibrosus II. Ultimate tensile strength and fatigue life.* Eur Spine J, 1993. **2**(4): p. 209-14.
222. Zak, M. and C. Pezowicz, *Spinal sections and regional variations in the mechanical properties of the annulus fibrosus subjected to tensile loading.* Acta Bioeng Biomech, 2013. **15**(1): p. 51-9.
223. Matsuzaki, H., et al., *Problems and solutions of pedicle screw plate fixation of lumbar spine.* Spine (Phila Pa 1976), 1990. **15**(11): p. 1159-65.
224. Chiu, Y.-C., et al., *Pedicle screw breakage in a vertebral body: A rare complication in a dynamic stabilization device.* Formosan Journal of Musculoskeletal Disorders, 2011. **2**(4): p. 143-146.
225. Zencica, P., et al., *[Adjacent segment degeneration after lumbosacral fusion in spondylolisthesis: a retrospective radiological and clinical analysis].* Acta Chir Orthop Traumatol Cech, 2010. **77**(2): p. 124-30.
226. Mobbs, R.J., et al., *Indications for anterior lumbar interbody fusion.* Orthop Surg, 2013. **5**(3): p. 153-63.
227. Palepu, V., M. Kodigudla, and V.K. Goel, *Biomechanics of disc degeneration.* Adv Orthop, 2012. **2012**: p. 726210.
228. Park, P., et al., *Adjacent segment disease after lumbar or lumbosacral fusion: review of the literature.* Spine (Phila Pa 1976), 2004. **29**(17): p. 1938-44.
229. Kurutz, M. and L. Oroszvary, *Finite element analysis of weightbath hydrotraction treatment of degenerated lumbar spine segments in elastic phase.* J Biomech, 2010. **43**(3): p. 433-41.

230. Polikeit, A., L.P. Nolte, and S.J. Ferguson, *Simulated influence of osteoporosis and disc degeneration on the load transfer in a lumbar functional spinal unit.* J Biomech, 2004. **37**(7): p. 1061-9.
231. Throckmorton, T.W., et al., *The impact of adjacent level disc degeneration on health status outcomes following lumbar fusion.* Spine (Phila Pa 1976), 2003. **28**(22): p. 2546-50.
232. Niinomi, M., *Mechanical properties of biomedical titanium alloys.* Materials Science and Engineering: A, 1998. **243**(1–2): p. 231-236.
233. Griza, S., et al., *Case study of Ti6Al4V pedicle screw failures due to geometric and microstructural aspects.* Engineering Failure Analysis, 2012. **25**(0): p. 133-143.